# Ex libris
# Universitatis
# Albertaensis

QUAECUMQUE VERA

THE UNIVERSITY OF ALBERTA


STUDIES WITH A TWO-DIMENSIONAL MAGNETOMETER ARRAY IN

NORTHWESTERN UNITED STATES AND SOUTHWESTERN CANADA


BY


( C )    P. ADRIAN CAMFIELD


A THESIS

SUBMITTED TO THE FACULTY OF GRADUATE STUDIES AND RESEARCH

IN PARTIAL FULFILMENT OF THE REQUIREMENTS FOR THE DEGREE

OF DOCTOR OF PHILOSOPHY

IN GEOPHYSICS


DEPARTMENT OF PHYSICS


EDMONTON, ALBERTA

SPRING, 1973

ABSTRACT

An array of 46 geomagnetic variometers was operated in the summer
of 1969 by the University of Alberta and the University of Texas at
Dallas, in the northwestern United States and southwestern Canada.
Magnetograms and contour maps of the Fourier transforms of magneto-
grams have been examined for effects of electromagnetic induction in
the earth.  In the North American Central Plains, one of the largest-
known variation anomalies has been mapped in a narrow region striking
north through the Black Hills of South Dakota.  The anomaly is
prominent in the period band of magnetic substorms (1/2 to 2 h) and
in three harmonics of the daily variation (8, 12 and 24 h).  In the
substorm band, vertical and horizontal anomalous fields due to internal
currents are larger than the regional normal fields; at the daily
variation periods, the anomaly persists in the vertical component but
not in the horizontal.  Substorm observations can be semi-quantitatively
explained by horizontal-field induction in a shallow two-dimensional
body of high conductivity, but a qualitative interpretation of the
anomaly requires concentration, by a local conductor, of current
induced over a much wider region such as the crust of the entire
Great Plains.  As period increases from the substorm band to the
daily variation, a change is indicated from predominantly horizontal-
field induction in the local conductor to vertical-field induction in
the large three-dimensional laminar crustal conductor.  The local
conductor is postulated to be a graphite schist body in the Precambrian
basement; a metamorphic belt containing schists and coincident with the

induction anomaly has been mapped by Lidiak using independent geophysical and geological techniques.

In the Northern Rocky Mountains, the vertical component of the daily variation is not attenuated relative to its value in the Great Plains, unlike the vertical component of substorms. A plane-layered earth fitting the observed values of normal-field Z/H ratios for appropriate spatial wave numbers k has a thin conducting layer at depths characteristic of the seismic low-velocity zone. Near its eastern edge, two thickenings of the layer separated by a resistive gap are required in the first-order modelling of two small local anomalies. The high conductivity may be related to partial melting, but if so, the melting is on a smaller scale than in the Basin and Range Province south of the array. The thickenings and gap might be explained by the lateral redistribution of hydrated ocean-floor material expected in the large-scale shearing involved in the overthrust of lithospheric plates.

Increasing complexity of the daily variation fields with increasing period has been interpreted provisionally as evidence for a new class of variation anomalies, termed <u>vartran</u> anomalies. They are believed to be caused by <u>var</u>iable lateral <u>trans</u>mission through the electrically heterogeneous upper mantle and crust, of fields associated with currents induced in deep structure south of the array. The combined refraction and absorption effects involved in the variable transmission make it unlikely that observations of these anomalies could be inverted to yield quantitative estimates of geoelectric structure.

ACKNOWLEDGEMENTS

I am indebted first and foremost to Dr. D.I. Gough, my thesis supervisor, for his guidance and encouragement during this project. I value greatly the stimulation and friendship which he has given me. The interpretation of the data in the thesis has evolved in the course of our joint discussions; I have tried to indicate where proper credit lies for the ideas which he has put forward.

The late Dr. Hartmut Porath, of the University of Texas at Dallas, was an extremely able and energetic partner in this joint study. His accidental death in Ethiopia in April, 1971 came as a severe shock to us.

I acknowledge the influence of the late Dr. Bernard Caner, of Victoria, who introduced me to geomagnetic deep sounding in western North America. I miss his criticism of this work.

I am grateful to investigators who have given us magnetic variation data: to Dr. G. Rostoker of the University of Alberta, for COC, which was operated by his students Dr. J.K. Walker, Dr. J.L. Kisabeth and Dr. J.C. Samson; to the staff of the Newport Geophysical Observatory (NEP), especially Mr. A. Travis; and to Dr. K.V. Paulson of the University of Saskatchewan, for TUO.

Dr. E.R. Niblett and others among my colleagues at the Division of Geomagnetism, Earth Physics Branch, E.M.R., Ottawa, have aided by their critical disection of our ideas.

Dr. F.W. Jones has helped us with the use of his programs for computing the response of electrical conductivity structures.

TABLE OF CONTENTS

# LIST OF TABLES

LIST OF ILLUSTRATIONS

CHAPTER  I

INTRODUCTION

## 1.1  Purpose of Investigation

The magnetometer array study described in this thesis was carried
out in the summer of 1969 to complete a reconnaissance survey of ano-
malies in geomagnetic variations in western North America.  This survey,
consisting of three arrays operated jointly by the University of Alberta
and the University of Texas at Dallas, provides coverage from the U.S.-
Mexico border north to the Trans-Canada Highway, and links the regions
explored by Schmucker in Arizona and New Mexico and by Caner in southern
Alberta and British Columbia.  The first array, in Colorado, Utah and
adjacent states, recorded two variation anomalies trending north-south,
one beneath the Southern Rocky Mountains between the Great Plains and
the Colorado Plateau, and a second beneath the Wasatch Front at the
contact of the Colorado Plateau with the Basin and Range Province.  These
have been interpreted in terms of large-scale conductive inhomogeneities
in the upper mantle, probably associated with regional variations in
upper-mantle temperature.  In addition, a station in northwestern
Nebraska showed an intense anomaly possibly associated with the Black
Hills of South Dakota.

The array study with which this thesis is concerned was designed
to look for northward continuation of the two upper-mantle anomalies
found by the first array, and to discover the connection, if any,
between them and the apparently-simpler and shallower conductive structure
reported by Caner in southwestern Canada.  Investigation of the Black
Hills area of South Dakota was also included.

## 1.2 Outline of Thesis

The remainder of this chapter (1) presents a review of previous geomagnetic depth sounding studies in western North America, to provide background for this report. Schmucker, in his pioneering work, used a small number of variometers installed along a profile, as did Hyndman, and Caner and his colleagues. Gough, Reitzel, Porath and their students introduced mapping with large two-dimensional arrays of variometers; this technique is free from some of the limiting assumptions which are necessary in analysing linear-profile data. Variation anomalies discovered over the past 15 years include those beneath the Rio Grande region, beneath the Southern Rockies and Wasatch Front, and beneath the Cordillera in Canada.

Chapter 2 describes the location of the 1969 array, the portable three-component geomagnetic variometer, and the field procedures used in operating the array.

Chapter 3 is concerned with short-period data, from polar magnetic substorms. Data conversion (analogue to digital) precedes data presentation in magnetogram form, and Fourier analysis yields contour maps of spectral components at various periods. A qualitative analysis of substorm fields reveals the location and intensity of anomalies in the regions of the Northern Rockies and the North American Central Plains (the latter passing through the Black Hills of South Dakota).

Chapter 4 describes the long-period data, from the geomagnetic daily variation. Data is again displayed in magnetograms and contour maps of Fourier components. Qualitative interpretation shows that the daily variation is affected by the Central Plains conductor but not by the Northern Rockies conductive structures.

Chapter 5 begins with a discussion of quantitative interpretation techniques which will be applied to the data. Short-period anomalous fields are approximately separated from normal fields, by assuming that features with short spatial wavelengths are anomalous fields associated with internal currents. Quantitative models are attempted for the anomalous fields in the Central Plains, and correlation with other geophysical and geological information is noted. In the Northern Rockies, models fitting short- and long-period normal fields and short-period anomalous fields have an internal consistency which matches constraints provided by other geophysical data. Suggestions for further work are included in this chapter.

1.3 Previous Geomagnetic Depth Sounding in Western North America

Geomagnetic depth sounding uses temporal variations in the external geomagnetic field as signal sources with which to investigate the electrical conductivity structure of the earth. Variations in the period-range from a few minutes to one day occur with sufficient energy and have penetration depths adequate to probe the crust and upper mantle. Internal currents induced by the external field will flow with a distribution determined by the electrical conductivity of the earth. Variations measured at the earth's surface will thus be a vector sum of the external fields and the internal fields associated with the induced currents. Hence spatial changes or anomalies in the character of variations may be caused by either external or internal sources; methods have been developed to average out the spatial variability of the external sources for different events (for single recording

instruments or linear profiles of instruments) or to separate out the external part (for two-dimensional arrays), so that internal source configurations can be isolated for interpretation in terms of conductive structure.

The electrical conductivity of the upper mantle is strongly dependent on temperature, since silicates at upper-mantle temperatures have the exponential dependence of conductivity on temperature which characterizes semi-conductors (Tozer, 1959). A change in temperature is assumed to affect the conductivity to a far greater extent than changes in composition. Hence an estimate of conductivity at depth should indicate at least relative temperature. In the crust under regions where heat flow is not abnormally high, enhanced conductivity is more likely to be caused by a compositional condition such as hydration (Hyndman and Hyndman, 1968) or conductive mineralization, rather than being due to high temperatures.

Schmucker (1964, 1969, 1970a), Hyndman (1963), Caner et al. (1967, 1971), and Gough and Reitzel (1969) used single profiles of seven or fewer geomagnetic variometers recording simultaneously in the pre-array era of geomagnetic depth sounding in western North America. Fig. 1.1 locates stations operated in the Cordillera of the western United States along profiles, as well as the 1967 array of Reitzel et al. (1970).

The five stations marked with crosses are part of a net of temporary observatories established by the U.S. Coast and Geodetic Survey during the International Geophysical Year (1957-58). Schmucker (1970a) notes that in this pilot study, stations LEA and ESP showed variations in the vertical component Z like those at the permanent
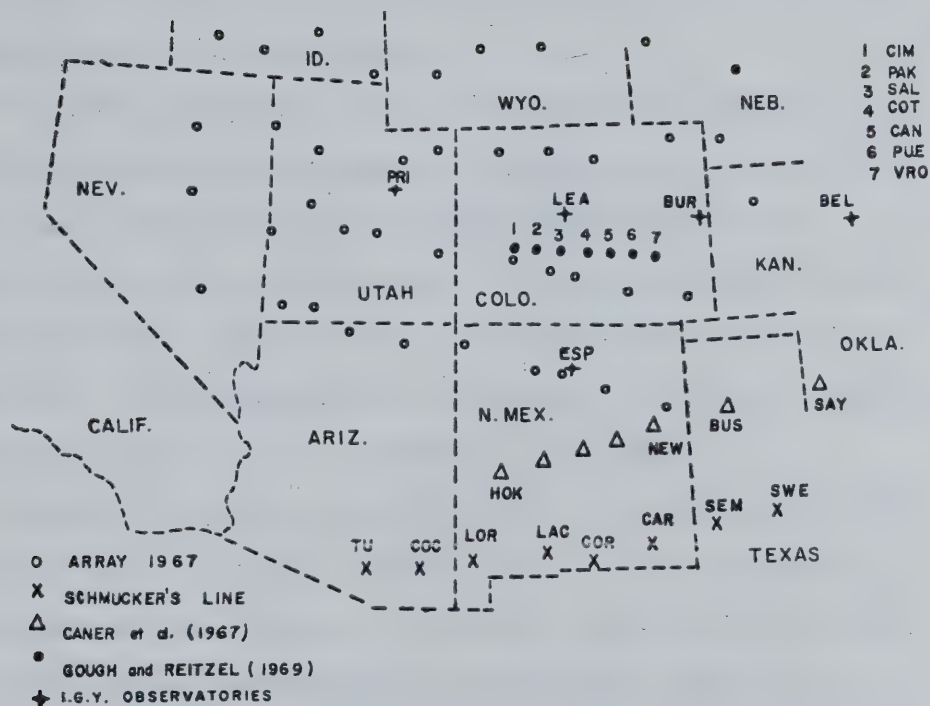
Fig. 1.1  Geomagnetic depth sounding profiles in the southwestern United
States, together with the array of Reitzel et al. (1970).
Diagram from Oldenburg (1969).

observatory at Tucson, Arizona (coded TU), with amplitudes strongly
reduced compared with those at BUR and BEL. At PRI, large-amplitude
Z fluctuations correlated well with the east-west horizontal component
D. The 400 km station spacing precluded any detailed analysis of the
internal conductivity distribution.

In 1959-62, Schmucker carried out an extensive recording program
in the southwestern United States, and described in his papers (1964,
1970a) the coastal and the inland (Sierra Nevada) anomalies in
California and the Rio Grande anomaly in New Mexico and Texas. Only
the latter will be considered here, in relation to the study of the
Cordillera. The relevant stations are shown by x's in Fig. 1.1, going
eastward from Tucson (TU) to Sweetwater, Texas (SWE).

A sample of the data on this profile is given in the upper half
of Fig. 1.2, a bay recorded on 10 May 1960. D and the north-south
horizontal component H along the profile are essentially uniform, and
are shown only for the station LAC (see Schmucker, 1970a, Fig. 7).
At TU the Z variation is similar in form to Z at CAR and SWE, but has
a much reduced amplitude; from these observations two different regions,
one eastern and one western, are identified. Schmucker considered
these stations normal, meaning that the variation fields are the
resultant of the external fields and internal fields induced in regions
of horizontally-stratified, although different, conductivity structures,
far from any lateral inhomogeneity. On the other hand, Z is anomalous
at LOR and especially LAC and COR, with a phase reversal evident at LAC.
The resemblance of anomalous Z to D suggests that a conductivity
structure striking north-south, between the two different normal regions
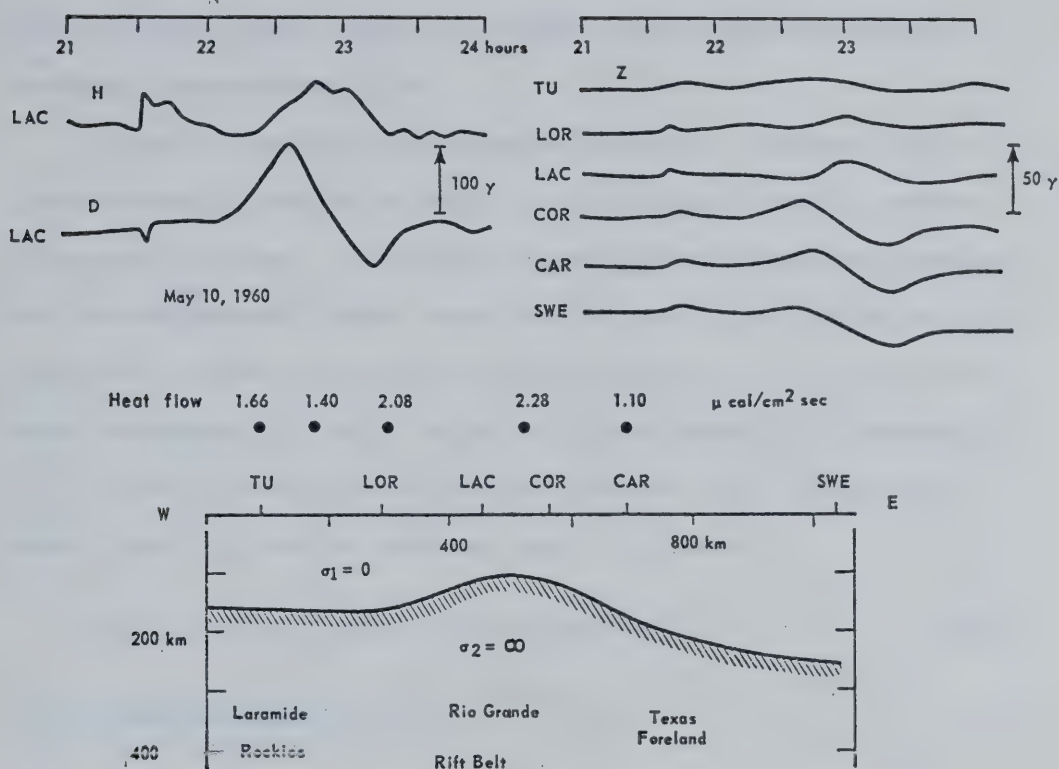
Fig. 1.2  (Upper) Bay of 10 May 1960 on the Rio Grande profile.  Note suppressed Z amplitudes at TU and LOR, a reversal between LAC and COR,  and enhanced Z at COR, CAR and SWE.

(Middle) Heat flow values from Warren et al. (1969).

(Lower) Schmucker's third model for the Rio Grande anomaly. A perfect substitute conductor rises beneath the Rio Grande Rift Belt, then falls to a greater depth beneath the Texas Foreland (Great Plains) than it had beneath the Laramide Rockies (Basin and Range Province).  From Schmucker (1969).

defined above, is the cause of the eddy-current concentration which produces the anomalous fields.

To isolate the effects of internal conductors, Schmucker used a transfer-function method of removing the effects of unknown geometry of external sources. He defined for each station a frequency-dependent but time-independent linear transformation matrix (or transfer function matrix) $f(\omega)$ which would relate anomalous fields in any or all of the three components H, D and Z to any or all the normal field components. If the observed variation as a function of time is $F(t)$, made up of a normal part $F_o(t)$ and an anomalous part $F_a(t)$, then

$$F(t) = F_o(t) + F_a(t) = F_o(t) + f(\omega) F_o(t) \tag{1.1}$$

In the frequency domain, for Z,

$$Z = Z_o + Z_a = Z_o + z(D) D_o + z(H) H_o + z(Z) Z_o \tag{1.2}$$

where the upper-case letters represent the spectra of harmonic time-functions. The lower-case letters represent elements of the 9-term transformation matrix, and are complex-valued functions of the form

$$z(D) = z_u(D) + i z_v(D) \tag{1.3}$$

For the Rio Grande anomaly, anomalous Z is seen in the magnetograms to correlate with D, so that (1.2) may be simplified to the approximation

$$Z \doteq Z_o + z(D) D_o + z(Z) Z_o \tag{1.4}$$

and if one has negligible anomalous Z induced by the normal vertical
field itself, approximately,

$$Z \doteq Z_o + z(D) \, D_o \tag{1.5}$$

Hence $z(D) \doteq \dfrac{Z - Z_o}{D_o}$ $\hspace{4cm}$ (1.6)

In actual practice $z(D)$ would be evaluated by analysis involving the
auto-power spectra of all three components and the cross-power spectra
between them.  Full details are found in Schmucker (1970a) or Everett
and Hyndman (1967).

In-phase values of the transverse-horizontal and vertical transfer
functions, projected into the direction of the profile and denoted by
$h_p(u)$ and $z_p(u)$ respectively, are shown in Fig. 1.3.  The out-of-phase
values (not shown) are very small.  This suggests that induction is in
a large deep-seated conductor for which self-induction is more impor-
tant than resistive induction, rather than in a conductive near-surface
layer which might include sediments (Schmucker, 1970a, section 6.2).
Geology shows that the Laramide Rockies (Basin and Range Province) in
the western region defined by low Z amplitudes have been the site of
continuous igneous activity from Cretaceous time to the present,
while the Texas Foreland (Great Plains) in the eastern region has been
tectonically stable almost since the Precambrian.  It is therefore
reasonable to ascribe the anomaly to topographic relief on the surface
of a conductive region of the mantle, correlated with temperature.
In support, heat flow measurements, such as those of Warren et al.
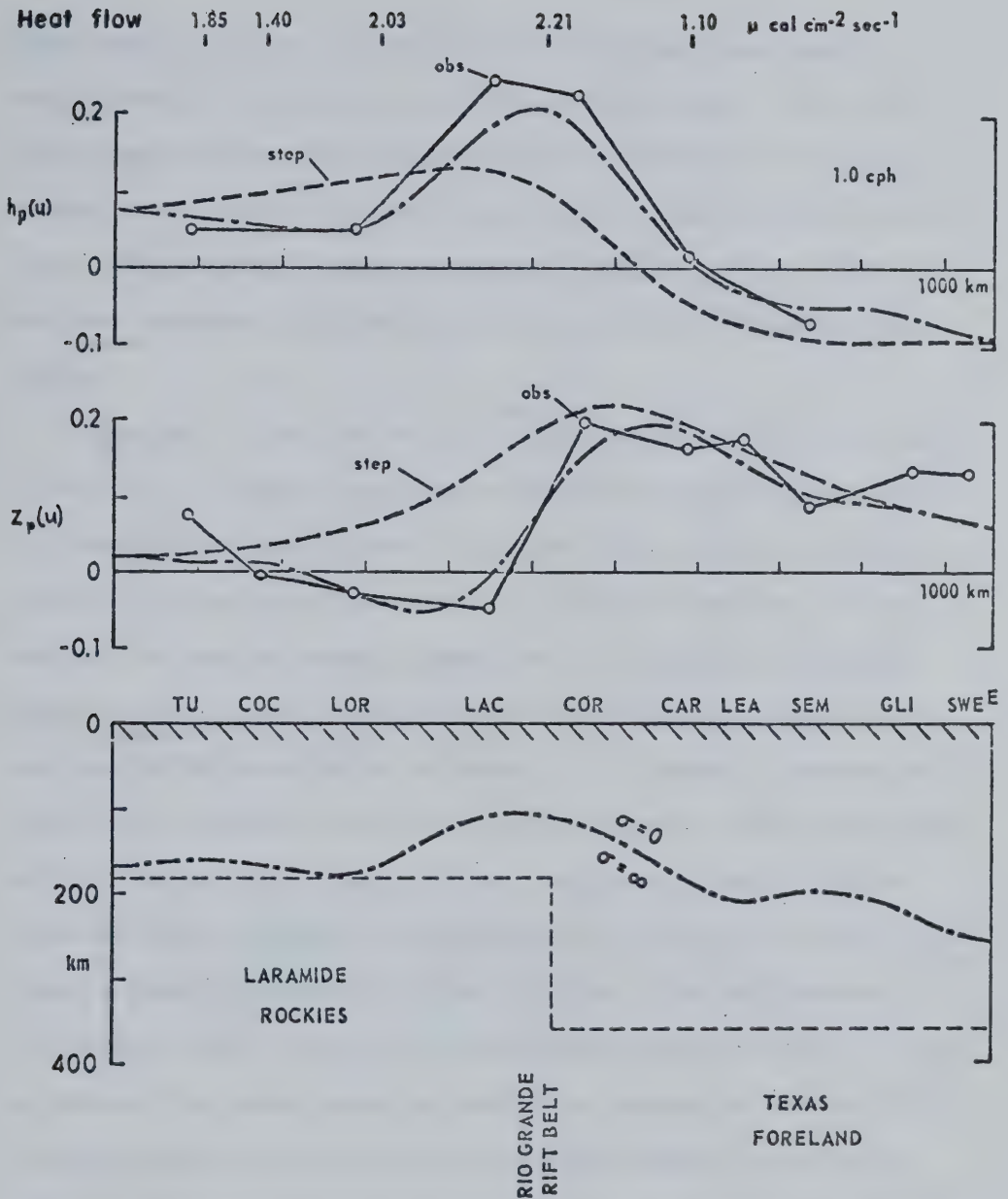
Fig. 1.3   Rio Grande anomaly for bays:  data, and interpretation by
           perfect substitute conductor at variable depth.  Circles
           joined by straight lines in the upper graphs are observed
           in-phase horizontal $h_p(u)$ and vertical $z_p(u)$ transfer functions.
           Theoretical curves are for the step model (equal-length
           dashes) and for the undulatory interface (long and short
           dashes) shown below.  From Schmucker (1970a).

(1969) shown in Figs. 1.2 and 1.3, indicate higher upper mantle temperatures in the Rockies than in the Texas Foreland. For this reason, and because the Z daily variation at stations on the profile is also affected by the internal conductivity structure (See Fig. 1.4; there is a systematic eastward increase in the Z/Y ratio), Schmucker has used conductive structures in the upper mantle to interpret his results.

Schmucker's first two models are given in Fig. 1.3, and the third in Fig. 1.2. A "perfect substitute conductor" of infinite conductivity is placed below a non-conductive crust and upper mantle at a depth such that its response, calculated by a conformal mapping technique, matches the observed transfer functions at a particular frequency; such a two-layer model substitutes for the integrated conductivity of that part of the earth which is sampled by an incident electromagnetic wave at that frequency. The depth to the conductor, 180 km under the Laramide Rockies with a step, aligned north-south, down to 360 km under the Texas Foreland, is consistent with the observed Z-amplitude relation between eastern and western stations. But the response of this initial model, given by the equal-length dashes in Fig. 1.3, does not predict the strong anomalous variations observed at LAC and COR. The second model, given by the short and long dashes in Fig. 1.3, brings the conductor closer to the surface in the centre of the profile and gives a satisfactory fit to the data. This model was derived by developing the difference between the observed and theoretical $z_p$ values in terms of three spatial harmonics with fundamental wave-length $2\pi/k_a$ set equal to the length of the profile. The difference
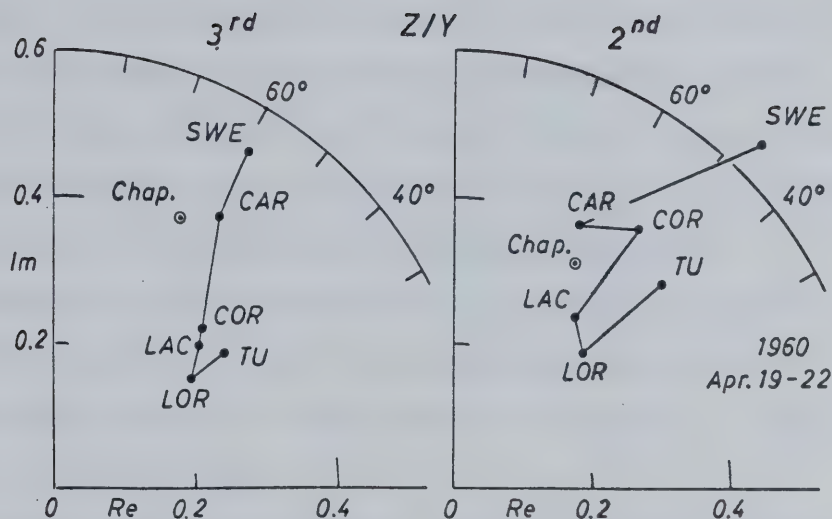
Fig. 1.4 Daily variation for the Rio Grande profile. Polar diagrams show the Z/Y ratio for the 2nd and 3rd harmonics of the daily variation averaged over four quiet days. Z leads in phase relative to Y. A systematic increase in Z from a minimum in New Mexico (LOR) towards Texas (SWE) results from an increase in the depth to the conductive mantle towards the east. "Chap." is a global average for Z/Y at this magnetic latitude. From Schmucker (1970a).

field was continued downwards with an assumed $\exp(nk_a z)$ depth dependence and superimposed on the field of the step model, to yield the shape of internal field lines at any subsurface point. Since the field line immediately above the interface between the perfect and the finite conductors used here must be tangential to the interface, the shape of the interface is thus defined. Schmucker (1970a) writes (p. 106) that this field line may be considered "to reflect the variable depth of penetration of bay-type disturbances along the profile".

Schmucker's (1969) third model for the Rio Grande anomaly is essentially a smoothed version of the second model; see Fig. 1.2. There is good correlation of high electrical conductivity at shallow depth with high heat flow.

The next profile in this region, marked by triangles in Fig. 1.1, was observed by Caner, Cannon and Livingstone (1967) to look for a northward continuation of the Rio Grande anomaly. The observatory at Norman, Oklahoma, 250 km to the east of SAY but not shown on the map, completed the profile. These authors classed the amplitudes of Z variations at these stations through the ratio

$$I = \frac{|\Delta Z|}{[(\Delta D)^2 + (\Delta H)^2]^{\frac{1}{2}}} \tag{1.7}$$

and also used the polar plots of Parkinson (1959, 1962) to check whether stations were normal or anomalous; a normal station shows no preferred azimuth in which horizontal variations can be correlated with Z variations. On this basis, all stations were classed as normal; all stations west of SAY were "low-I", while Norman was clearly "high-I" in the way that Z amplitudes at Schmucker's stations CAR and SWE

were clearly higher (two or three times greater) than those at TU. I
at SAY was intermediate. From this, Caner et al. (1967) located a
transition at or east of SAY, implying that the Rio Grande anomaly
swings 500 km eastward from the mountains into the Great Plains. Work
in 1968 with an array of magnetometers led Porath and Gough (1971) to
conclude that concentration of current in the deep conductive sediment
of the Anadarko Basin was in fact responsible for this low-I to high-I
transition; array work in 1967 (Reitzel et al., 1970; Porath et al.,
1970) suggested that the Rio Grande anomaly turns to the northwest, to
follow the contact between the Basin and Range Province and the
Colorado Plateau.

The last profile in this region was that of Gough and Reitzel
(1969), which was operated in a field-test of a new variometer design
(Gough and Reitzel, 1967). Stations are the numbered dots in Fig. 1.1,
and were located knowing that the IGY stations LEA and BUR were respec-
tively low-Z and high-Z, but before the publication of Caner et al.
(1967). A transition station was found at SAL, about 100 km west to
the Front Range of the Southern Rockies. Gough and Reitzel had expec-
ted that the transition between LEA and BUR would be the northward
extension of the Rio Grande anomaly. However, the 1967 array of
Reitzel et al. (1970) and Porath et al. (1970) showed, as mentioned
above, that this was not the extended Rio Grande feature, but was
caused by a separate upper-mantle structure beneath the Southern
Rockies between the Great Plains and the Colorado Plateau.

During and after Schmucker's pioneering work in the southwestern
United States, Hyndman and then Caner and his colleagues established

a series of profiles of geomagnetic recording stations in southwestern
Canada, in British Columbia and Alberta. The map in Fig. 1.5 shows
the locations; stations are coded according to their I-value (defined
in equation 1.7). Profile A is the original line of Hyndman (1963)
from WES on the Pacific coast near Vancouver across the Cordillera
to Lethbridge (LET) in the Great Plains. Lambert and Caner (1965)
subsequently extended this profile to TOF on the west coast of Vancouver
Island in a study of the coast effect. Profile B, from CAC across
the Cordillera to Calgary (CAL) has been described by Caner, Cannon
and Livingstone (1967). This line was reoccupied at greater station
spacing and extended eastward as part of the 1969 array considered
in this thesis. The remaining Cordilleran profiles C and D and the
coast-effect profile E are the work of Caner, Auld, Dragert and
Camfield (1971). The area in the dashed rectangle in the Kootenay
Lake region of B.C. was covered in great detail (20 stations) by
Lajoie and Caner (1970) in a second-order survey.

The principal feature of the transition from the Cordillera to
the Great Plains, observed on the east-west profiles, is a general
notable decrease in normal Z amplitudes at stations in the Cordillera,
relative to those in the Plains. Recall that Schmucker reported a
similar result for stations near Tucson, relative to those in the Texas
Foreland. This attenuation can be clearly seen in the magnetograms
of Fig. 1.6, taken for pairs of stations on profiles A, B and D.
Each station in the pair is far from the transition zone between the
regions.

Caner's (1971) calculation of power-spectral ratios for Z at
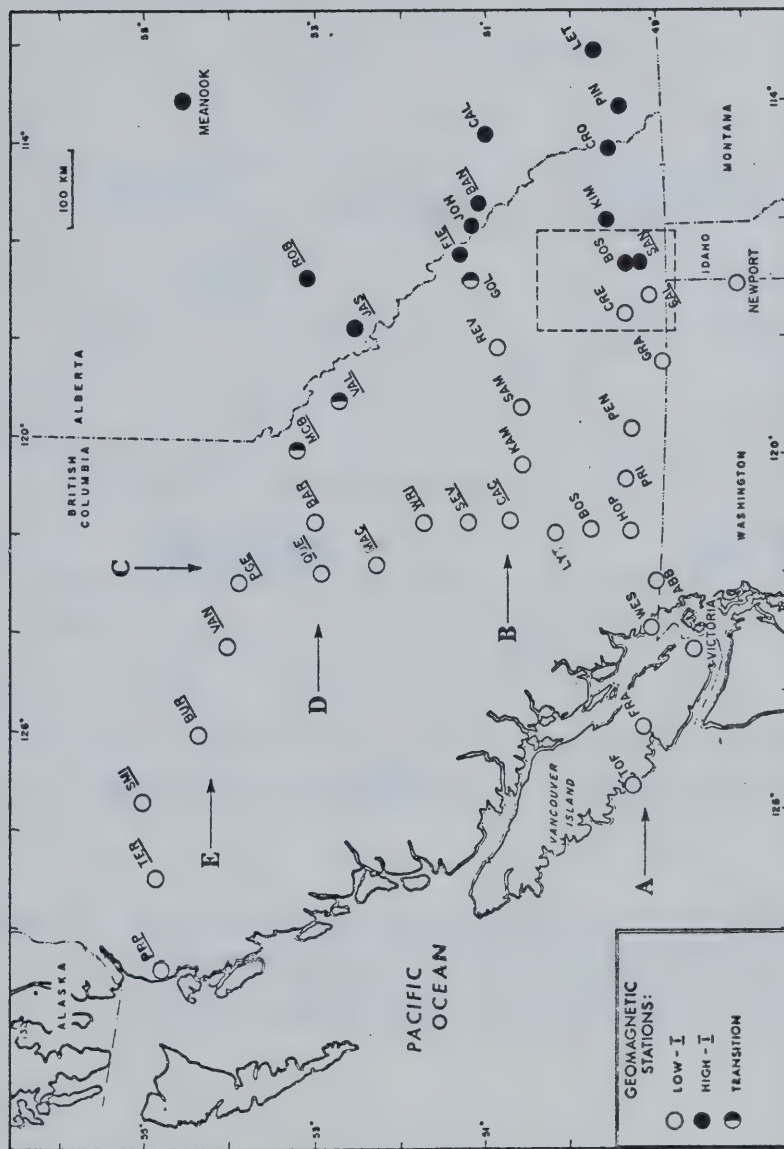
Fig. 1.5 Geomagnetic recording stations in western Canada, including those of Hyndman and of Caner and his colleagues. Stations in the Great Plains and foothills are high-Z, while those in the Cordillera west of the Rocky Mountain trench are low-Z. From Caner et al., 1971.
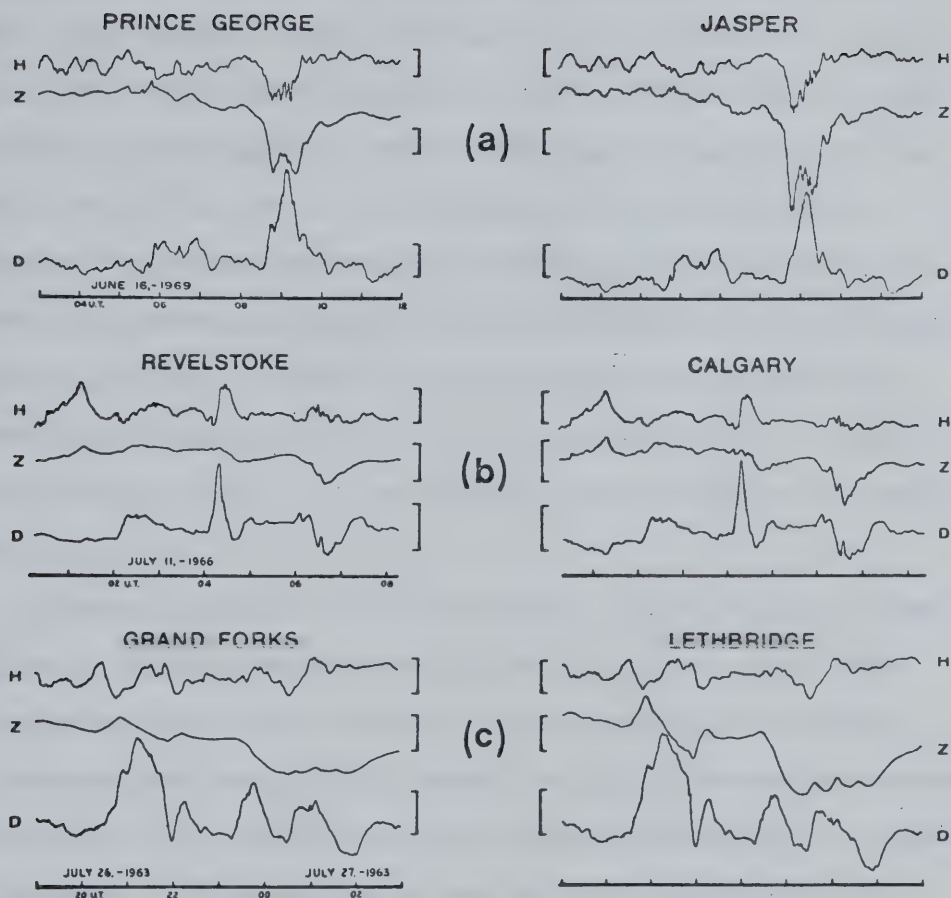
Fig. 1.6 Magnetograms for pairs of stations at (a) 53°N (profile D); (b) 51°N (profile C); and (c) 49.5°N (profile A). Scale bars are 50 gammas; time marks are at 1 h intervals. Suppression of Z at western stations (left) is easily seen. From Caner et al. (1971).

stations east and west suggests that the attenuation is greatest at
the shortest periods measured (about 20 min) and is not important
above about 120 min. Unlike Schmucker's data for the daily variation
(Fig. 1.4), Caner's (1971) records at stations PEN and PIN on profile
A (Fig. 1.5) show that the Z daily variation has essentially the same
amplitude on both sides of the Cordillera. This would indicate a
fundamental difference between the subterranean conductivity structure
beneath the southwestern United States and beneath southwestern Canada.
The conductor which attenuates short-period variations west of the
Cordillera in Canada must be too thin and shallow or have an integrated
conductivity too small to affect the much longer periods of the daily
variation.

Anomalous fields in this area are small; Parkinson plots by Caner
apparently show no confinement of the variation vector which might
be correlated with gross geological structure striking north-south
to northwest-southeast. Caner assumed that fields measured at locations
distant from the transition zone were in fact normal fields, and chose
to interpret his observations in terms of the frequency-dependent
normal-field ratio Z/H above a layered conductivity structure. The
calculation of the response of such a structure requires direct
knowledge of the wavelength $\lambda$ of the inducing field, a quantity which
can hardly be estimated with a short linear profile. For this reason,
when dealing with data for a given external source measured simulta-
neously at an eastern and a western station, Caner worked with a
parameter

$$M = \frac{(Z/H) \text{ west}}{(Z/H) \text{ east}} \tag{1.8}$$

where each of these four quantities is an auto-power spectral estimate. M depends less strongly on $\lambda$ than the Z/H ratio itself, but is not independent of $\lambda$.

The conductivity models of Caner (1971) based on station PIN for the foothills of the Northern Rockies (southwestern Alberta) and on PEN for the Cordillera (western region) are sketched in Fig. 1.7. A thin, highly-conductive layer is placed in the lower crust beneath the Cordillera to attenuate the short-period vertical-field variations. High conductivity in the lower crust is explained on the basis of hydration (Hyndman and Hyndman, 1968); water required to raise the conductivity is assumed to originate from adsorbed oceanic crust and trench systems (Caner, 1970). With the addition of water, partial melting towards the base of the crust is also possible, with an associated increase in electrical conductivity, since the temperature at which partial melting commences in rocks is depressed by the presence of water (Lebedev and Khitarov, 1964, for granite) to temperatures appropriate for these depths under this region of (assumed) relatively high heat flow (Roy et al., 1972).

To fit the shallow layer to his data, in the period range 0.5 to 24 h, required a very short source wavelength (600–1000 km) which Caner kept independent of period. Porath (1971b) has criticized the use of this very short scale length, pointing out that Swift (1967) and Oldenburg (1969) report magnetic disturbance fields with dimensions of at least several thousand kilometers. Cochrane and Hyndman (1970) suggest that 5000 km is an appropriate value in this region. Results to be presented in Chapter 5 of this thesis support this suggestion.
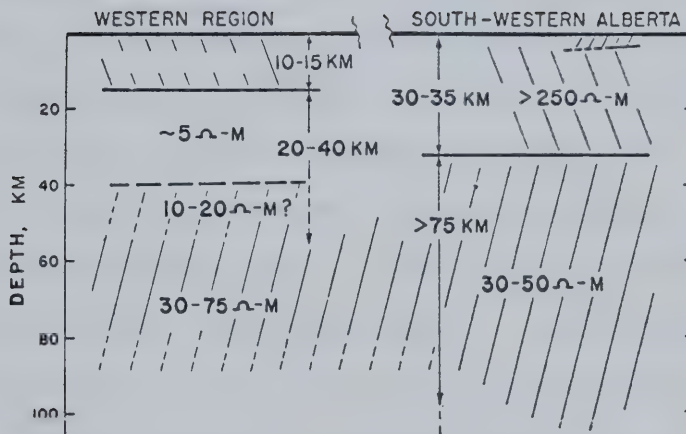
Fig. 1.7 Caner's (1971) models of conductive structure for southwestern Alberta and south central British Columbia, based on data from both geomagnetic depth sounding and magnetotellurics.

The conductivity models from Caner's geomagnetic depth sounding are supported to a certain extent by his magnetotelluric observations (Caner et al., 1969) at PEN and GRA (western); and at a third location between KIM and CRO, and PIN (eastern); see the map of Fig. 1.5. Magnetotelluric interpretation at longer periods is less sensitive than depth sounding to the choice of spatial wavelength (Madden and Nelson, 1964); on the other hand, magnetotelluric data at longer periods are more difficult to measure accurately and are more likely affected by distant lateral inhomogeneities (Wright, 1970). There is sufficient scatter in the apparent resistivity curves that, although the conductivity models of Fig. 1.7 will fit them, other configurations are certainly possible. Among these would be a smooth decrease in apparent resistivity toward longer periods for the western stations, and almost constant resistivities over the observed period range for the eastern stations (Porath, 1971b).

Cochrane and Hyndman (1970) have reinterpreted the data for profile A of Fig. 1.5. Transfer functions calculated for three pairs of stations were used to obtain normal vertical fields $Z_o$ from measured fields D, H and Z, by correcting for the anomalous fields with a rearrangement of equation 1.2:

$$Z_o = Z - z(D) \ D_o - z(H) \ H_o - z(Z) \ Z_o \tag{1.9}$$

Further assumptions require negligible induction by the normal vertical field, so that the last term of equation 1.9 can be dropped, and small or negligible anomalies in the horizontal fields, so that $D_o$ and $H_o$ could be approximated by D and H.

$$Z_o \doteq Z - z(D)\ D - z(H)\ H \qquad\qquad (1.10)$$

Corrected $Z_o$ data and measured horizontal data for stations removed
from the transition zone (GRA, west; LET, east) were used to form M
ratios over the period range 10 min to 4 h; these were then interpreted
with models of horizontally-stratified structure. The resulting
models, fitted with a source wavelength 5000 km as mentioned above,
do not differ appreciably from Caner's for PEN/PIN, although the
resistivities of both the conducting layer and the base on which it
rests are somewhat higher than Caner's (10 $\Omega$m as opposed to 5 $\Omega$m,
and 100–200 $\Omega$m vs 30–75 $\Omega$m). These higher values may arise because
Cochrane and Hyndman included in their models a highly-conductive 1 $\Omega$m
mantle of infinite extent beginning at depth 300 km under the western
region and 400 km under the eastern; this is plausible, but the
absence of daily-variation signals from their data allows no direct
confirmation. Caner, even with daily-variation data, did not feel
confident in assigning such depths to the ultimate conductor, but
simply reported no increase in conductivity down to 100 km.

Turning now to studies with two-dimensional arrays of variometers,
Fig. 1.8 shows the location of joint operations of the University of
Alberta and the University of Texas at Dallas in the summers of
1967-69. The instruments deployed were expecially designed for such
work by Gough and Reitzel (1967). Papers by Reitzel et al. (1970),
Porath et al. (1970) and Porath and Gough (1971) describe and interpret
the results of the 1967 array in Utah, Colorado and adjacent states.
Porath and Gough (1971) also report on the 1968 array which continued
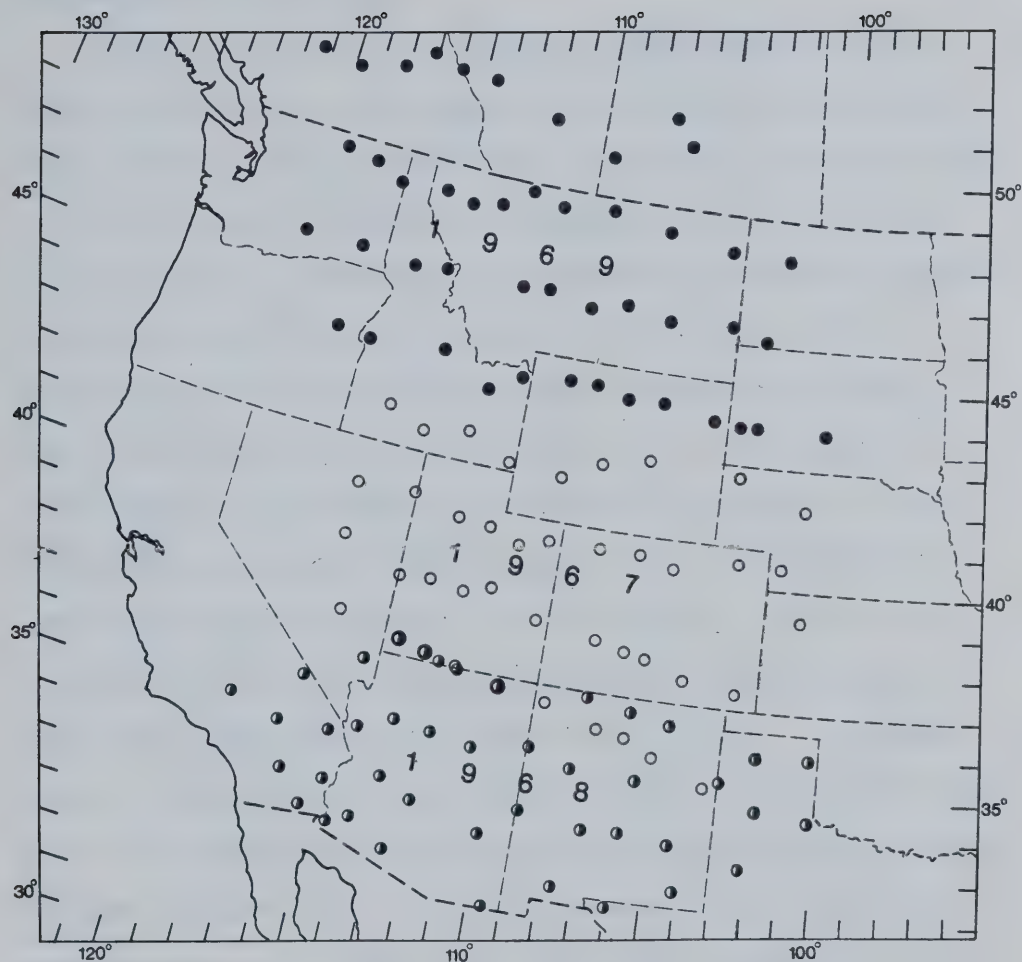
Fig. 1.8 Location of joint magnetometer array studies in western North
America by the University of Alberta and the University of
Texas at Dallas.  Open circles, 1967 field season; half-filled
circles, 1968; filled circles, 1969 - this thesis.

coverage southward to the U.S.–Mexico border. The 1969 array is the subject of this thesis; publications include Camfield et al. (1971), Porath et al. (1971), Camfield and Gough (1972) and Gough and Camfield (1972a, 1972b).

Reitzel, Gough, Porath and Anderson (1970) present the 1967 results in three ways: magnetograms for simultaneous disturbances along profiles, as did previous workers (see Figs. 1.2 and 1.6); plots of Fourier spectral components vs. frequency, from the transforms of the time series representing the magnetograms, at several stations; and contour maps of Fourier components over the entire array at given periods. An example of the contour presentation is shown in Fig. 1.9 at period 30 min from the analysis of a single substorm on 1 September 1967 (0500–0830 UT). This period corresponds to a peak in the amplitude spectra; Reitzel et al. (1970) also include maps at other periods similarly chosen: 45, 60 and 89 min. In Fig. 1.9, the contours of the Z amplitude map show two north–south ridges of high values separated by a flat valley of low values. In a similar way, the Y amplitude map has two ridges which are west of the Z maxima, at locations consistent with north–south internal line-current sources for both anomalies. The X amplitude map is relatively featureless over the array, to be expected where the Y and Z maps show that the major structures strike north–south.

The phase maps for X and Y show a smooth variation across the array, with a lag to the west connected with the westward surge of the auroral-zone source currents (Rostoker et al., 1970). The Z phase map is dominated by two local anomalies, found at stations where
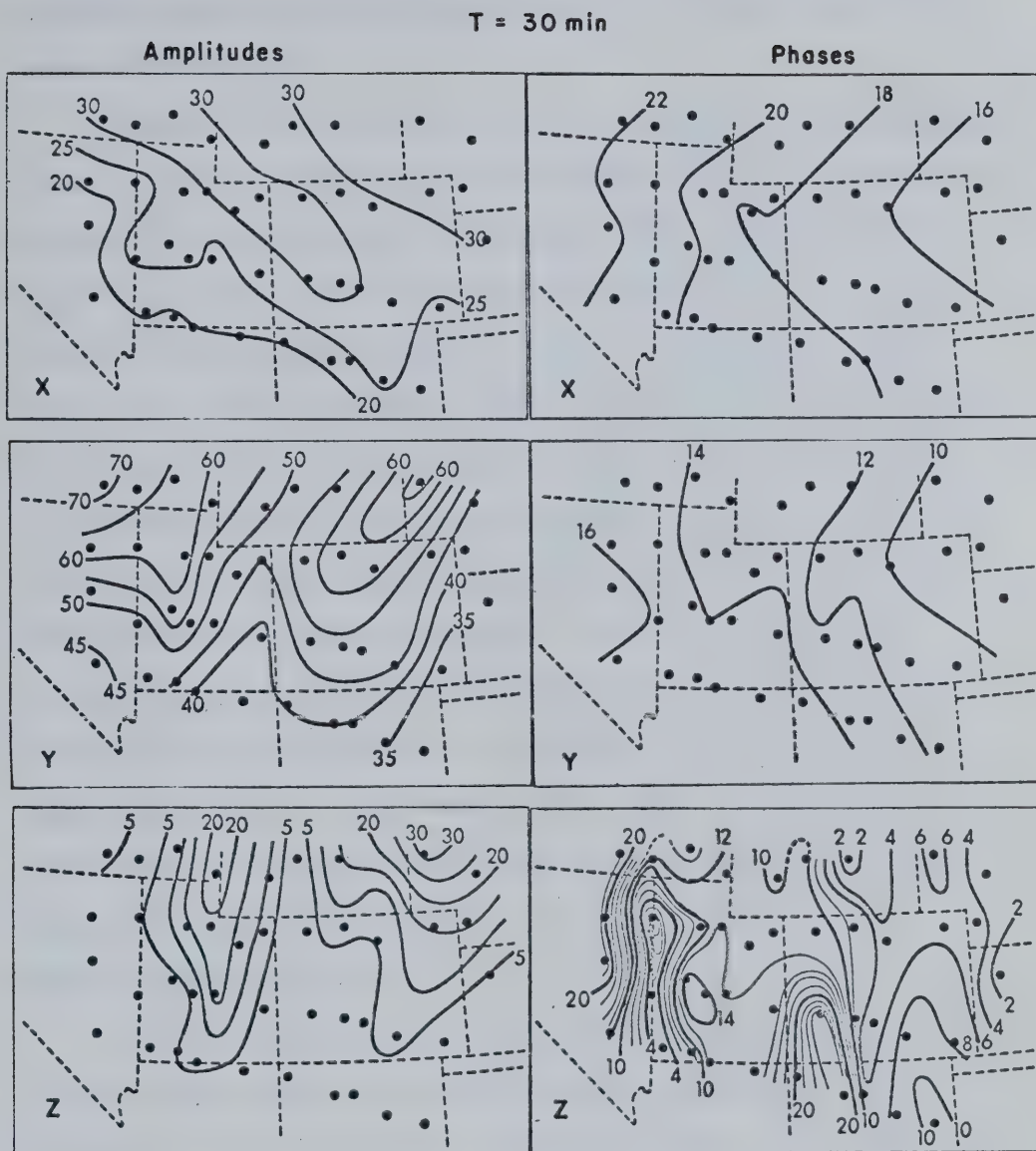
Fig. 1.9   Contour maps of Fourier amplitudes (in 0.1 gammas, with contour
interval 0.5 gammas) and phases (in minutes of time, with
interval 2 min) at period 30 min for the substorm of 1 September
1967 recorded in the western United States.   From Reitzel et al.
(1970).

the magnetograms show phase reversals due to anomalous Z from internal currents induced by Y.

In physiographic and geologic terms, the western anomaly indicates internal currents flowing at the Wasatch Front fault zone, between the Colorado Plateau and the Basin and Range Province. Suppression of Z amplitudes at the extreme western stations, easily seen in the magnetograms of Reitzel et al. (1970), is similar to Schmucker's observations (Fig. 1.2) for Tucson-type stations further south, and indicates in both cases a rise in the conductive mantle beneath the Basin and Range Province caused by increased temperature at smaller depth. The eastern anomaly is over the Southern Rockies, which lie between the Great Plains and the Colorado Plateau. The observed weakening of the western Z phase anomaly with increasing period, relative to the eastern one, and the asymmetry of the western amplitude anomaly, are taken to mean that the upward step in the surface of the conducting mantle from the Colorado Plateau to the Basin and Range Province, at the Wasatch Front, is not nearly as tall as the step up to the Southern Rockies conductor.

At the northeastern limit of the 1967 array, in Nebraska, an apparent strengthening of the Southern Rockies anomaly in Y and Z is suggested by the data in Fig. 1.9 (period 30 min). It is far more evident in the maps at 89 min, which are not given here. Reitzel et al. (1970) recognize that this feature may be due to local high conductivity related to the Black Hills thermal zone of South Dakota immediately to the north. Mapping in the Black Hills region, to follow up this indication, forms a major part of this thesis.

Phase relationships in the substorm fields and the Z amplitude of the geomagnetic daily variation confirm that anomalous currents at the Wasatch Front and the Southern Rockies are induced in mantle conductive structures, not in conductive near-surface sediments. The contour map in Fig. 1.10 of the range in the vertical component on a quiet day ($\Sigma Kp = 9+$) shows increases at the eastern front of the Southern Rockies and at the Wasatch Front. Sedimentary conductors would be essentially transparent to the 24, 12 and 8 h harmonics of the daily variation, so the topography on the map must be due to induction in structures which extend to great depth. These are undoubtably the same as the conductive inhomogeneities which cause the anomalies in the substorm fields.

One of the original goals of the array operation was knowledge of the variation fields in two dimensions, so that a formal separation of the fields into parts of internal and external origin could be carried out using surface-integral methods. Porath, Oldenburg and Gough (1970) applied this procedure to the substorm data of Reitzel et al. (1970), using formulae derived by Hartmann (1963) and Weaver (1964). Initial contouring of the horizontal fields by linear interpolation between stations was adjusted to satisfy the curl-free condition ($\partial X/\partial y = \partial Y/\partial x$) which arises from the requirement that $\nabla \times \vec{H} = 0$ on the earth's surface. The same condition was used in extrapolating the fields beyond the array, to allow an attempt at separation for points near the edge of the array. Separations were executed in both the time and frequency (or period) domains, the former to reveal instantaneous configurations of internal currents, and the latter to
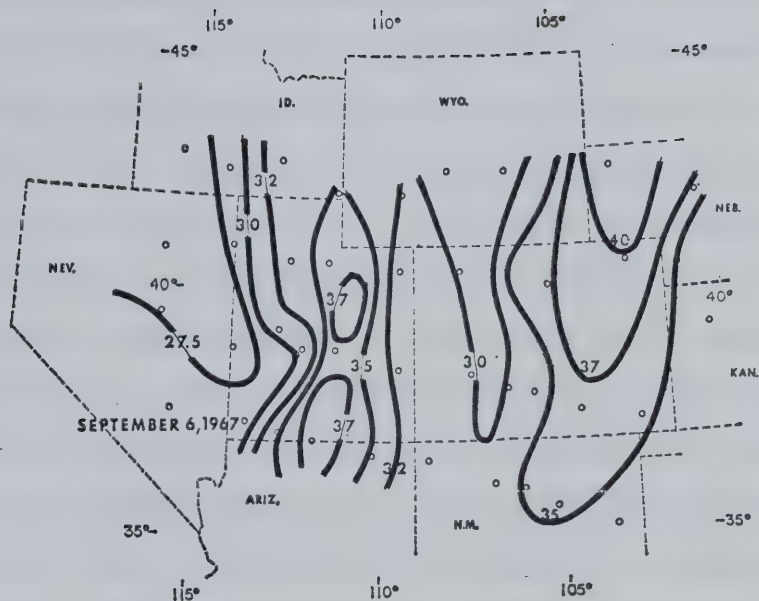
Fig. 1.10   Contour map of vertical component ranges, in gammas, for the
daily variation on 6 September 1967.   The Southern Rockies
and Wasatch Front anomalies are evident in the daily variation
as well as in the substorm fields.   From Reitzel et al. (1970).

obtain an average over the whole event for given periods.

Porath et al. (1970) confirmed that features in the measured field
with spatial wavelengths short relative to the size of the array are
separated into the internal part, as expected in these mid-latitudes
where rather uniform source fields should exist. They also found that
the internal part contained an inseparable fraction β of the normal
fields which have spatial wavelengths greater than the size of the
array, while the external part included the complementary fraction 1-β.
This follows from the definition of the normal field. To estimate the
normal field, for use in isolating and normalizing the anomalous fields,
required a series of steps following the separations. First, approxi-
mations to the normal horizontal fields were obtained by fitting planes
to the curl-free observed data by least squares; anomalous horizontal
fields were then computed by subtracting the normal fields from the
observed fields. Then the anomalous vertical component was calculated
from an expression involving the difference between the (separated)
vertical internal and external parts plus derivatives of the normal
horizontal fields. Also involved was an assumption that β = 0.5,
which follows from the separation equations upon recognizing that the
external part of Z is relatively uniform over the array. Normal Z
follows from the difference between observed and anomalous fields.

Depths to conductive structures were estimated from the in-phase
normalized anomalous fields over the period range 30-90 min. The
depth to a line current in the earth is given by the half-width of the
transverse horizontal field, i.e. the distance between the peak value
and either half-peak value, or by half the separation between the

positive and negative peaks in the vertical component. On this basis, the average maximum depth to the top of the conductive structure beneath the Southern Rockies is 190 km, while the figure for the Wasatch Front is about 115 km. If the anomalies are modelled instead by long isolated conducting cylinders in a less-conductive medium, estimates involving the same distances yield maximum depths to the centre of possible cylinders: 390 km under the Southern Rockies and 250 km under the Wasatch Front. All these values increase somewhat with period, reflecting the increased penetration with longer period; the range of values is however small, implying that the material in which the currents flow is highly conductive.

Two-dimensional models are appropriate for these linear anomalies. Trial values for two semi-circular upwellings on the surface of a perfectly-conducting mantle come from the depth estimates above; in addition, a step in the surface is necessary to bring it to shallower depths beneath the Basin and Range Province, as implied by the asymmetry of the Wasatch Front anomaly and the suppressed normal Z amplitudes of westernmost stations. The response of such a model was computed by conformal mapping (Schmucker, 1964). An appropriate function $w(z) = u + iv$, where $z = x + iy$, maps the surface $y = 0$ of a half space into the model structure; the function is used to compute equipotentials ($x$ = constant) and field lines ( $y$ = constant) above the conductor. Theoretical anomalous fields to compare with profiles of observed values are derived from gradients of the potential.

The correspondence (Reitzel et al., 1970) between the location of the conductivity anomalies and regions of high heat flow (Roy et al.,

1972) is excellent, supporting the premise that the upwellings are associated with long-lived upheavals of the mantle isotherms (Gough and Porath, 1970).

Porath and Gough (1971) report from the 1968 array that the conductive structures discovered in 1967 continue southward, and that "the Basin and Range Province as a whole overlies a highly conducting (and, by inference, hot) region in the mantle." From this work it follows that Schmucker's Rio Grande anomaly, at the transition between the Basin and Range Province and the Great Plains, must turn northwest to merge with the Wasatch Front anomaly. Porath and Gough (1971) have also re-examined the problem of determining normal fields, concluding that the method of Porath et al. (1970), involving planes fitted by least squares and the separations as described above, resulted in phase differences of 30-35° between the anomalous fields and the normal Y field, whereas the magnetograms of Reitzel et al. (1970) would not support differences greater than 15°. They have rederived the normal fields using the condition of small phase differences and further assumptions that the Southern Rockies anomaly in Z arises only from currents flowing beneath the Rockies, and that normal Z is constant across the array. Their profiles of normalized anomalous fields at 38.5°N are shown in Fig. 1.11; these are quite similar to the profiles of Porath et al. (1970) except near the ends, where the errors in a separation would be most troublesome.

The response of the model sketched in Fig. 1.11 was computed using Madden and Swift's (1969) transmission-surface analogy for solving Maxwell's equations in a two-dimensional structure with a uniform
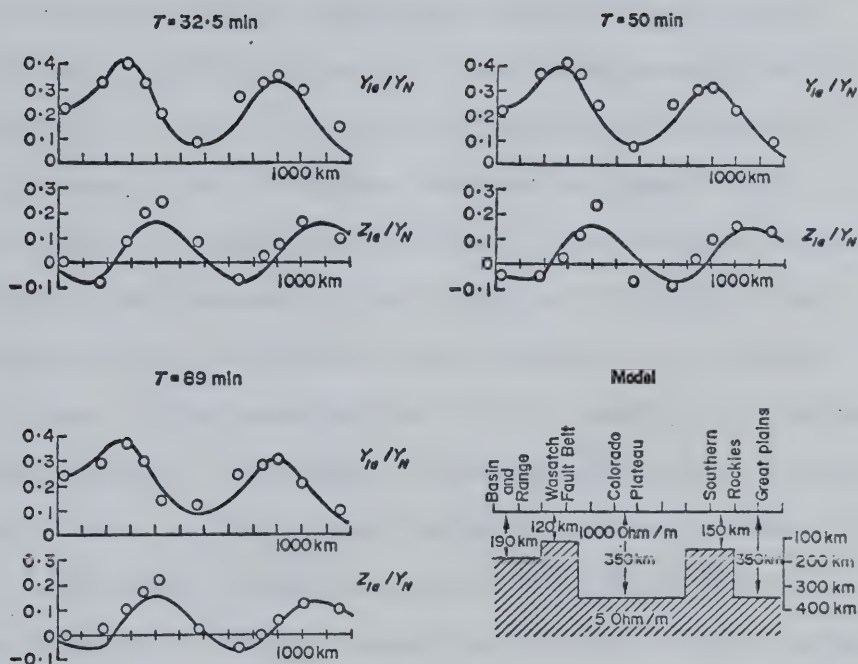
Fig. 1.11 Observed normalized anomalous fields (circles), and calculated fields (solid curves) for the model of conductive structure shown, along a profile at 38.5°N. The subscript ia denotes an internal anomalous field; the subscript N is for a regional, normal field. Circles indicate variometer stations closest to the profile. From Porath and Gough (1971).

transverse horizontal inducing field. Wright's (1969) computer formu-
lation was employed. Shallow (crustal) structures of realistic
conductivity did not fit the data, since they have phase differences
of 35° or more and anomalous fields whose amplitudes vary conside-
rably more with period than those observed. The upper-mantle model,
with ridges and a step on a half-space of resistivity 5 $\Omega$m below a
1000 $\Omega$m top layer, fits the observed anomalous horizontal fields
reasonably well. It predicts vertical fields less than those observed,
likely because this component is more sensitive to details of the
structure than are the horizontal fields. Depths to the conductor
are as follows: 350 km under the Great Plains, jumping to 150 km under
the Southern Rockies, 350 km under the Colorado Plateau, 120 km under
the Wasatch Front, and 190 km under the Basin and Range Province. The
numbers for the Basin and Range and for the Great Plains are similar
to those of Schmucker (1970a) obtained further south. The resolution
of the data would permit the conductor under the Colorado Plateau
to be placed at a somewhat shallower depth, but the structure there
is certainly closer to that under the Great Plains than to that
beneath the Basin and Range Province.

Another interpretation of these fields by Porath (1971a) places
the conductor at shallower depths, coincident with the seismic
low-velocity zone delineated in this region by Archambeau et al.
(1969) and others. The justification for this is based on the premise
that both the low seismic velocity and the high electrical conductivity
result from partial melting of the rocks at these depths. (The upper-
mantle conductor of Porath and Gough (1971) would arise from semi-

conduction processes at the appropriate higher temperatures.) In his model, Porath (1971a) has a 30 km-thick layer of 2 $\Omega$m with its top at depth 160 km under the Great Plains. Under the entire profile, the basement consists of 100 $\Omega$m from 190 km to 400 km, and 10 $\Omega$m below that. The surface layer is 1000 $\Omega$m, as in the model of Porath and Gough (1971). Depths to the 2 $\Omega$m conductor then are 160 km under the Great Plains, tapering to 45 km under the Southern Rockies, 80 km under the Colorado Plateau, 27 km under the Wasatch Front, and 45 km under the Basin and Range. Note that in this case the depth under the Colorado Plateau is intermediate between the values for the Great Plains and the Basin and Range. This model fits the data just as well as that of Porath and Gough (1971) for substorm periods, although its response to the daily variation fields has apparently not been tested. This exercise serves to demonstrate just how non-unique is the indirect inversion process.

Smaller arrays operated by Porath and Dziewonski (1971) in the Great Plains have mapped variation anomalies associated with crustal structures, such as the Anadarko Basin (thick conductive sediments) and the Ouachita tectonic belt (boundary between the Paleozoic sediments in West Texas and the younger sediments of the Gulf Coast). A small anomaly near the mid-continent gravity high in the U.S. is apparently caused by "currents in the sedimentary troughs on the steep flanks of the Precambrian basalts which give rise to the gravity anomaly."

CHAPTER II

DATA ACQUISITION

## 2.1 The Array

During the summer of 1969, the geomagnetic deep sounding
groups at the University of Alberta and at the University of
Texas at Dallas operated jointly a two-dimensional array of 43
geomagnetic variometers in southwestern Canada and the northwestern
United States. With three additional magnetometers operated by
other groups (named in Section 2.2), a total of 46 instruments
was deployed along four east-west lines between latitudes 44° and
51°N and longitudes 100° and 121°W. The two northern lines (21
variometers) were installed and serviced by the Alberta group,
while the two southern lines (22 variometers) were the responsibility
of our colleagues from Texas.

The array was placed to search for possible northward
continuation of the Wasatch Front and Southern Rockies anomalies
in geomagnetic variations which had been defined in the 1967 field
season (Reitzel et al., 1970; Porath et al., 1970), and to
determine the connection, if any, between them and the feature
mapped in southern Alberta and British Columbia by Hyndman (1963)
and by Caner and his colleagues (Caner and Cannon, 1965; Caner et al.,
1967; Caner et al., 1969; Caner, 1970, 1971; Caner et al., 1971).

The station arrangement for the array is shown in Fig. 2.1
superposed on a map of the large-scale tectonic features of the
region. Geographic and corrected geomagnetic coordinates for the
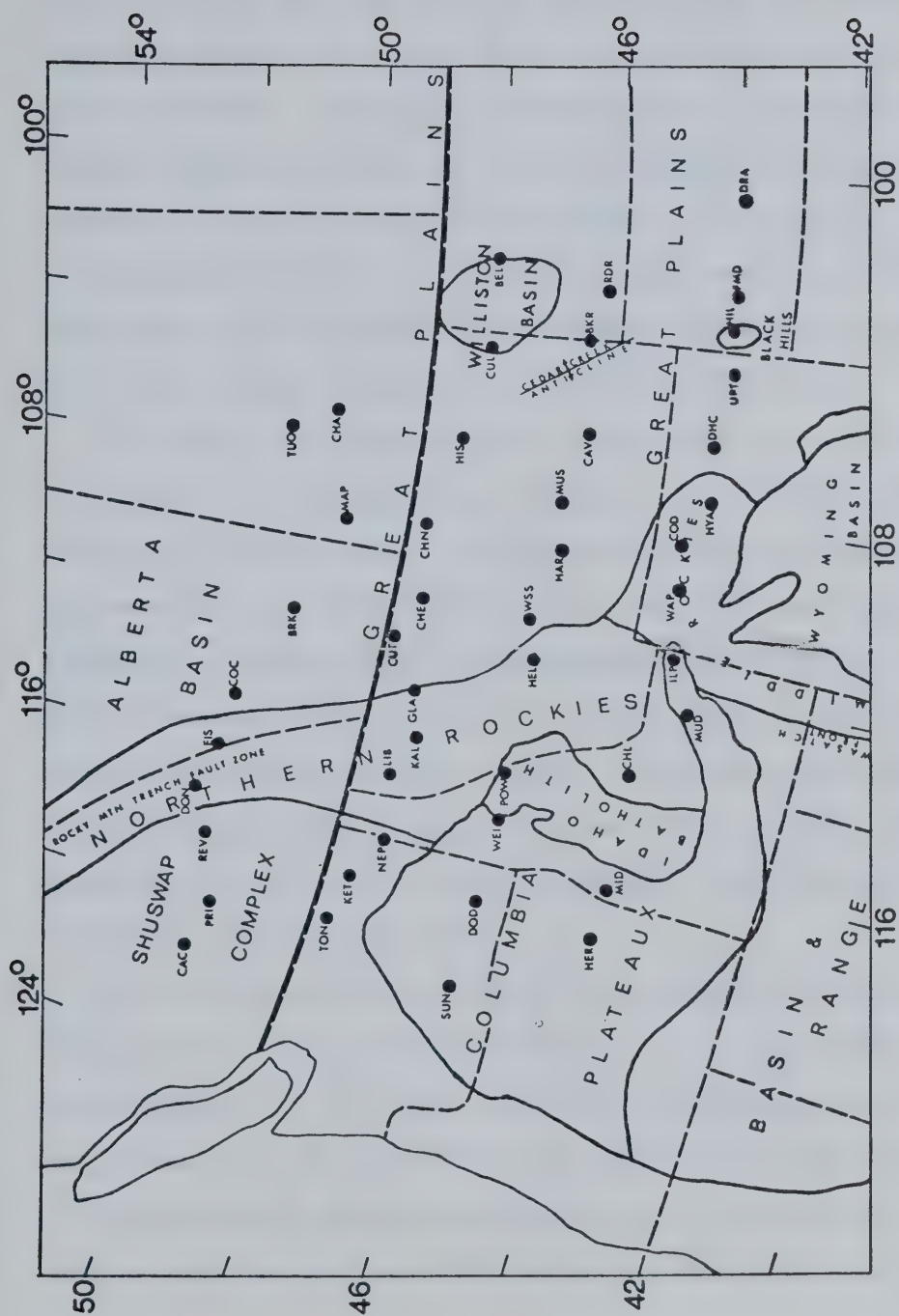
Fig. 2.1 Variometer array of 1969 on a simplified tectonic map of southwestern Canada and the northwestern United States.

stations are given in the Appendix . The north-south interval
between lines is about 250 km, while along each line the spacing
between stations varies between 50 and 190 km, although typically
120 km or greater. The smaller spacings were used near the boundaries
between tectonic provinces, where maximum anomalous fields were
expected. A station in the 1967 array (CRW of Reitzel et al., 1970)
in northwestern Nebraska had registered enhanced variation fields
just south of the Black Hills of South Dakota; the 1969 array was
therefore stretched eastward to cover the Black Hills uplift.

The station arrangement is shown again in Fig. 2.2, this time
on a grid of corrected geomagnetic coordinates interpolated from
the tables of Hakura (1965). It would perhaps have been desirable
to locate the lines of variometers along parallels of corrected
geomagnetic latitude, rather than along geographic parallels, so
that the external fields of substorms recorded along any one line
would be less-strongly varying. However, the contour maps adopted
for presenting the data from the array make this unnecessary, and
so instruments were located along the geographic east-west road
network for convenience of access.

After the installation of Alberta's 21 variometers had been
completed under the supervision of Prof. D.I. Gough, the author
was responsible for the initial switch-on, for three-quarters of
the routine servicing and for the final pull-out of the instruments.
At the beginning of the recording program, all the variometers
were in operation by 17 July 1969, and at the end of the program
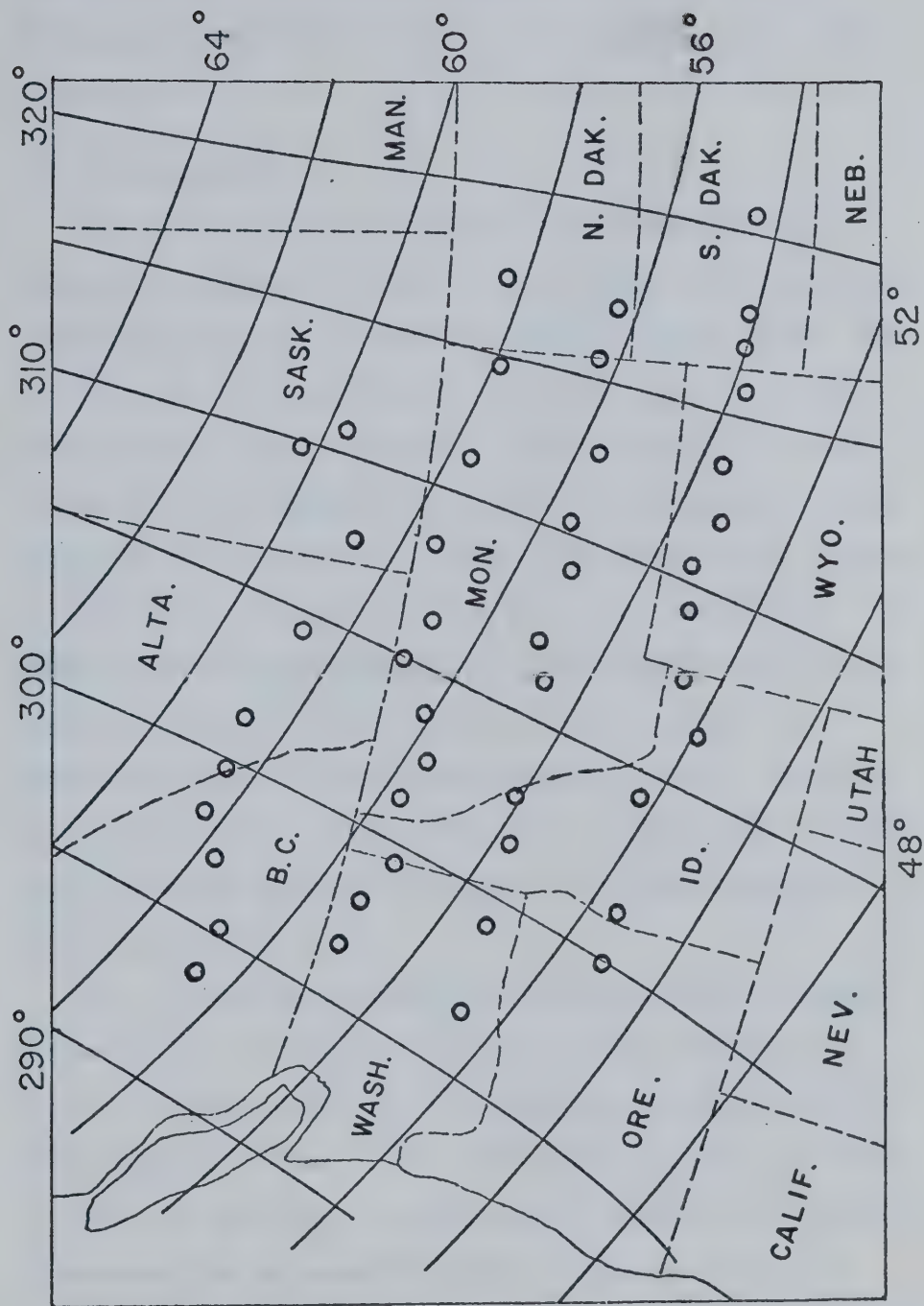
Fig. 2.2  1969 array on grid of corrected geomagnetic coordinates of Hakura (1965).

the first to be shut down was removed on 30 August 1969. The
Texas group's half of the array ran for a slightly longer period
of time.

## 2.2 The Variometer

The basis for all the joint array work by the University
of Alberta and the University of Texas at Dallas is an inexpensive
geomagnetic variometer designed by Gough and Reitzel (1967). The
instrument has as transducers the three classical small magnets,
hung on taut fine-wire suspensions, which rotate when the torque
on them due to the respective components of the geomagnetic field
changes as the field varies. A light beam reflected from a mirror
polished onto each magnet magnifies the angular deflections. The
reflected beam is then focussed onto 35 mm film to record the
magnet positions in terms of linear displacements from two
baselines provided by reflections from fixed mirrors. The pulsed
light source and the stepped rather than continuous film transport
result in traces formed on the film by an unbroken sequence of
discrete rectangular dots.

In a non-varying geomagnetic field, the D magnet is aligned
horizontally in the magnetic meridian, and hence there is no
torque on the magnet due to the horizontal field, nor any torsion
in the suspension fibre. The H and Z magnets, however, are held
in their zero positions (transverse to the relevant field component)
by counteracting the magnetic torques on them with torsion in
their suspension fibres. The torque depends directly on the magnet

moment, ie. on the intensity of magnetization of the magnet material, while the torsion involves the modulus of rigidity of the suspension wire. Both these parameters are temperature-dependent, although the rigidity much less so than the magnetization through the choice of a special alloy for the suspension wire. Thus to prevent zero drift in the H and Z records it is necessary to thermostat the instrument and/or apply temperature compensation.

Maintaining a constant temperature was most easily accomplished by encasing the instrument in a long aluminum tube which is buried vertically in the ground during a recording program. In the summer of 1969, the University of Alberta variometer was 50 cm shorter than the University of Texas' which had the dimensions of the original design by Gough and Reitzel (1967). For the short version in good thermal contact with non-frozen soil of average diffusivity ($5x10^{-3}$ $cm^2$/sec), a weekly variation in surface temperature of 30C° is predicted to be attenuated to 0.5C° at the depth of the H sensor (125 cm), and to 0.2C° at the Z sensor (25 cm deeper). For a daily temperature variation of the same amplitude, the corresponding numbers are $7x10^{-4}$ and $8x10^{-5}$ C°. Measurements by Carson (1963) in a sandy clay moraine soil near Chicago detected no daily temperature variation at the 100 cm level, supporting the prediction. Dawson and Fisher (1964) report similar results in a soil of unconsolidated pumice in New Zealand. Thus the variometer has good temperature stability from its method of installation. In addition, a first-order temperature compensation

effective to 3 or 4 $\gamma/C°$ is provided by auxiliary magnets made of the same material as the sensing magnets, which have been positioned to cancel, at some temperature, half the relevant component (H or Z) of the earth's main field at the sensing magnets. These two approaches combine to give excellent temperature stability.

The "brain" of the instrument is an electric watch (tuning-fork controlled, the Accutron made by Bulova) which initiates the observing cycle. A sampling interval of 10 sec is adequate for this work because aliasing is prevented by the steep fall (more than two orders of magnitude) in the average power density spectrum for geomagnetic fluctuations as the period decreases from about 30 to 12 sec (Herron, 1967). So, at intervals of 10 sec, a lamp is turned on for about 1 sec to record the magnet positions. A time-delay circuit then allows the lamp filament to cool before the film is advanced 0.2 mm by a solenoid and ratchet arrangement, ready for the next cycle. Film requirement is thus about 1.7 m/day. In 1969, the original cork-disc clutch in the camera's film takeup was replaced by a more reliable mechanical clutch which used slippage between spring-loaded gears.

The Accutron also provides contact closures at 1 h and 24 h intervals, which are used to mark time on the records by switching current through small coils near the suspended magnets to give them small deflections. In this application, the Accutron's rate of drift is adequate.

The instrument requires the equivalent of about 1.2 W of

continuous power.  One lead-acid automotive battery (6V, 135 A.h)
and one 6V "Hotshot" dry battery, buried beside the variometer,
will provide almost a month's operation at summer soil temperatures.

When the University of Alberta variometers were shortened
in 1968 from their original length, a rather strong interaction
between the H and Z magnets was discovered; it had not been
noticeable in the long instruments.  Typically, a real 100$\gamma$ change
in the Z field produced an apparent 2$\gamma$ change in H, while a 100$\gamma$
change in the H field gave a 4$\gamma$ change in Z.  The effect of H
on Z is twice the effect of Z on H because of a sensitivity-
doubling reflection in the Z optical path.  A correction for the
interaction is made to first order, in the initial stage of data
processing.

Data for three stations in the array came from magnetometers
operated by others.  Station TUO, of the University of Saskatchewan,
used a Hartmann-Braun analog chart recorder driven by an IGY
fluxgate magnetometer (Serson, 1957).  Only short-period (substorm)
data was available from TUO.  At station NEP, the USCGS Geophysical
Observatory Newport, the short-period equipment provided by the
Killam Earth Sciences group at the University of Alberta was
operated by the observatory staff.  Here, an updated fluxgate
magnetometer (Trigg et al., 1971) was coupled with a Leeds &
Northrup analog chart recorder.  Long-period data (daily variation)
for NEP was taken from the standard-run Ruska magnetograms.
Station COC, also of the Killam group, used the updated fluxgate
but recorded on digital magnetic tape via a system described by

Samson (1971). COC had short-period data in all components and
long-period in D and H; long-period Z was rejected because of
unacceptable drifts.

The author is grateful to the above groups for supplying
data. The appropriate names are given in the Acknowledgements.

2.3 Field Procedure

As mentioned in the previous section, the variometers are
installed in the ground at magnetically-quiet sites, in a hole
bored with a soil auger, for constant-temperature and undisturbed
operation. The instruments were initially oriented with a Brunton
compass to 1/4° or better, and were levelled to 0.1° or better,
to prevent variations in any one component from causing erroneous
readings in the others.

At periodic service visits (in 1969, at 12-day intervals),
in-situ calibration and time were recorded on the film by applying
a known field, from a coil carrying a measured current, to each
component in turn, at a time known from the WWV radio service.
The deflections of the traces due to known fields allowed the
displacement sensitivities or scale constants of the instruments
to be calculated, to better than 2%; on the 35 mm film, these are
about 14 $\gamma$/mm for D's, 10 $\gamma$/mm for H's, and 8 to 14 $\gamma$/mm for Z's.
Under a magnification of ten times, a resolution of the records
to better than 1 $\gamma$ can be expected. The absolute time marks allowed
the time of adjacent hour marks to be determined to better than 10
sec. Hour marks timed in this way at both ends of a 12-day record

yielded a rate of drift (assumed linear) for the Accutron watch; rates ranged from 1 to 10 sec/day for the 21 watches, although they were relatively constant for a given watch from one record to the next.

Loss of data due to problems with the variometers was small; the main cause of trouble was the Accutron watch, which in this application is not as reliable as the manufacturer would suggest. Even though the watch was shock-mounted in plastic foam, the mechanical "clunks" of the nearby solenoid in the film transport probably did not enhance its operation.

Installation, servicing and pull-out of the 21 University of Alberta variometers required about 22,000 miles of driving during the 2 1/2 month field project. Data acquisition cost, excluding capital costs and salaries, is estimated at $11,000 for the whole array. Data processing, including digitizing and model computations, probably totalled about twice this amount when estimated on the same basis.

CHAPTER III

THE SUBSTORM DATA

## 3.1 Introduction

Initial analysis of data obtained with the 1969 array was
concentrated on three disturbances which were recorded, with optimum
amplitude, by the equivalent of about 90% of the variometers. The
disturbances are sequences of polar magnetic substorms (see the
review by Rostoker, 1972), occurring a few hours before and after local
midnight, plus in one case some daytime storm-time activity during
which the planetary magnetic three-hour-range index Kp was between 4+
and 5o. These events constitute the short-period data, as opposed to
the long-period data of the daily variation to be considered in
Chapter IV. A description of the short-period events and a qualitative
interpretation of the induction effects seen in them has been given
by Camfield et al. (1971), while a more quantitative interpretation
has been put forward by Porath et al. (1971). A quantitative inter-
pretation of conductive structure beneath the Northern Rockies, based
on both short- and long-period data (see Chapter IV), will be presented
by Gough and Camfield (1972b). This chapter elaborates somewhat on the
material of Camfield et al. (1971).

The 35 mm film recordings of the events selected were printed
electrostatically at ten-times magnification, edited, and smoothed by
hand to prevent aliasing during the subsequent commercial digitizing
at 1 min intervals from the prints. Full-scale plots of the digital
values were superposed on the prints to check the accuracy of the

digitizing, and corrections were made where necessary.  The values
were normalized to gammas using scale factors derived from the field
calibrations of the variometers, and, for the University of Alberta's
stations, were corrected to first order for the H-Z interaction
mentioned in Section 2.2.

## 3.2  Magnetograms

Magnetograms showing the normalized data are presented for 10
August (Figs. 3.1 and 3.2), for 12 August (Figs. 3.3 to 3.6), and for
20 August 1969 (Figs. 3.7 and 3.8).  These were drawn by Calcomp drum-
plotter controlled off-line by computer-produced magnetic tape.  Hour
time-lines are marked in Universal  Time (UT).  Line 1 is the northern-
most line of instruments; line 4, the southernmost; see the map of Fig.
2.1.  Stations in each line are arranged from east to west going down
the page.  All stations are shown on the magnetograms, even though there
may be partial data or no data at some of them.  Downward Z, northward
H and eastward D are positive, and scale bars show the plotting
sensitivities.  Each of the observed induction anomalies is discussed
below as it is seen in the three sets of magnetograms.

The most striking feature in the data is the anomaly found at the
eastern edge of the array trending northward from the eastern side of
the Black Hills of South Dakota to the U.S. - Canada boundary.  Camfield
et al. (1971) have named this the North American Central Plains anomaly.
It is very narrow; a reversal in the vertical variation field occurs
in less than 50 km between stations FMD and HIL on line 4 (Figs. 3.2
and 3.6), and in less than 110 km between RDR and BKR on line 3 (Fig. 3.8,

# 10 AUGUST 1969
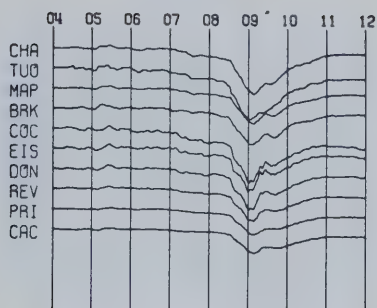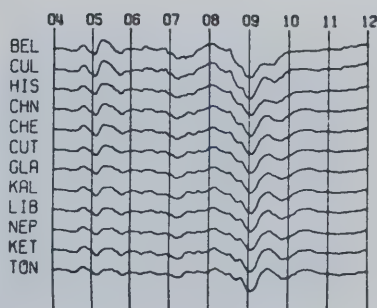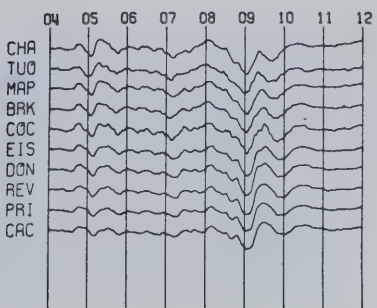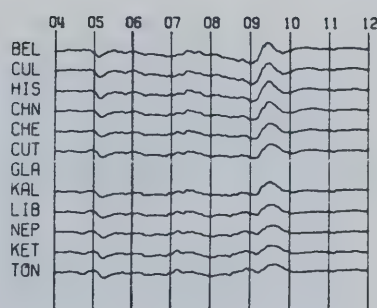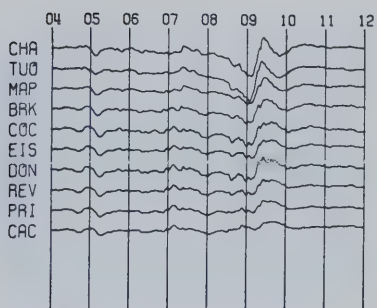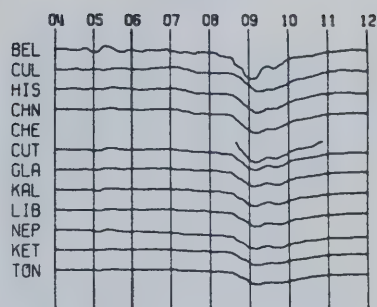


Fig. 3.1  Magnetograms for disturbance of 10 August 1969, northern lines.

# 10 AUGUST 1969
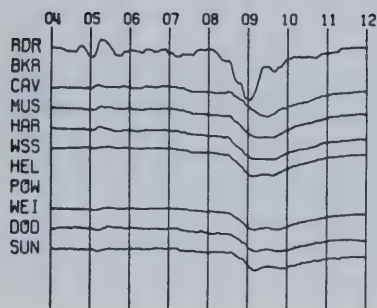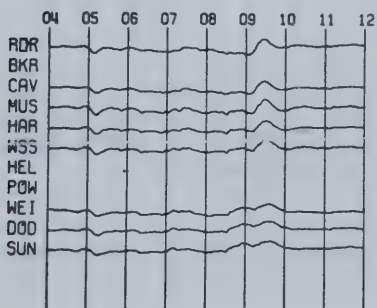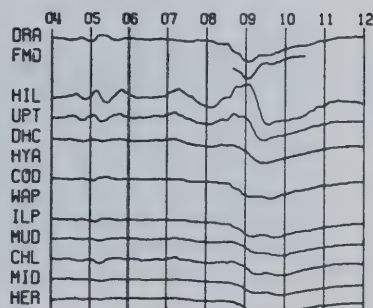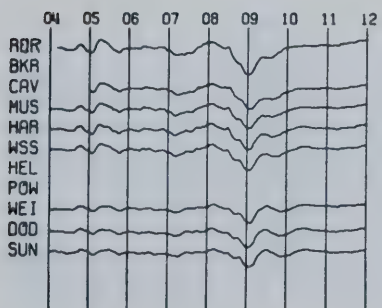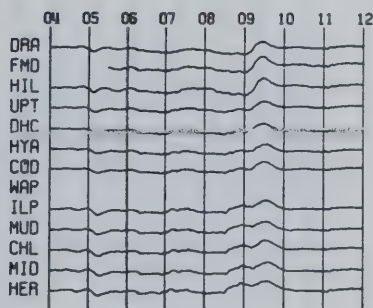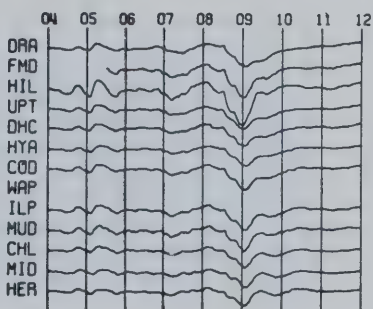


Fig. 3.2  Magnetograms for disturbance of 10 August 1969, southern lines.

# 12 AUGUST 1969

## LINE 1
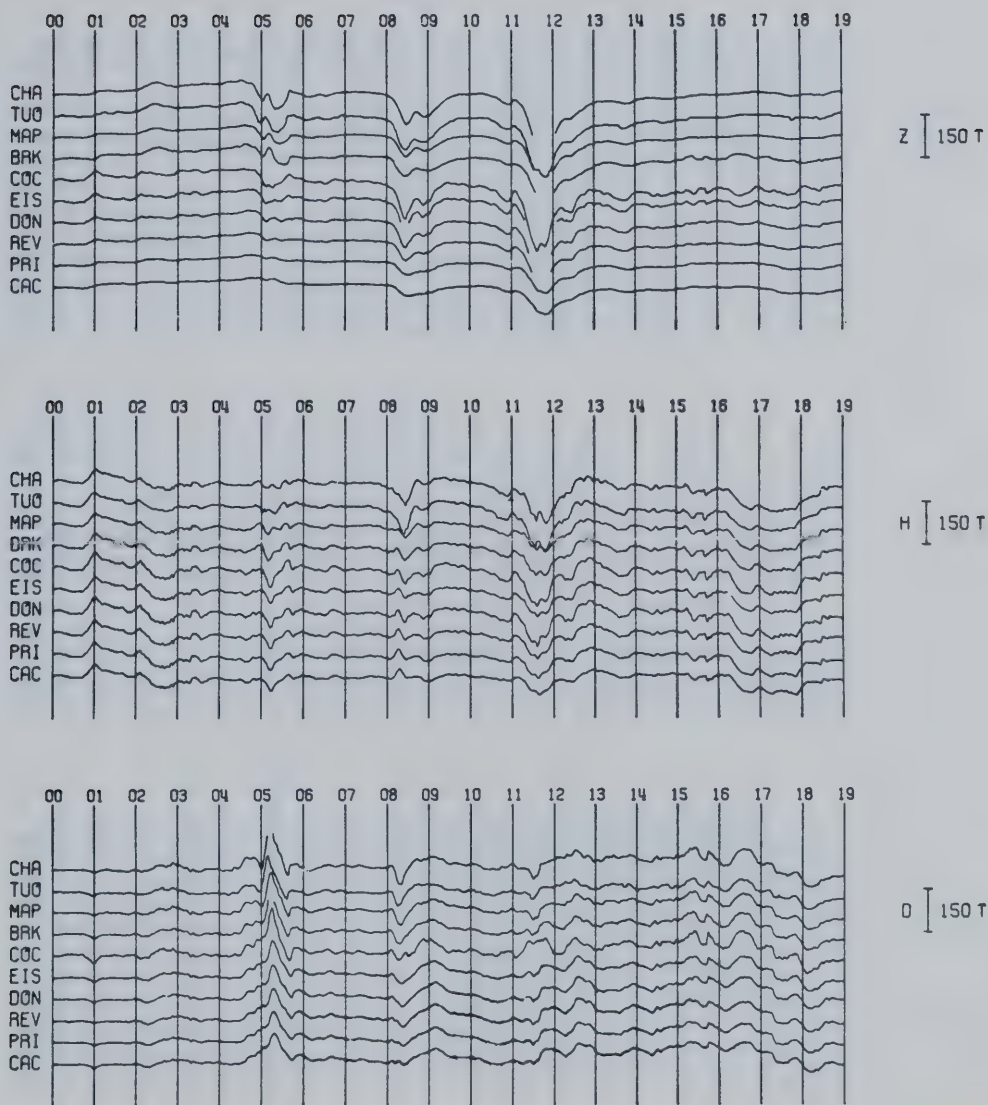


Fig. 3.3  Magnetograms for storm of 12 August 1969, line 1.

# 12 AUGUST 1969

## LINE 2
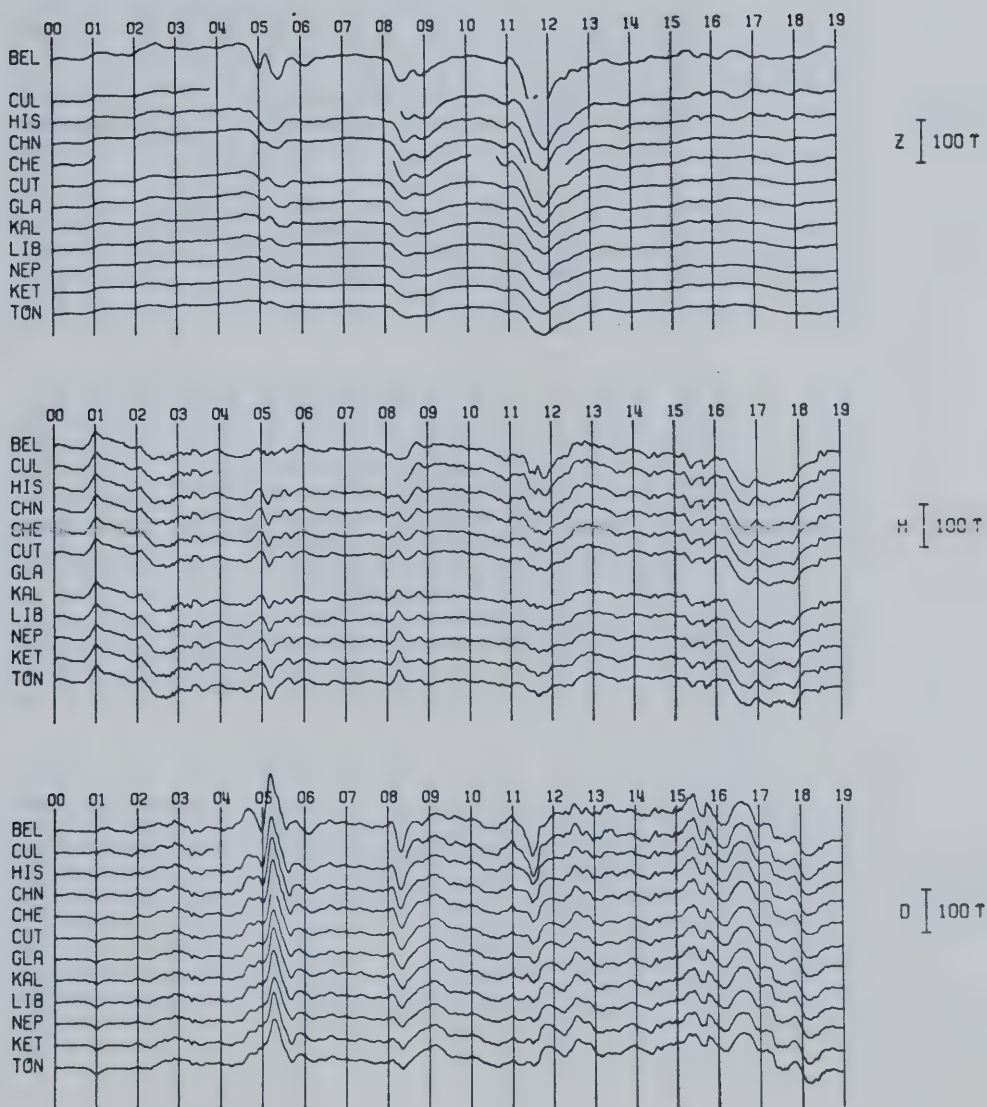


Fig. 3.4  Magnetograms for storm of 12 August 1969, line 2.

# 12 AUGUST 1969

## LINE 3
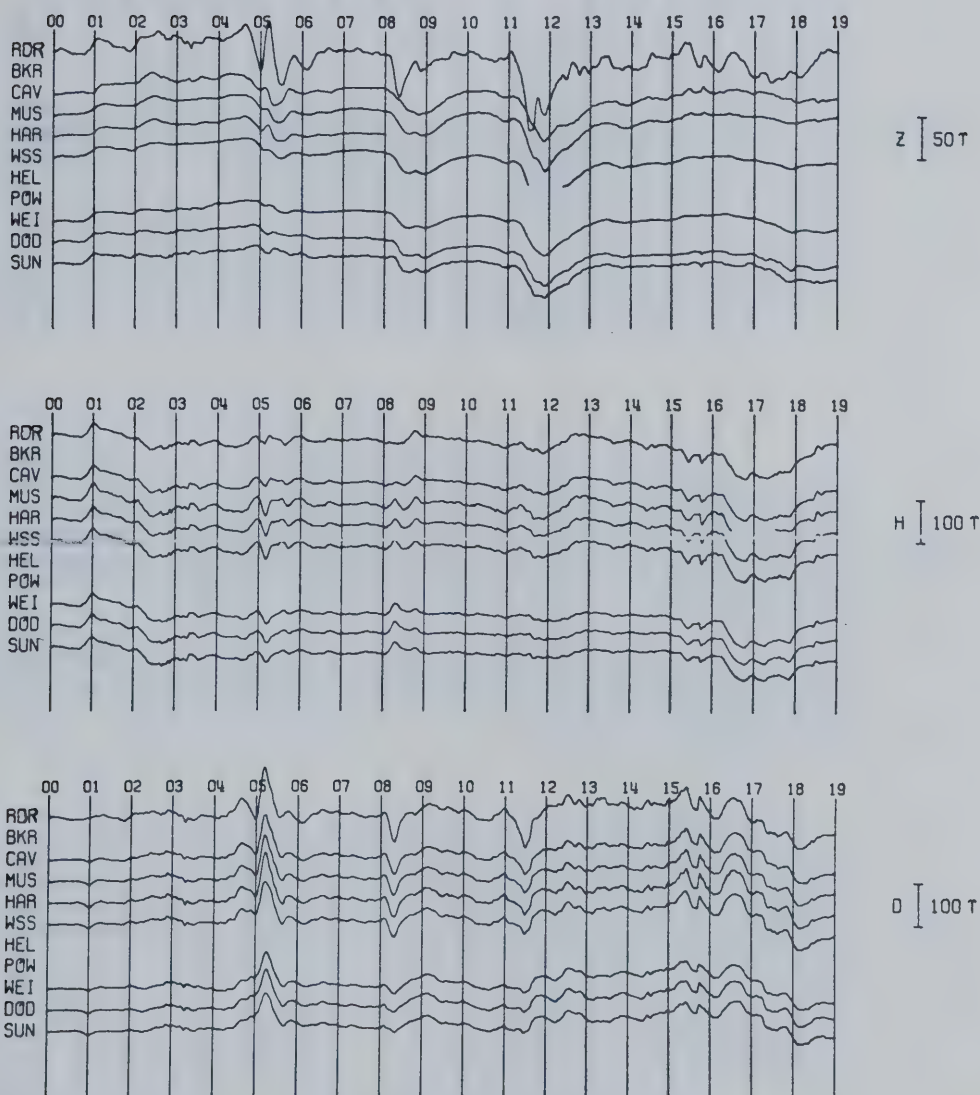


Fig. 3.5  Magnetograms for storm of 12 August 1969, line 3.

# 12 AUGUST 1969

## LINE 4
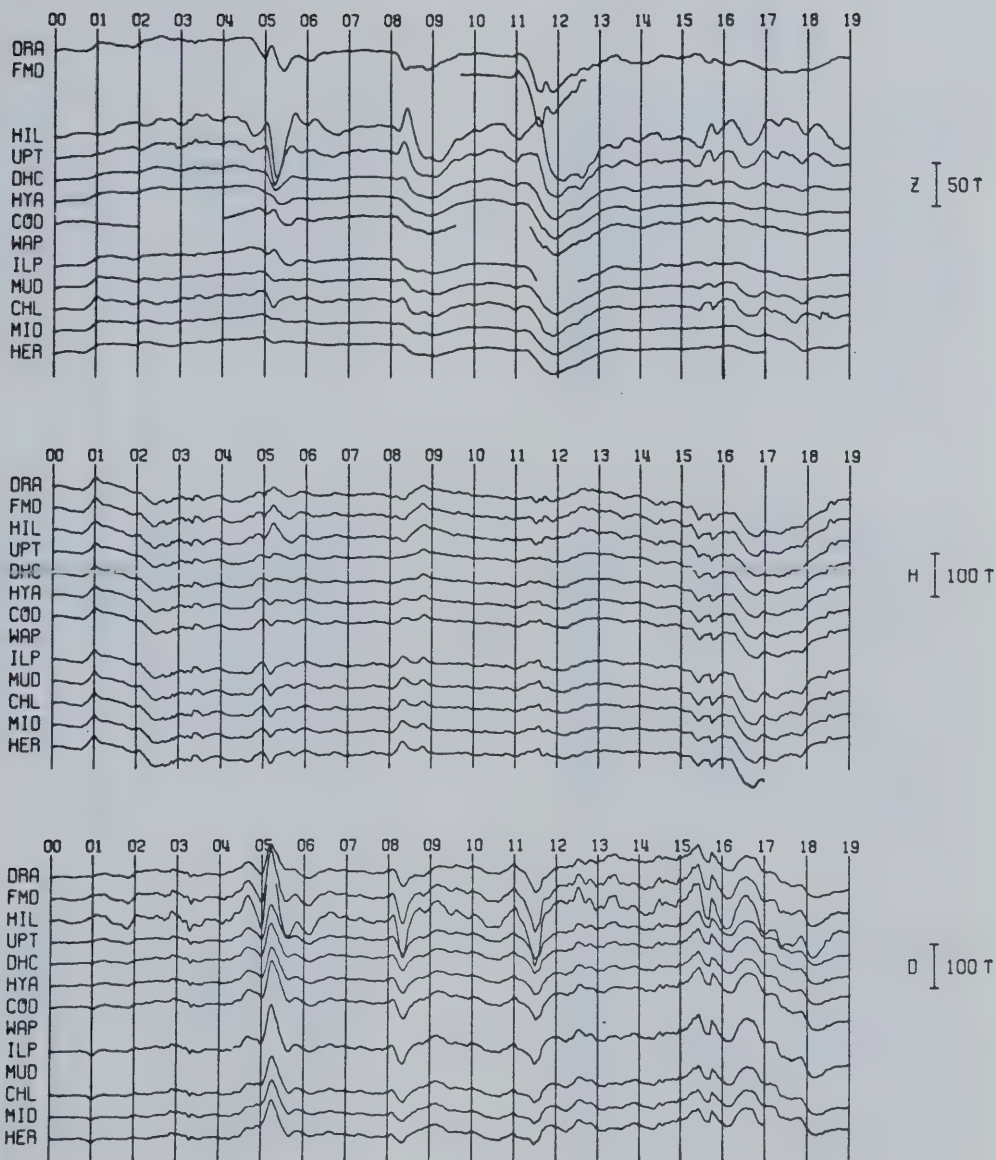


Fig. 3.6  Magnetograms for storm of 12 August 1969, line 4.
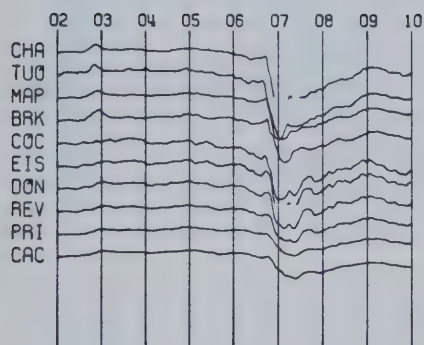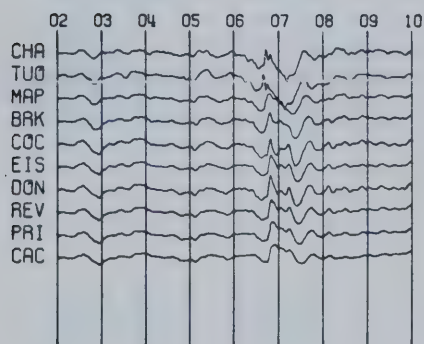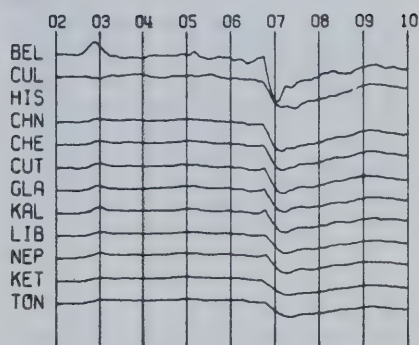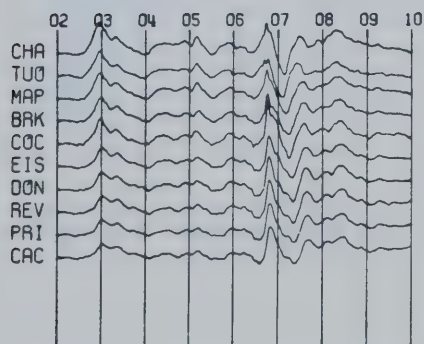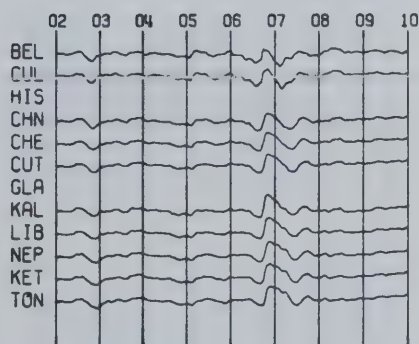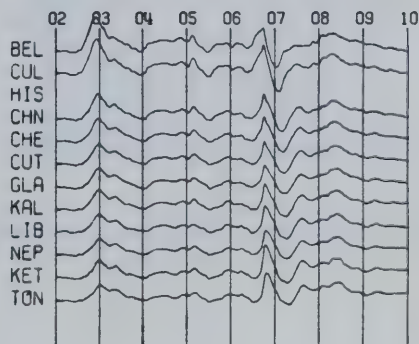
Fig. 3.7  Magnetograms for disturbance of 20 August 1969, northern lines.

# 20 AUGUST 1969

## LINE 3



## LINE 4
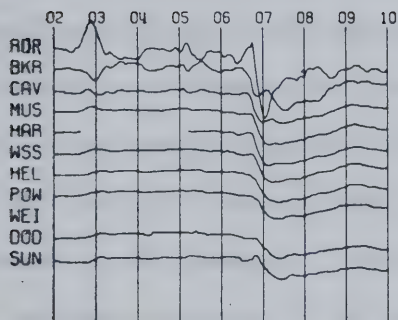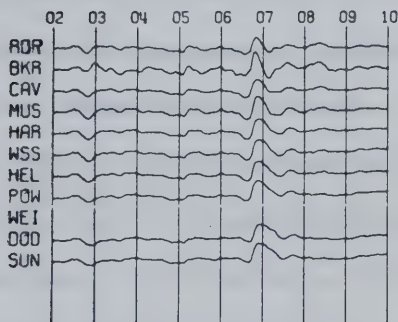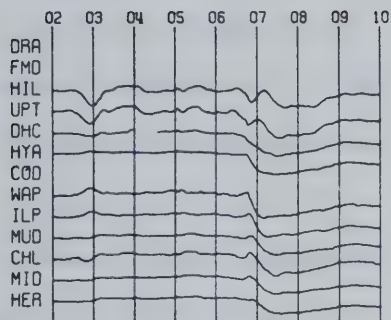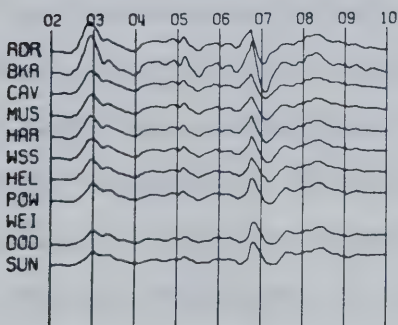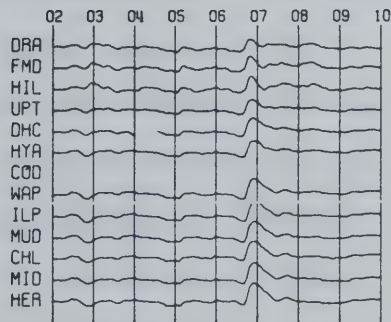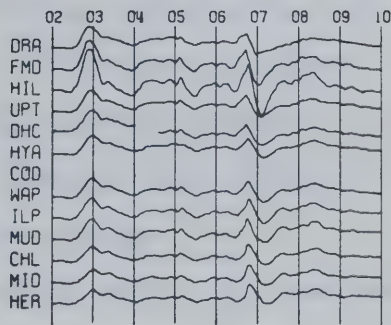
Fig. 3.8 Magnetograms for disturbance of 20 August 1969, southern lines.

especially clearly at 03 UT). On line 2 the anomaly is between BEL and CUL (Figs. 3.1 and 3.7). For the substorms at 05 and 09 UT on 10 August, the Z trace at BEL (Fig. 3.1) is similar in form to that at DRA, to the east of the anomaly on line 4 (Fig. 3.2); Z at CUL (Fig. 3.1) shows little or no anomalous field and resembles Z at DHC, well to the west of the anomaly on line 4 (Fig. 3.2). The separation between BEL and CUL (160 km) was possibly too great to record a narrow zone of reversed Z, if it exists. The horizontal variation fields, especially the east-west component D, are noticeably enhanced at HIL (Figs. 3.2, 3.6 and 3.8), at BKR (Fig. 3.8), and at CUL (Figs. 3.4 and 3.7). This implies that the maximum concentration of induced current must be nearly beneath these stations. On line 2, D at BEL (Figs. 3.4 and 3.7) shows almost as much enhancement as at CUL; an additional station between these two would be necessary to decide whether the anomaly is diverging at this latitude, or merely that the maximum had not been observed with the large station spacing between BEL and CUL.

At their station CRW in northwestern Nebraska, 150 km south of HIL, Reitzel et al. (1970) have reported D and Z fields enhanced similarly to those at HIL. If the anomaly does extend another 250 km further south to their variometer at STE in northeastern Colorado, it has become very weak and has merged with the Southern Rockies anomaly.

Whatever the geometry of the induced current system, its magnitude must be very great, to give the large reversed vertical fields on either side and the large horizontal fields above it. The magnetograms show that the anomalous D and Z fields associated with the induced current are closely in phase with the normal, regional D field, and that the

anomalous fields, considered as functions of time, resemble the normal
D field. (Normal D is defined as the resultant of external D, and inter-
nal D induced in the absence of lateral conductivity inhomogeneities.)
This resemblance suggests that the anomalous currents are driven by
normal D, and thus that this is a case of induction by the horizontal
field. The anomaly indicates the existence of a shallow, elongated
body of extremely high conductivity.

The second major phenomenon observed in the data is the attenua-
tion of the normal vertical force variations at stations west of the
Cordillera. This was first reported with single lines of magnetometers
by Hyndman (1963) in southern British Columbia at latitude 49°N and
then by Schmucker (1964) in Arizona and New Mexico at 32°N. Caner et
al. (1967) added coverage with lines at 35°N and 51°N, and Caner et al.
(1971) at 54°N. The 1967 and 1968 arrays (Reitzel et al., 1970; Porath
and Gough, 1971) confirmed that this feature is continuous in the
western and southwestern U.S. In the 1969 array magnetograms considered
here, the westward attenuation of normal Z is easily observed on all
lines except at stations where it may be partially obscured by anoma-
lous Z associated with induced currents flowing along the boundaries
of local conductive structures. On line 1, where normal Z is both
large and non-uniform in space because of the relative closeness of
auroral-zone ionospheric source currents, the transition to the region
of attenuated Z is rather abrupt. It occurs between stations DON and
PRI, with REV being intermediate in the three events of Figs. 3.1, 3.3
and 3.7. On the basis of a statistical estimate of $\Delta Z/(\Delta H^2 + \Delta D^2)^{\frac{1}{2}}$ for
many events, however, Caner et al. (1967) chose a station slightly east

of DON as the intermediate.

This attenuation of the normal Z field of substorms points to a regional enhancement of subterranean electrical conductivity. Various models have been proposed: a thin layer of high conductivity in the lower crust or at the depth of a seismic low-velocity zone, or a rise in the surface of the conductive part of the mantle. These will be discussed further in Chapters IV and V.

Smaller induction anomalies at various locations within the array are evident from anomalous Z fields whose waveforms mimic the normal horizontal field which induces them. Stations COD and ILP on line 4 in Fig. 3.6 show anomalous Z resembling normal D at 05 UT. This is likely a weak northward continuation of the Wasatch Front anomaly (Reitzel et al., 1970; Porath and Gough, 1971). In the same figure, strong anomalous Z similar to normal H was recorded at CHL, and moderate anomalous Z at MUD, MID and HER. This can best be seen when normal H has a different waveshape from normal D, as at 01 and 08-09 UT. The same Z-H correlation was observed more intensely in the 1967 array at a station about 200 km south of mid-point between MUD and CHL, just south of the Idaho Batholith (station BRU of Reitzel et al., 1970). This Z-H correlation is due to currents flowing along the east-west interface formed by the rise of the conductive upper mantle southward from under the Columbia Plateaux to shallower depths beneath the Basin and Range Province.

On line 3 at 05 UT on 12 August (Fig. 3.5), anomalous Z following the large normal D peak is evident at CAV, MUS and HAR, is transitional at WSS, and is attenuated at WEI. At other times in these data, these

stations do not show anomalous effects. At 01 and 05 UT in the same figure, there is a hint of anomalous Z resembling H at DOD and SUN, rather more so at SUN than at DOD.

On line 2, again at 05 UT on 12 August (Fig. 3.4), anomalous Z associated with the large D excursion appears at stations farther west than on line 3, i.e. at CUT, GLA, KAL, LIB and NEP. This is the Northern Rockies anomaly, which will be discussed further. KET and TON show only the westward attenuation of normal Z.

On line 1, as mentioned above, normal Z is strong and non-uniform in space. In spite of this, anomalous effects were observed under some conditions at stations in the Cordillera east of the Rocky Mountain Trench, and in the Great Plains. When the normal horizontal field varies in a NE-SW direction (H positive or negative when D positive or negative), as in Figs. 3.1 and 3.7, anomalous Z appears at the six stations EIS to CHA. If the horizontal field is NW-SE (H positive or negative when D negative or positive), as in Fig. 3.3 at 05 UT, the two westernmost of these six stations, EIS and COC, do not have anomalous Z while the other four do. This difference must be connected with local changes in the direction of the discontinuity in conductivity which gives rise to the anomalous fields; perhaps it strikes east-west near EIS and COC.

## 3.3 Fourier Spectra

Discrete Fourier transforms of the time series were computed to study the frequency content of the variation fields and the frequency response of anomalies. The discrete Fourier series of a sequence of

data $x_j$, $j = 0, 1, \ldots N-1$ is given by

$$x_j = a_o + \sum_{k=1}^{N-1} (a_k \cos \omega_k j + b_k \sin \omega_k j)$$

where $a_k$ and $b_k$ are the Fourier coefficients, and $\omega_k = 2\pi k/N$. This may be written

$$x_j = a_o + \sum_{k=1}^{N-1} c_k \cos(\omega_k j - \theta_k)$$

where $c_k = \sqrt{a_k^2 + b_k^2}$ is the Fourier component amplitude, and

$\theta_k = $ arc tan $(b_k/a_k)$ is the phase.

With this definition, a more positive value for phase implies a waveform shift to a later time.

A rotation of the horizontal components from H and D (local geomagnetic coordinates) to X and Y (geographic coordinates) was first carried out to remove the distortion of the change of declination from 11°E to 23°E from east to west across the array:

X = H cos d - D sin d

Y = H sin d - D cos d

The rotation angle d (the declination of the geomagnetic main field) is listed for each station in the Appendix. To remove the mean and any linear trend from the data before transformation, a straight line pinned at each end of the series to the mean of the first or last ten minutes of data was subtracted from the series; to reduce end effects

from the finite length of data, the first and last ten minutes were multiplied by a $\sin^2$-taper to bring the data smoothly to zero at each end. The fast Fourier subroutine RHARM (Cooley-Tukey algorithm) from the IBM Scientific Subroutine Package requires the number of data points to be an integral power of 2; zeros were added to the data to increase the series to 2048 points. More zeros were added than would have been necessary to reach the closest power of 2, in order to obtain more output values in the period range of interest (20-120 min). See Oldenburg (1969), pp. 50-51, who found no adverse effect in adding more zeros than necessary. The justification for adding any zeros lies in the transient nature of a magnetic substorm; any small deflection in the magnetograms before or after a substorm can be regarded as having an independent source (Reitzel et al., 1970, p. 220).

Single polar magnetic substorms were picked from the data for transformation, as follows: 10 August, 0630-1200 UT; 12 August, 0330-0730 UT; and 20 August, 0600-1000 UT. Spectra for the longer sequences 04-12 UT on 10 August and 02-10 UT on 20 August will also be discussed. Amplitude spectra for the single substorm on 12 August as recorded at CHL, SUN and MUD are drawn in Fig. 3.9. It can immediately be seen that the horizontal fields D and H have quite different spectra. All three D spectra have one peak at short periods while all the H have two; at period 60 min, H has a maximum while D has a minimum, and at 40 min almost the opposite occurs. This suggests that the event is not as simple as it appears in the magnetograms. The horizontal field is elliptically polarized with a phase difference between the horizontal components, a situation which Porath and Gough (1971) mention as
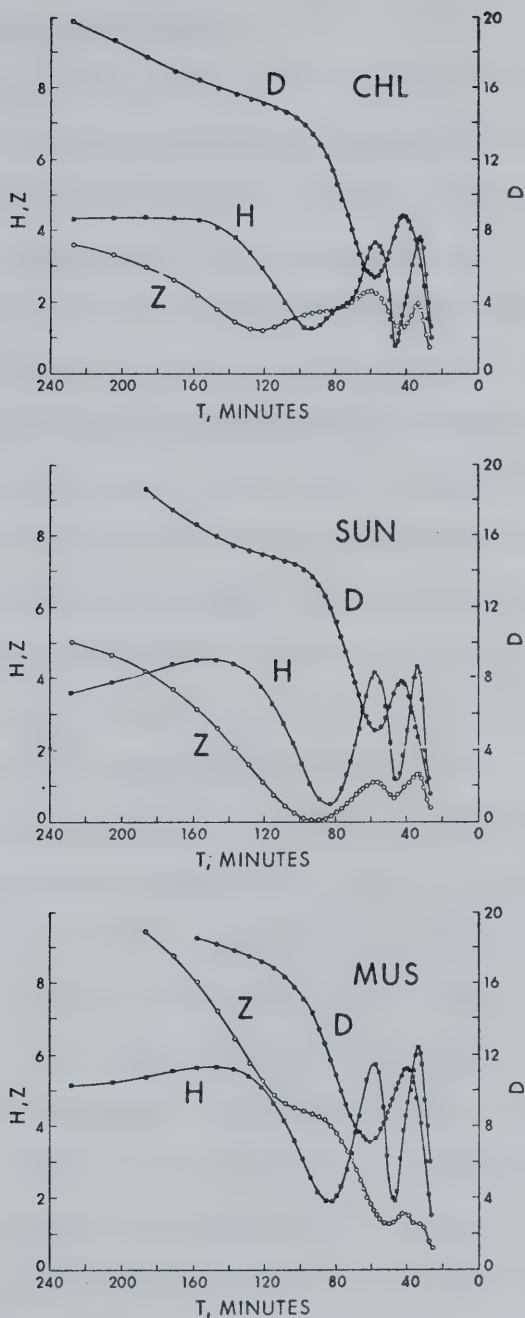
Fig. 3.9  Fourier amplitude spectra in the period range 25–225 min for
0330–0730 UT, 12 August 1969, for stations CHL (top), SUN
(middle), and MUS (bottom).

generally occurring in substorms.

If a station records anomalous Z resembling one of the horizontal components, then the Z spectrum should resemble that of the horizontal component. In the previous section, anomalous Z associated with H was observed at CHL in Fig. 3.6. Here in Fig. 3.9, the Z spectrum for CHL has the same shape as the H spectrum, with maxima at 30 and 60 min and a minimum at about 40 min. It is quite unlike the D spectrum. At SUN, the Z spectrum again shows a strong correlation with the H spectrum but not with D; unlike the effect at CHL, this is harder to see in the magnetograms except at 01 and 05 UT in Fig. 3.5. At MUS, the Z spectrum does not have the two short-period peaks found at the other two stations, but has a single peak correlated with the only D peak. Anomalous Z associated with D was observed at MUS (near the east front of the Northern Rockies) in the magnetograms of Fig. 3.5.

Other Z spectra for this event (not presented here) at CAC and HER have double peaks correlating with X; and at CHA and DRA, a single peak matching with Y. In the magnetograms this matching is evident at DRA and HER (Fig. 3.6) and perhaps at CHA (Fig. 3.3), but it is obscure at CAC because Z is so highly attenuated there (Fig. 3.3). This spectral method of defining Z correlation with D or H has been used by Porath and Gough (1971) at a station east of the Southern Rockies.

The next two figures show spectra for the longer sequences 04-12 UT on 10 August (Fig. 3.10) and 02-10 UT on 20 August (Fig. 3.11) at stations in the four corners of the array. Both sequences contain at least two substorms, and the spectra hence are more complex than the transforms of a single substorm. Porath and Gough (1971) point out

that the Fourier results, which are integrals over the length of a series, will depend on the amplitude and phase characteristics of each substorm in the series and also on the time separation between them. As in Fig. 3.9, maxima in one horizontal component may coincide with minima in the other.  Peaks in the spectrum of one or more components may shift slightly in period from one side of the array to the other, in response to phase changes between the components of the external field which are associated with the development of the substorm's ionospheric/magnetospheric current system (Rostoker et al., 1970). Returning to the substorm of 0330-0730 UT on 12 August for an example, the centre periods of peaks in X and Y for four stations are given in the following table:

Table 3.1

Location of spectral peaks for 12 August event

| Station | Period, min | |
|---------|-------------|---|
| | X | Y |
| CHA | 34.7, 56.9 | 40.2 |
| CAC | 35.3, 58.5 | 42.7 |
| HER | 34.1, 56.9 | 42.7 |
| DRA | 28.8, 66.1 | 39.4 |
| Apparent resolution, min | 0.6,  1.6 | 0.9 |

Most of these values differ by only a few times the apparent resolution of the spectra (1/2048 cycles per minute).  The large shifts in X at DRA may be due to the proximity of the Central Plains anomaly; X at DRA

has an additional peak at 41.8 min (close in period to the Y peak),
which reinforces this explanation.

The spectra given in Figs. 3.10 and 3.11 for the longer  sequences
containing multiple substorms are very complex, as predicted and as
observed in the 1967 array by Reitzel et al. (1970).  The "interaction"
between the substorms in the Fourier calculation has produced many more,
narrower peaks than showed in the spectra for a single substorm.  It
has also made the spectra of the horizontal components less obviously
different from one another; most spectral lines are found in both com-
ponents, in comparison to the spectra in Fig. 3.9 for the single sub-
storm which have two short-period peaks in H but only one in D.  This
similarity of horizontal components can be advantageous when one is
choosing a period at which energy is high in all components across the
array, for presentation, via contour maps, of data at such periods.
It is less likely that a peak in one component will correspond with a
trough in the other.  Arrows in Figs. 3.10 and 3.11 show several exam-
ples.  On the other hand, the reliability of the peak height, which
depends both on the individual substorms and on their "interaction",
may not be as firm.  Contour maps in the next section are drawn using
transforms of both single and multiple substorm sequences, as will be
noted; results are essentially similar.

3.4  Maps of Spectral Components

The most comprehensible way of presenting the Fourier parameters
for an array of magnetometers is via contour maps of amplitude and phase
at discrete periods corresponding to spectral peaks.  This is the only

# FOURIER AMPLITUDES

# 10 AUGUST 1969
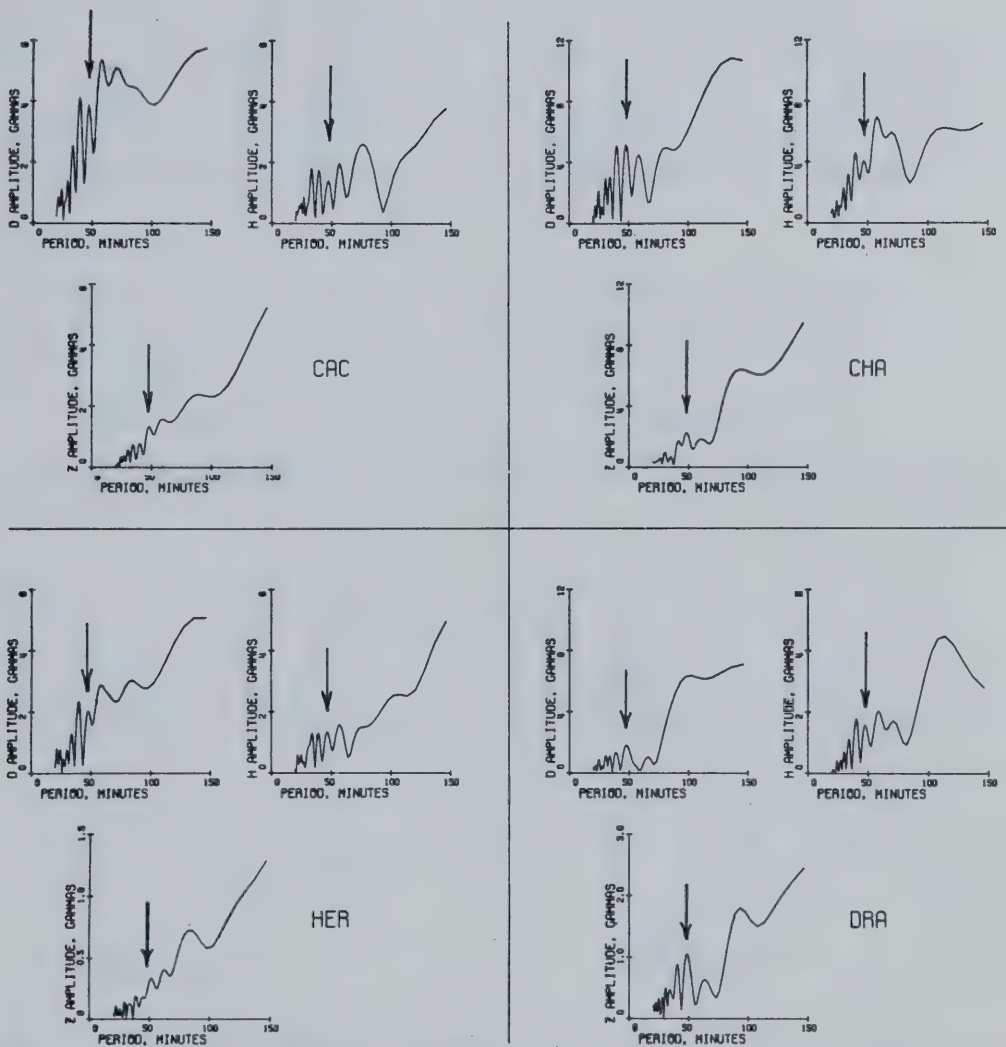


Fig. 3.10  Fourier amplitude spectra in the period range 20-150 min for
04-12 UT, 10 August 1969, for stations at the corners of the
array.  In each of the four sets, the D spectrum is to the
upper left, H to the upper right, and Z below.  Ordinate
scales are as marked.  Arrows indicate period  47.6 min.

# FOURIER AMPLITUDES

# 20 AUGUST 1969
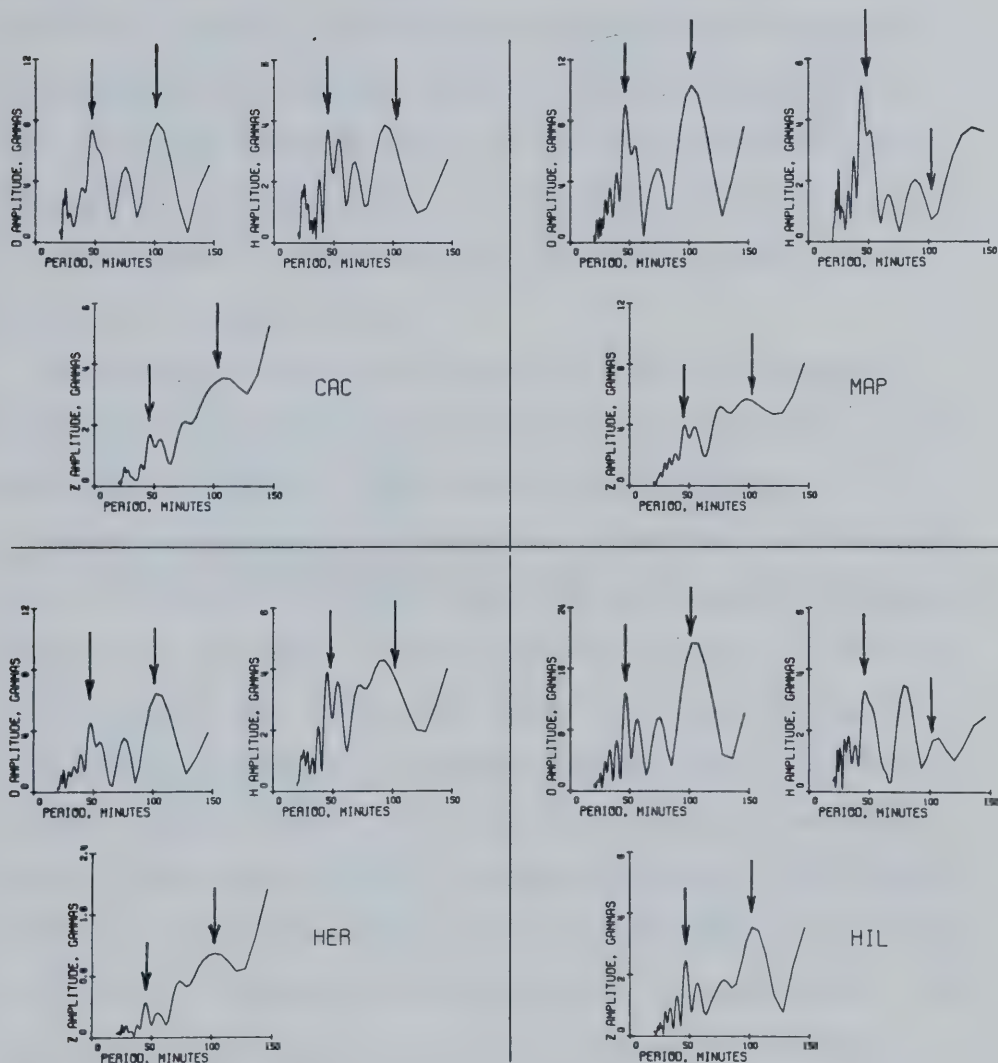


Fig. 3.11  Fourier amplitude spectra in the period range 20–150 min for 02–10 UT, 20 August 1969, for stations at the corners of the array.  In each of the four sets the D spectrum is to the upper left, H to the upper right, and Z below.  Ordinate scales are as marked.  Arrows show periods 47.6  and 102.4 min.

arrangement in which the data can easily be considered in array form; the magnetograms (Section 3.2) and Fourier spectra (Section 3.3) can only be grouped along profiles.  Periods were chosen where energy was high in, if possible, all three components of the variation field, all across the array; in considering disturbances where maxima at a given period in two components corresponded with a minimum in the third, as for the 12 August spectra in Fig. 3.9, priority was given to securing high energy in Y and Z.  In such a case, the phase map for X is unreliable because of instability in the phase spectrum near a minimum in the energy spectrum.

Contouring has been done by hand using linear interpolation between stations.  Small circles on the maps indicate the location of magnetometers; stations are not shown if data are missing.

Seven sets of maps are included here:  one (Fig. 3.12) from the event on 10 August, at period 47.6 min (the peak marked in the spectra of Fig. 3.10); two (Figs. 3.13 and 3.14) from 12 August, at 40.2 and 102.4 min (the former is the period of the D and Z peak in Fig. 3.9, and the latter is arbitrarily chosen); and four (Figs. 3.15-18) from 20 August, at 25.3, 47.6, 85.3 and 102.4 min (the second and fourth of these periods are indicated in the spectra of Fig. 3.11).  Maps for X are at the top of these figures; for Y, in the middle; and for Z, at the bottom.  Amplitudes are on the left, phases on the right.  The 20 August data were recorded by the largest number of instruments, equivalent to 91% serviceability.  Differences between the maps in the 20 August set should yield information regarding depths to conduc-tive structures, since the depth of penetration of the time-varying

AUGUST 10,1969    T=47.6 MIN.
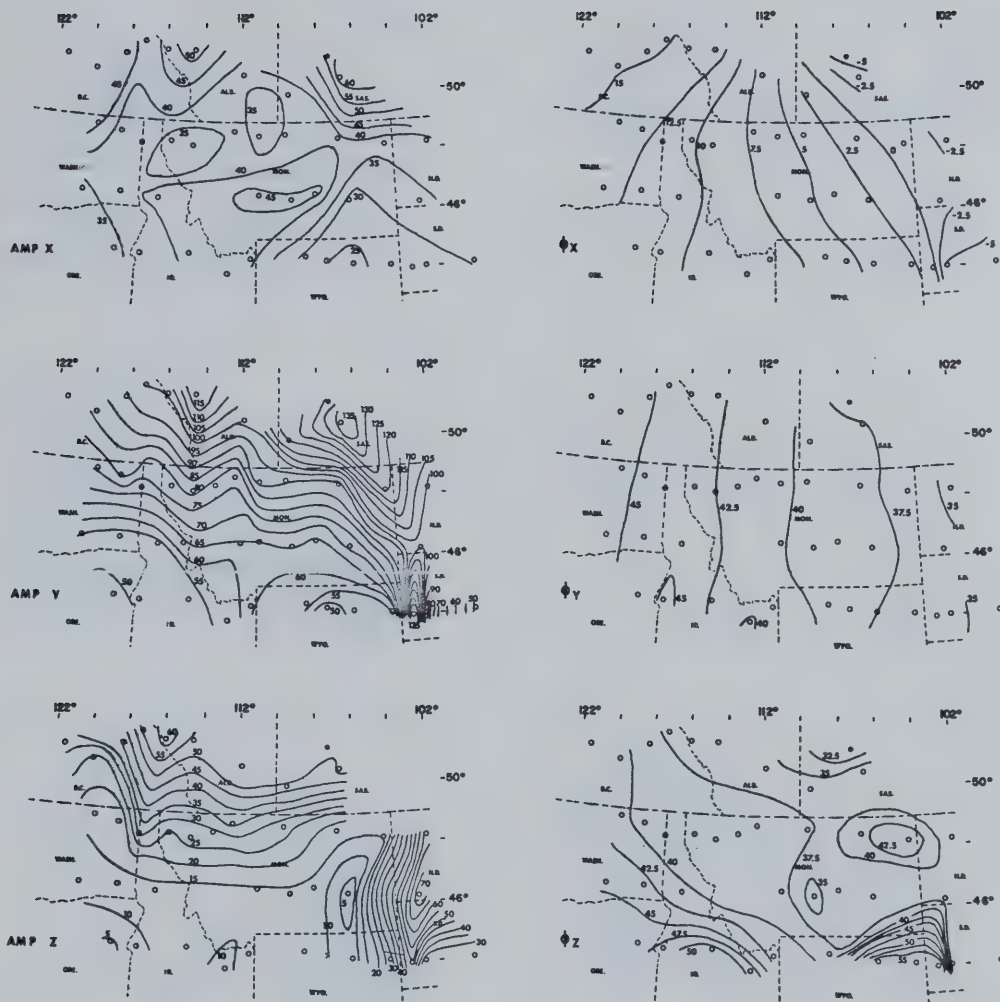


Fig. 3.12  Fourier amplitudes (in arbitrary units, with contour interval
5 units) and phases (in minutes of time, with interval 2.5 min)
for 0630–1200 UT, 10 August 1969, at period 47.6 min.

AUGUST 12,1969  T=40.2 MIN.
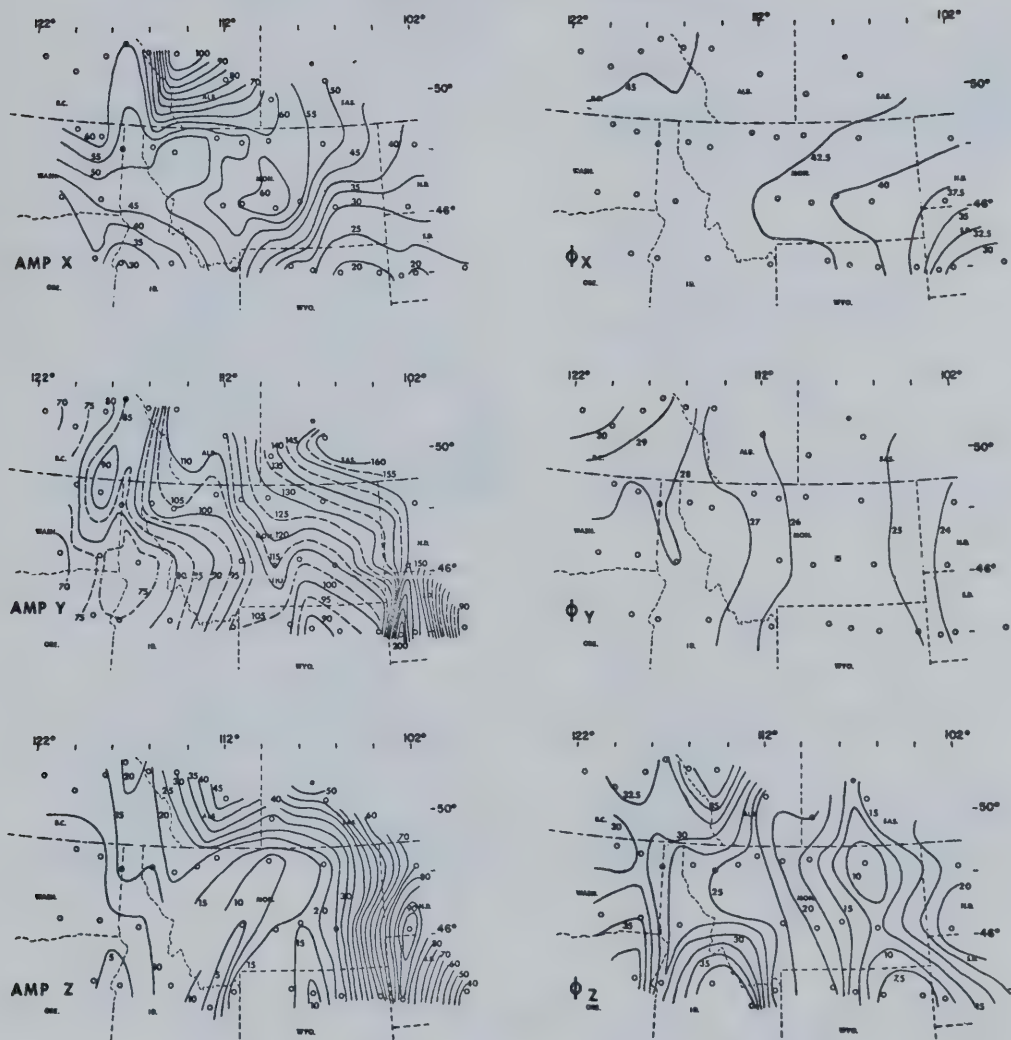
Fig. 3.13  Fourier amplitudes (in arbitrary units, with contour interval 5 units for X and Z, and 5 or 10 units for Y) and phases (in minutes of time, with interval 1 min for Y and 2.5 min for X and Z) for 0330-0730 UT, 12 August 1969, at period 40.2 min.

AUGUST 12,1969    T=102.4 MIN.
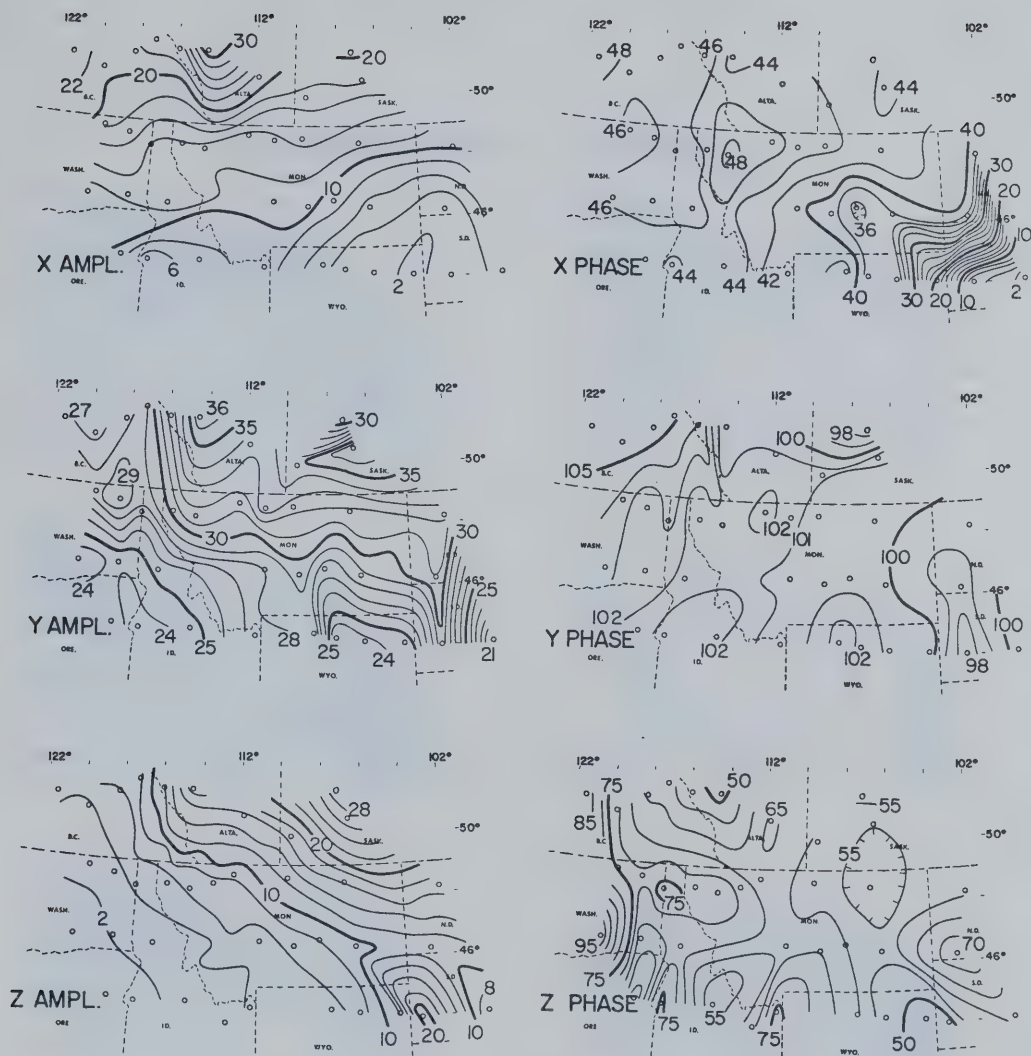


Fig. 3.14   Fourier amplitudes (in arbitrary units, with contour interval
1 unit for Y and 2 units for X and Z) and phases (in minutes
of time, with interval 1 min for Y, 2 min for X, and 5 min for
Z) for 0330-0730 UT, 12 August 1969, at period 102.4 min.

**AUGUST 20,1969   T = 25.3  MIN.**
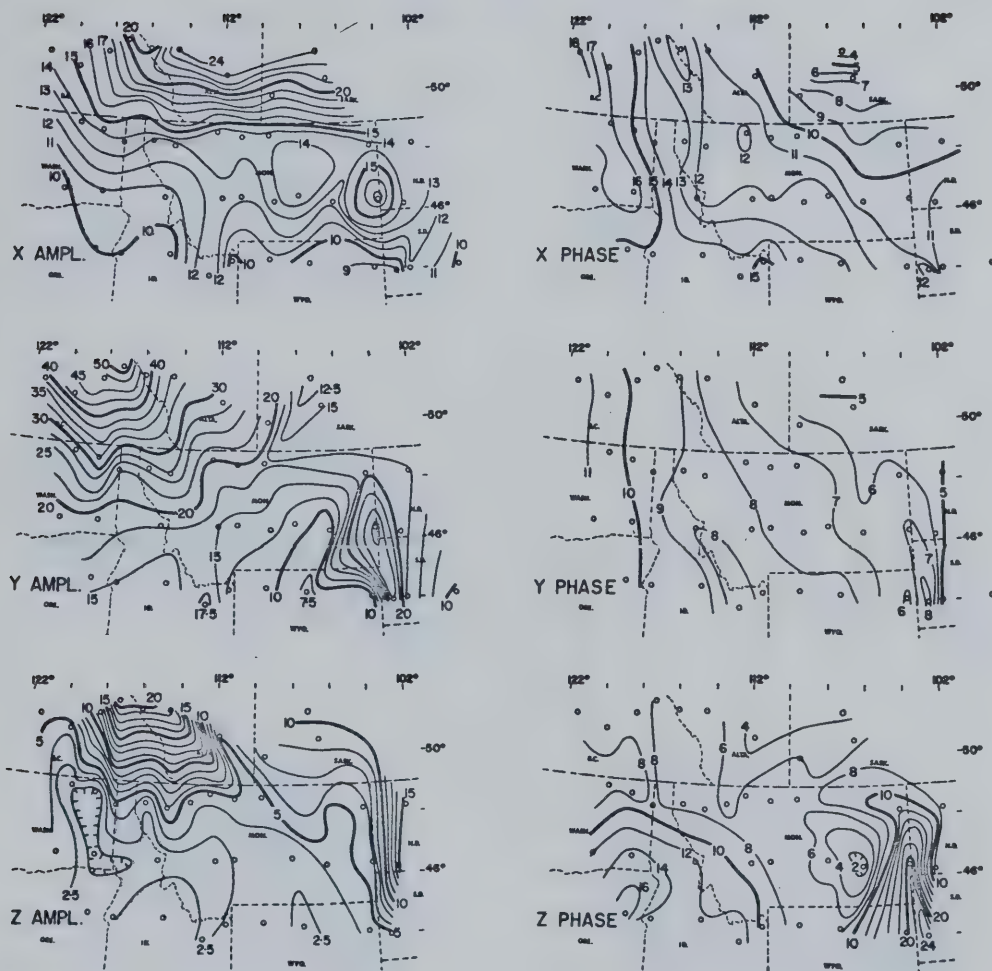
Fig. 3.15   Fourier amplitudes (in arbitrary units, with contour interval
1 unit for X, 1.25 units for Z and 2.5 units for Y) and
phases (in minutes of time, with interval 1 min for X and Y
and 2 min for Z) for 02-10 UT, 20 August 1969, at period
25.3 min.
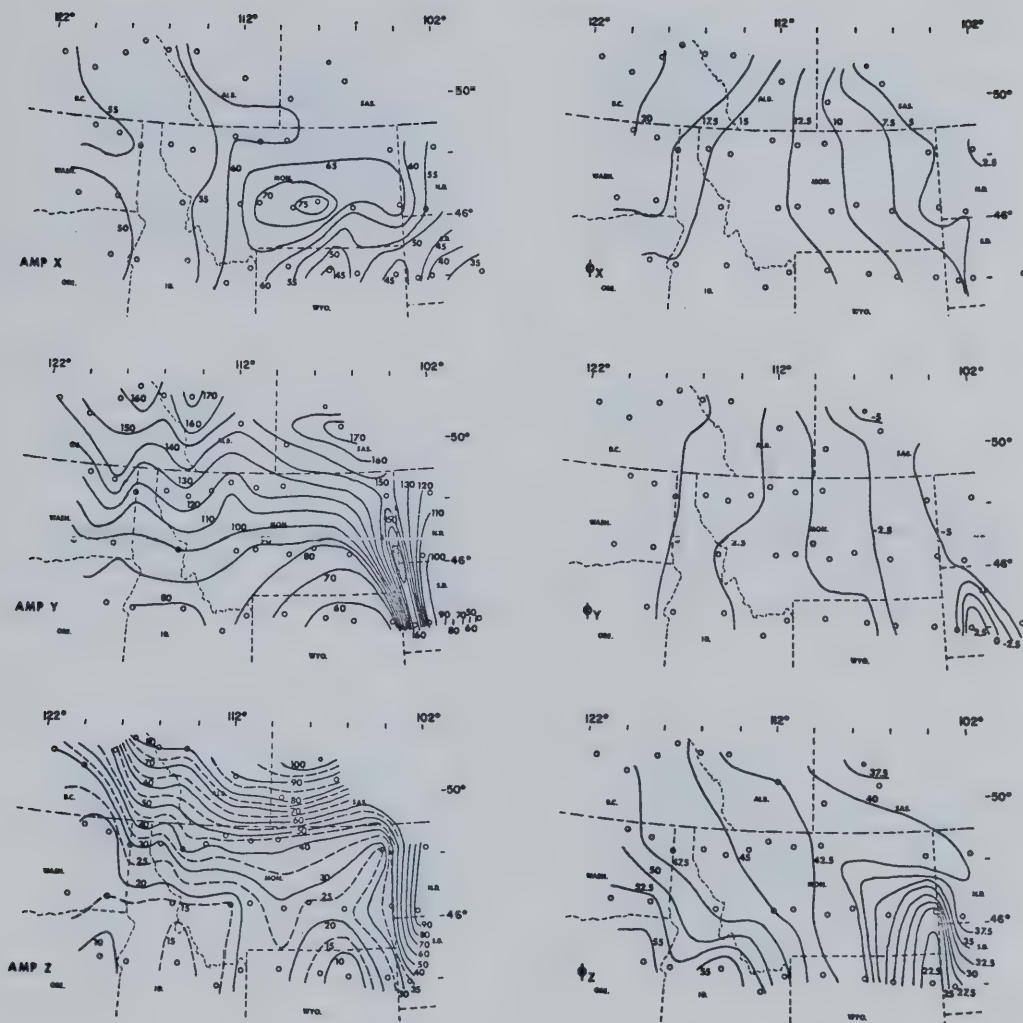
Fig. 3.16   Fourier amplitudes (in arbitrary units, with contour interval
5 units for X, 10 units for Y, and 5 or 10 units for Z) and
phases (in minutes of time, with interval 2.5 min) for 06-10
UT, 20 August 1969, at period 47.6 min.

Fig. 3.17 Fourier amplitudes (in arbitrary units, with contour interval
5 units for X and Y, and 5 or 10 units for Z) and phases (in
minutes of time, with interval 2.5 min) for 06–10 UT,
20 August 1969, at period 85.3 min.
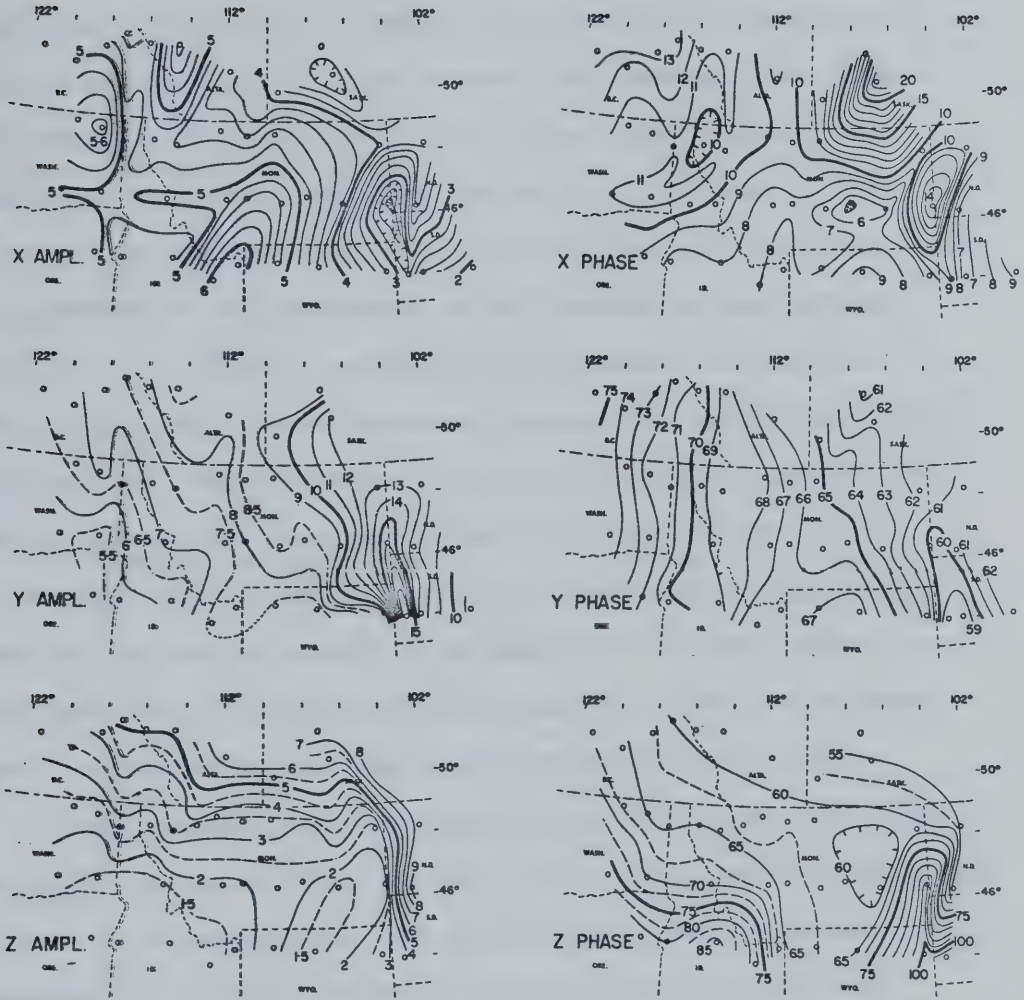
Fig. 3.18 Fourier amplitudes (in arbitrary units, with contour interval
0.2 units for X, and 0.5 or 1 unit for Y and Z) and phases
(in minutes of time, with interval 1 min for X and Y, and 2.5
or 5 min for Z) for 02-10 UT, 20 August 1969, at period 102.4
min.

fields and the process of induction in conductive structures are frequency-dependent.

First, some general comments about the normal fields as seen in the maps. Recall that the normal field is defined as the resultant of the external field and the internal field induced in the absence of lateral conductive inhomogeneities. The normal vertical field amplitude has a strong northward gradient in all of Figs. 3.12-18; the slope of the contoured surface is especially steep between lines 1 and 2, sometimes forcing an increase in the interval between contours (Fig. 3.17). This is a consequence of the proximity of the array to the auroral zone currents which are the source of the external fields. The maps show that in addition to having this gradient, normal Z at the western side of the array is strongly attenuated west of the Cordillera, likely because of induction in material of enhanced conductivity at smaller depths. This causes the Z contours, which run east-west over the central part of the maps, to strike to the north over the Cordillera then bend westwardly towards the Pacific.

The Z amplitude map at period 85.3 min for 20 August (Fig. 3.17) contains a puzzle which has not been solved. In at least the northern part of the array away from the Central Plains anomalous feature, the magnitude of the average normal Z measured by the ratio $Z/\sqrt{X^2+Y^2}$, east or west of the Cordillera, is two to three times greater than corresponding values at periods 47.6 and 102.4 min for this event. There may be something peculiar about the source field here, but on the other hand at 47.6 min both this event (Fig. 3.16) and the one on 10 August (Fig. 3.12) yield the same normal field ratios. Because the

ratios at 85.3 min are so much greater than those at other periods, Porath et al. (1971) rejected them when fitting layered conductivity models to the normal fields. (See also Chapter V.)

The phase maps for both horizontal field components generally show a very clear uniform phase increase across the array, corresponding to waveform shifts to later time from east to west. Rostoker et al. (1970) have interpreted the phase results in connection with the development of the current system of polar magnetic substorms, and have associated the shifts with the lengthening of the intensified part of the auroral electrojet, termed the westward surge, which occurs at the time of an auroral breakup. The phase pattern appears in all X and Y phase maps except those for X in Figs. 3.14, 3.17, and 3.18, which are unavoidably at periods close to minima in the X amplitude spectra. The instability of phases in such cases has been mentioned above; the negative results for X phase in these figures are hence not significant.

Next, a comment on a feature which may be either a normal field or an anomalous field effect. (Again, an anomalous field is associated with current induced in the earth at a lateral inhomogeneity in electrical conductivity.) The X amplitude maps in Figs. 3.17 and 3.18 at periods 85.3 and 102.4 min differ from the others in an unusual way: X increases southward over most of the array. At the shorter periods of the other maps, the X field generally increases in the other direction, northward towards the auroral zone, due to source effects. If the southward increase at longer periods is also a (normal field) source condition, the mechanism is unknown. Similar observations of a

southward increase in X at periods greater than 90 min were however made with the 1967 array by Reitzel et al. (1970), who have interpreted them as an anomalous effect due to the rise in the surface of a good (mantle) conductor from under the Colorado Plateau south to the Basin and Range Province. Such a situation under the Basin and Range and the Middle Rockies near the southern edge of the 1969 array (see Fig. 2.1) might be invoked to explain the southward gradient in X of Figs. 3.17 and 3.18. It would not be inconsistent with the southward decrease in normal Z which was ascribed solely to increasing distance from the source currents.

Thirdly, a discussion of features which are anomalous field effects. The North American Central Plains anomaly (Camfield et al., 1971) is dominant in the eastern part of the array. It always appears in Y and Z amplitude and Z phase, and at some periods in Y phase as well (Figs. 3.14-16, 3.18). It strikes north from the Black Hills of South Dakota to the U.S.-Canada border, and has very large magnitude and very small width. Interpretation in terms of shallow (crustal) conductivity structure is attempted in Chapter V.

In the region of the Northern Rockies in the northwest part of the array, two anomalies have been mapped, rather small in magnitude compared with the Southern Rockies anomaly to the south (Reitzel et al., 1970) but persistent at various periods for all three events. There is no obvious connection between the Northern Rockies anomalies and those associated with either the Southern Rockies, or the Wasatch Front. The Northern Rockies anomalies show best in the Y amplitude maps in Figs. 3.12-18, but they also appear in Z amplitude, and, in some maps, in X amplitude. The Y and Z maps are consistent, in that

the maxima in Z are offset to the east of those in Y, as would be ex-
pected for north-south internal line currents. The currents would be
located beneath the Y maxima, in this case roughly along the eastern
front of the Northern Rockies and along the Midway-Kettle River ranges
west of the Rocky Mountain Trench. (These geographical features are
labelled in the map of Fig. 2.1). Interpretation of conductive
structure in this region is discussed in Chapter V.

In Figs. 3.15-17, there are vague indications in Y and Z amplitude
at the southern edge of the array that we have detected the northern
end of the Wasatch Front anomaly. The data do not show a link, if
one exists, between it and the two Northern Rockies anomalies. Just
south of the array, in Utah, Cook and Montgomery (1971) have suggested
from gravity data the existence of large-scale east-west structural
trends which may be "related to transform faults formed as a result
of crustal and upper mantle movement". These may mark the termination
of the Wasatch Front anomaly, which hence would not be expected to
continue northward into the territory of the 1969 array. In Chapter
IV, data from the daily variation, at the much longer periods 8, 12
and 24 h, show that the anomalous fields associated with the Wasatch
Front terminate in Montana. The conductive ridge in the upper mantle
probably has its northern end near 44°N.

An anomaly in Z phase in the southwestern corner of the array
(Figs. 3.13-16) may be associated with the northern edge of the highly
conductive mantle beneath the Basin and Range Province (Reitzel et al.,
1970), a feature for which evidence was also found at southwestern
stations on line 4, in the resemblance of anomalous Z waveforms with

those of normal H in the magnetograms of Section 3.2, and in the correspondence of H and Z peaks in the spectra of Section 3.3

At periods up to 47.6 min, a maximum in X amplitude is located in central Montana (Figs. 3.12-13 and 3.15-16). Because this anomaly does not appear at longer periods, it is likely due to shallow structure such as the conductive sediments in synclines and mountain basins in the region, as outlined on the Tectonic Map of the United States (U.S.G.S. and A.A.P.G., 1962).

A final remark should be made about Fig. 3.14, the Fourier results at 102.4 min for 0330-0730 UT on 12 August. As an experiment, this period was arbitrarily chosen at a point in the spectrum where energy was relatively high; see Fig. 3.9, where one can see that 102.4 min is not the centre of a peak, as it is in the spectrum for the 20 August event (Fig. 3.11). What can be said about the comparison between the maps in Figs. 3.14 and 3.18? (Both are at the same period, but are from different events.)

One reason for the differences between the amplitude maps is the lack of data in all three components at stations CUL (line 2) and BKR (line 3) in Fig. 3.14, and in Z at DRA and FMD in Fig. 3.18. Since these stations are very important in defining the Central Plains anomaly, it is not surprising that their absence changes the appearance of the maps. Similar, but less drastic, effects are caused at period 47.6 min by the loss of all data from BKR in Fig. 3.12 and Z data from DRA and FMD in Fig. 3.16.

A difference which is more difficult to explain is the disorga-nized Y phase in Fig. 3.14, compared to Y phase in Fig. 3.18; this

cannot be ascribed to phase instability near a minimum in the Y ampli-
tude spectrum, as was done above for X phase in Figs. 3.14, 3.17 and
3.18, because Y energy is high at 102.4 min (Fig. 3.9). Nor does X
amplitude in Fig. 3.14 have the general southward increase which was
described above for X at periods greater than 50 min, i.e. in Figs. 3.17
and 3.18; on the other hand, in both Fig. 3.14 and 3.18, X amplitude
does have a minimum over the Central Plains feature. These peculiari-
ties of X amplitude and Y phase in Fig. 3.14 at the arbitrarily-chosen
period 102.4 min may well result from the way the period was picked,
or they may represent some unknown characteristic of the source field.

One characteristic of the source field which has not been consi-
dered in the data presentation of this chapter is the polarization of
the horizontal field. By using standard monochromatic equations
Bennett and Lilley (1972) have computed the horizontal polarization
parameters at a particular period for an event observed by an array
in southeast Australia. The axes of the normal-field polarization
ellipse are in this case approximately perpendicular to the ocean-
continent interfaces at the East and Southwestern coasts. The relative
size of the Z coast-effect anomalous fields, induced by the normal
horizontal fields, is qualitatively predicted by the ratio of the major
to minor axes. In addition, when the horizontal data are rotated
into the directions of the axes, the phase relationships between
anomalous Z and the normal horizontal components are clarified. To
quote Bennett and Lilley,

... the complicated vertical amplitude and phase

maps ... can be understood more fully by recourse

to the horizontal field polarization ...

Such an approach might help to explain the pecularities of the fields in Fig. 3.14, discussed in the previous paragraph, as well as improve the general results of this chapter.

CHAPTER IV

THE DAILY-VARIATION DATA

4.1  Introduction

Following the analysis of substorm fields described in the previous
chapter, the field observations were scanned to see if a section of
record was available for a study of the geomagnetic daily-variation
fields over the array.  In such a study of data from the 1967 array,
Reitzel et al. (1970) presented a contour map of the range of daily
variation in the Z component on a magnetically-quiet day; refer back
to Fig. 1.10.  The Wasatch Front and Southern Rockies anomalies, which
had been mapped at the periods of substorm fields and attributed to
deep (upper mantle) electrical conductivity structure by Porath et al.
(1970) and Porath and Gough (1971), were obvious on this map also,
in the much longer periods making up the daily variation.  Stations
on the eastern side of these features showed ranges up to 25% greater
than stations to the west of them.  Schmucker (1970a) had observed
similar enhancement in the Z daily variation on his profile further
south at latitude 32.5°N; see Fig. 1.4.  Since these long-period fields
have increased depth of penetration and hence are relatively less
affected by shallow (crustal) structures than the short-period fields,
the observation of these features in the Z daily variation supported
interpretation in terms of deep structure.

One must contrast these large differences in the Z daily variation
with the results of Caner (1971).  At two stations in southwestern
Canada (one in the interior plateau and one in the foothills of the

Rocky Mountains), the Fourier amplitudes at 24-, 12- and 8-hour

periods calculated from 14 consecutive days of simultaneous recordings

of the Z component are equal within the errors of measurement and

computation.  This supports the thesis of Caner et al. (1967) and

Caner (1970, 1971) that the attenuation, west of the Cordillera in

southwestern Canada, of the normal Z field of substorms is due to a

thin conductive layer rather than enhanced conductivity in the upper

mantle as reported in the western and southwestern United States.

## 4.2  Data Selection and Handling

With the two different results of the previous section in mind,

and with a desire to investigate the behaviour at long periods of the

conductor which affects substorm fields so drastically in the

Central Plains, data were selected for a study of the daily variation

over the 1969 array.  From the standard graphical presentation of

the planetary magnetic three-hour-range index Kp, shown as the

"musical diagram" of Fig. 4.1, the time interval 17-22 July 1969 was

chosen as relatively free from disturbance.  The following table shows

the $\Sigma$Kp values, which are the sum of the eight Kp values for each

day, and also the indices Ap and Ci:

Table 4.1

Disturbance indices for 17-22 July 1969

| 1969 July | | $\Sigma$Kp | Ap | Ci |
|---|---|---|---|---|
| | 17 | 8o | 4 | 0.1 |
| | 18 | 6+ | 3 | 0.1 |
| Q | 19 | 4o | 2 | 0.0 |
| Q | 20 | 6+ | 3 | 0.2 |
| | 21 | 9o | 4 | 0.3 |
| | 22 | 15o | 7 | 0.4 |

Q denotes one of the five international quiet days for the month.
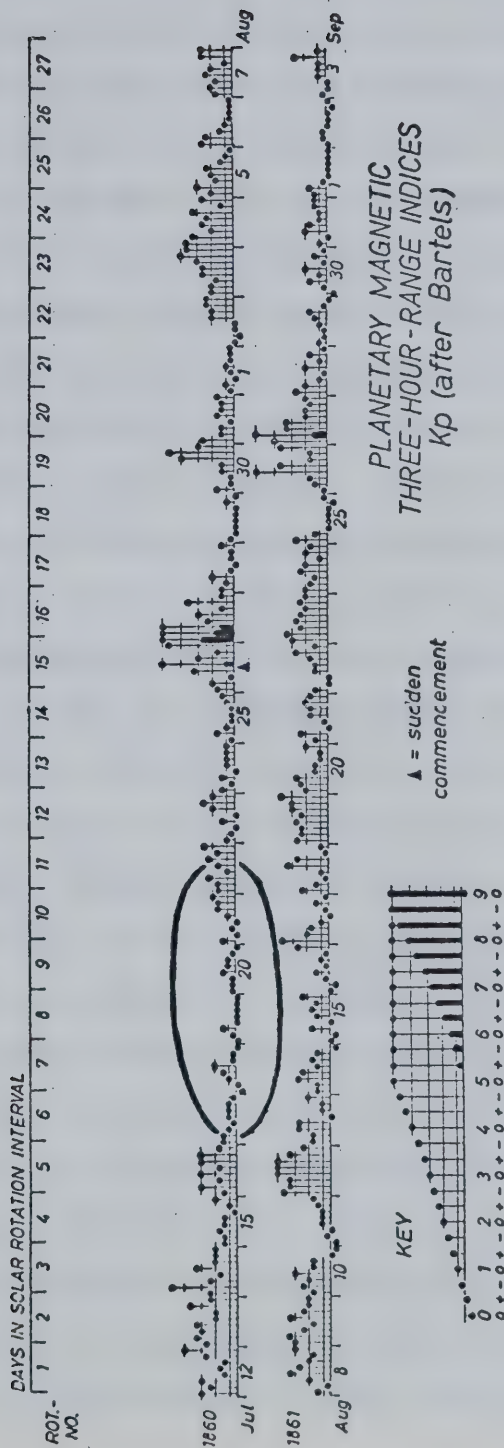
Fig. 4.1  Planetary magnetic three-hour-range indices Kp for 12 July to 3 September 1969.  The array was operational from 17 July to 30 August.  The time interval chosen for daily variation study is encircled.

In this time window, complete data were available for 31 stations, with incomplete observations from 7 others and none from the remaining 8. This gave 106 full traces from a possible 138 (3 components at each of 46 stations) and some partial traces. The recording efficiency here is less than was attained for the substorms of the previous chapter, mostly because of problems with the Accutron watch in some of the variometers. Again a relative timing accuracy of better than 1 minute (perhaps as good as 30 seconds) was maintained, with the aid of the Pi2 micropulsations which accompanied small substorms at about 05 UT on 17 July, 06 UT on 19 July, and 23 UT on 21 July. The micro-pulsations were assumed to occur simultaneously (within a minute or less) over the whole array (Rostoker, 1968).

The analogue records on 35 mm film were projected at a magnifi-cation of 9.4 times by a Durst photographic enlarger onto the D-Mac pencil-follower digitizing table in the Division of Geomagnetism, Ottawa. Only about 1½ hours of record could be projected at one time. This created a problem in choosing a sampling interval. For example, for an interval of ½ hour, energy in the period-band 28 to 32 minutes (associated with substorms) would alias or fold back onto the 24-, 12-, and 8-hour periods of the daily variation. The corresponding period-band for a 1 hour interval is 53 to 69 minutes. The spectra for substorms in the previous chapter show that there can be apprecia-ble energy in both these bands. Unless the energy could be smoothed out before digitizing ("anti-alias filtering"), the daily variation harmonics would be contaminated. It was felt that it would be im-possible to remove variations in these period-bands consistently by

eye when only 1½ hours of record could be viewed at once.  For this
reason, and because a standardized computer processing system was
available in the Division of Geomagnetism, the author decided to use
a much shorter sampling interval (1 min) to avoid the aliasing
problem.

Digitizing was carried out at a sampling interval of 1 cm along
each trace, yielding about 66 points per hour; points at a 1 min
interval were subsequently selected by linear interpolation between
the measured points.  Five and one-half days of records were converted,
from 0000 on 17 July to 1159 on 22 July, yielding 7920 points per
trace for a total of about 800,000 data points.  The data were norma-
lized to gammas using scale factors derived from the in-situ calibra-
tions of the variometers, and were corrected for the interaction
between the H and Z sensing magnets of the University of Alberta
instruments.

The time series were smoothed with a digital recursive low-pass
filter operated in zero phase-shift mode following the fourth-order
Butterworth filter of Alpaslan (1968).  The impulse response and the
gain vs. period characteristic of the filter are shown in Fig. 4.2.
The gain of the filter is flat within 0.1 db to 60 min period and is
down by 6 db at 30 min and by more than 45 db at 15 min.  The impulse
response is about 180 minutes long; data points to at least this
length were rejected from the beginning and end of the filtered series.
Every fifth point was selected from the filtered series, producing
1440 points at a 5 min sampling interval covering the 5 days from 0600
on 17 July to 0555 on 22 July.
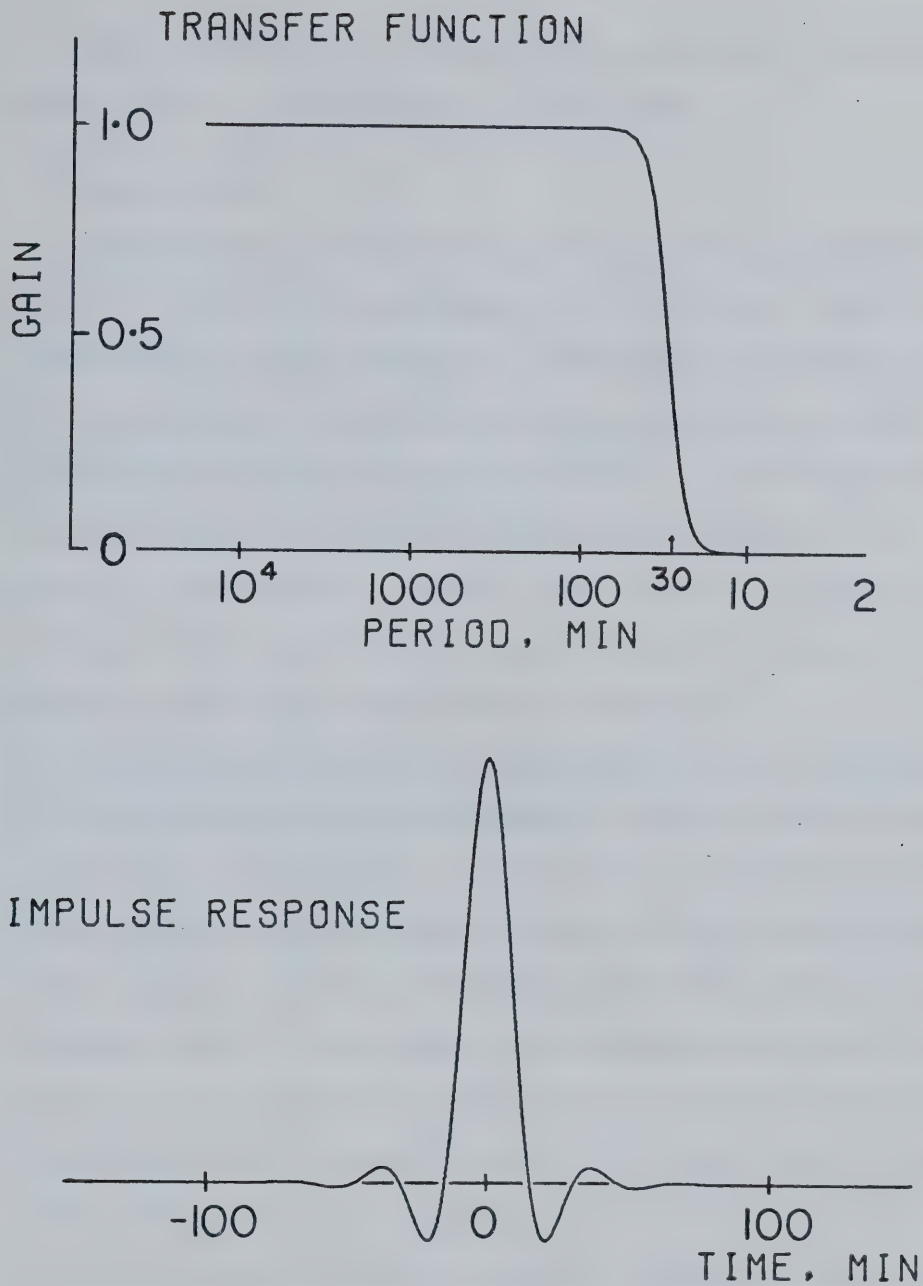
Fig. 4.2 Characteristics of the digital low-pass filter (fourth-order Butterworth, recursive, zero phase-shift) with high-frequency cutoff (-6db) at T = 30 min.

These are termed the long-period data, by contrast with the short-period data for substorms of the previous chapter.

4.3 Magnetograms

Magnetograms for the five days 17-22 July 1969 are presented in Figs. 4.3 (line 1, the northernmost), 4.4 (line 2), 4.5 (line 3), and 4.6 (line 4, the southernmost). The format is the same as used for the short-period data of the preceding chapter, with stations plotted from east to west going down the page. All the station code-names are shown on the figures, even though some components are missing at some stations. Vertical lines mark 00 UT. Downward Z, northward H and eastward D are positive. Note that Z is plotted with twice the sensitivity of the other two components.

General impressions from the magnetograms include the uniformity of the daily-variation wave from station to station across the array, especially in the horizontal components; and the variability of the shape of the wave from one day to the next. Similar generalizations could be made for the data of Riddihough (1969) from observatories in northwest Europe. In more detail, the H component here, while changing slowly from one station to the next, decreases rather consistently in amplitude from the northeast corner of the array (station CHA on line 1 of Fig. 4.3) to the southwest (station MID on line 4, Fig. 4.6). D does not. The Z component can apparently change much more rapidly from one station to the adjacent one than do H and D, presumably because anomalous Z fields, associated with inhomogeneous electrical conductivity structure in the earth, add to a normal Z field which is
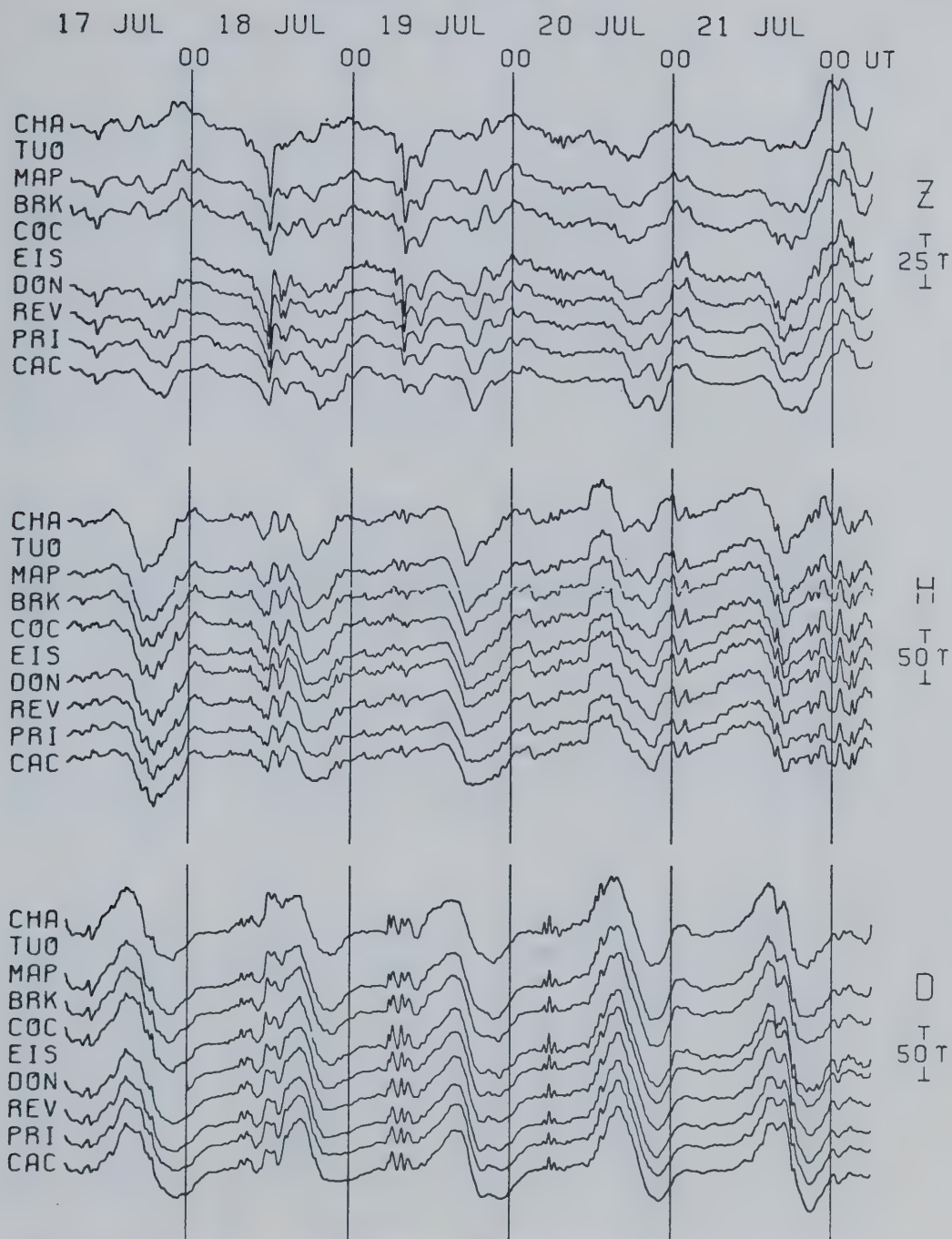
Fig. 4.3  Magnetograms for 17-22 July 1969, line 1.
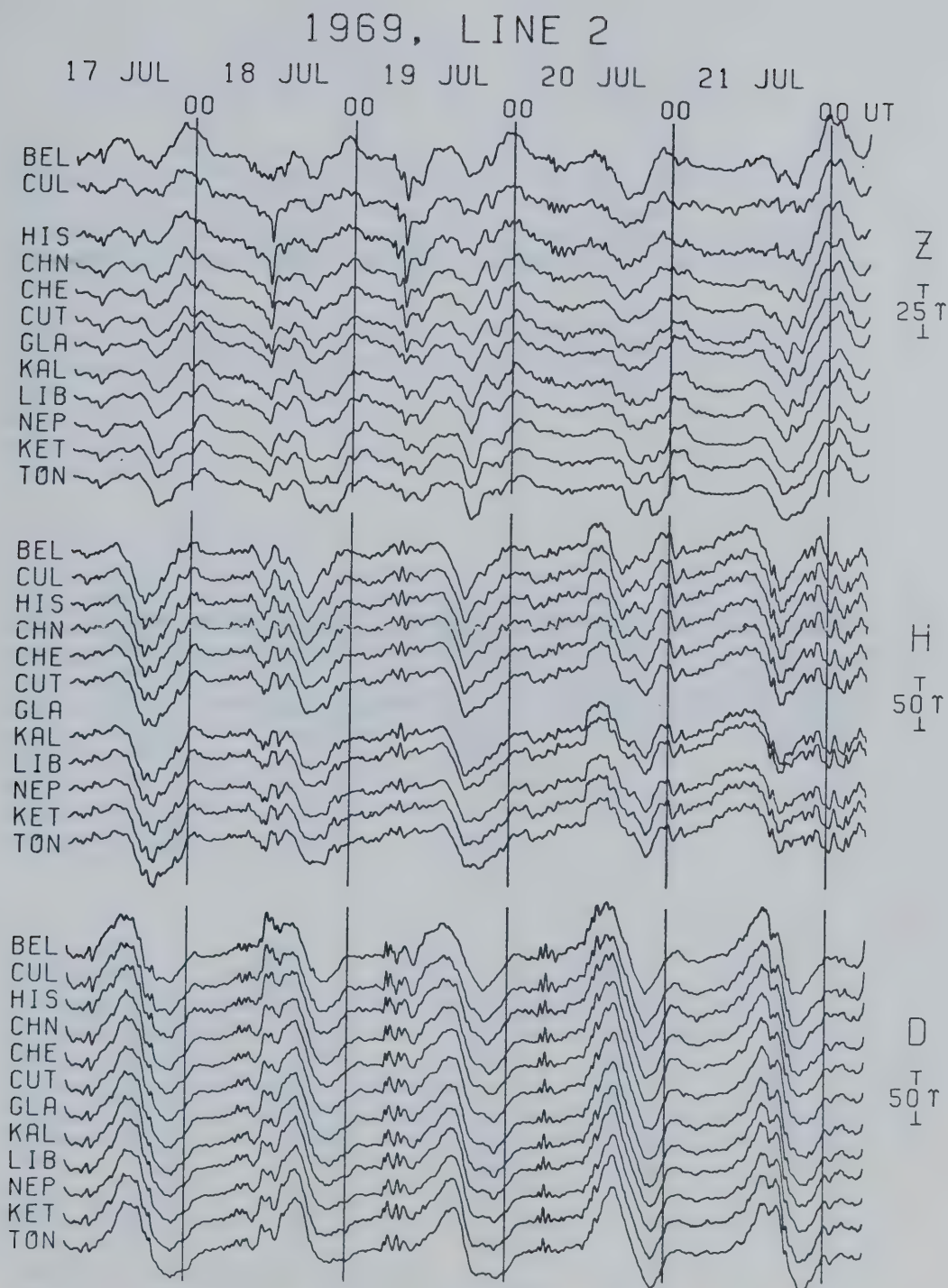
Fig. 4.4  Magnetograms for 17-22 July 1969, line 2.
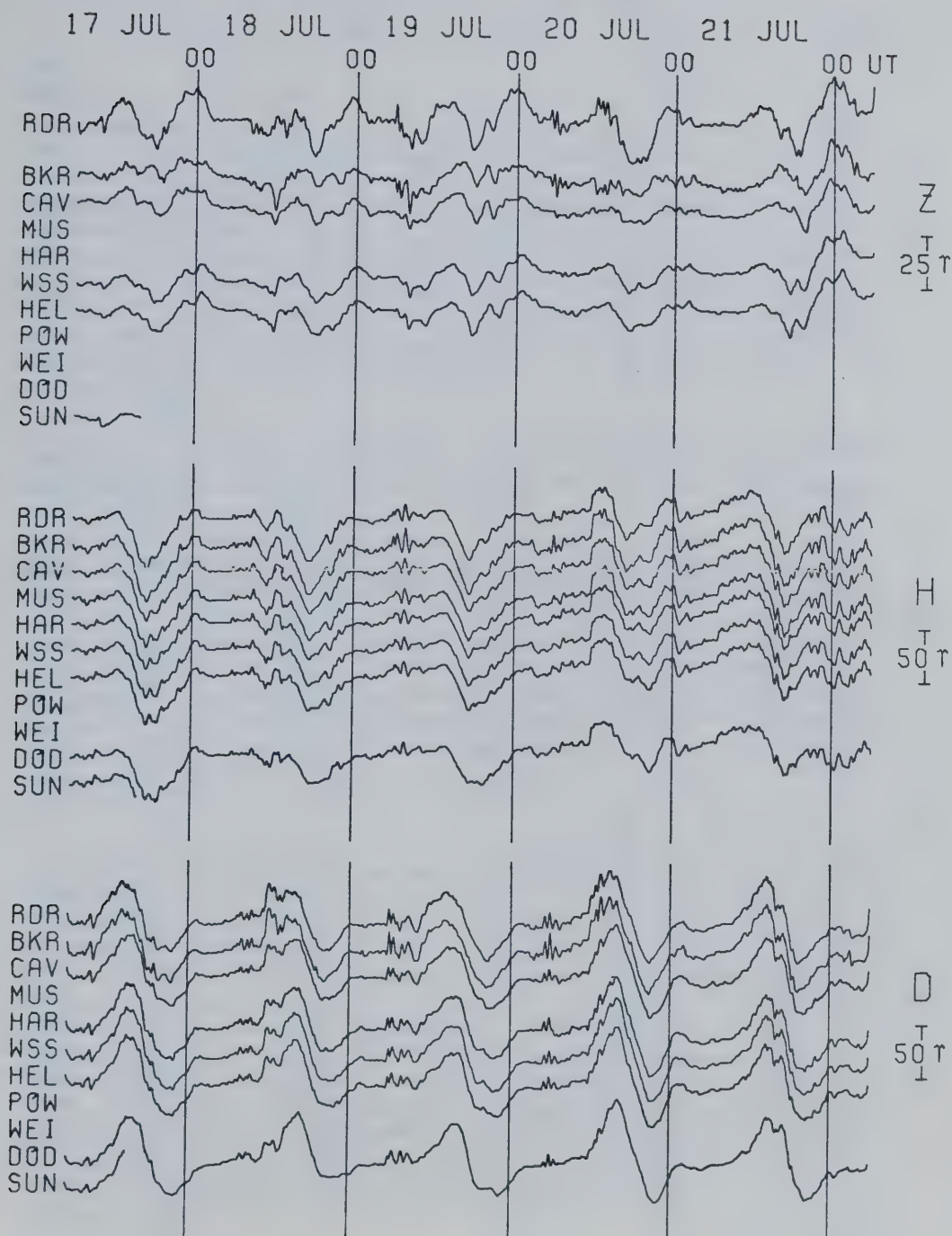
Fig. 4.5  Magnetograms for 17–22 July 1969, line 3.

# 1969, LINE 4
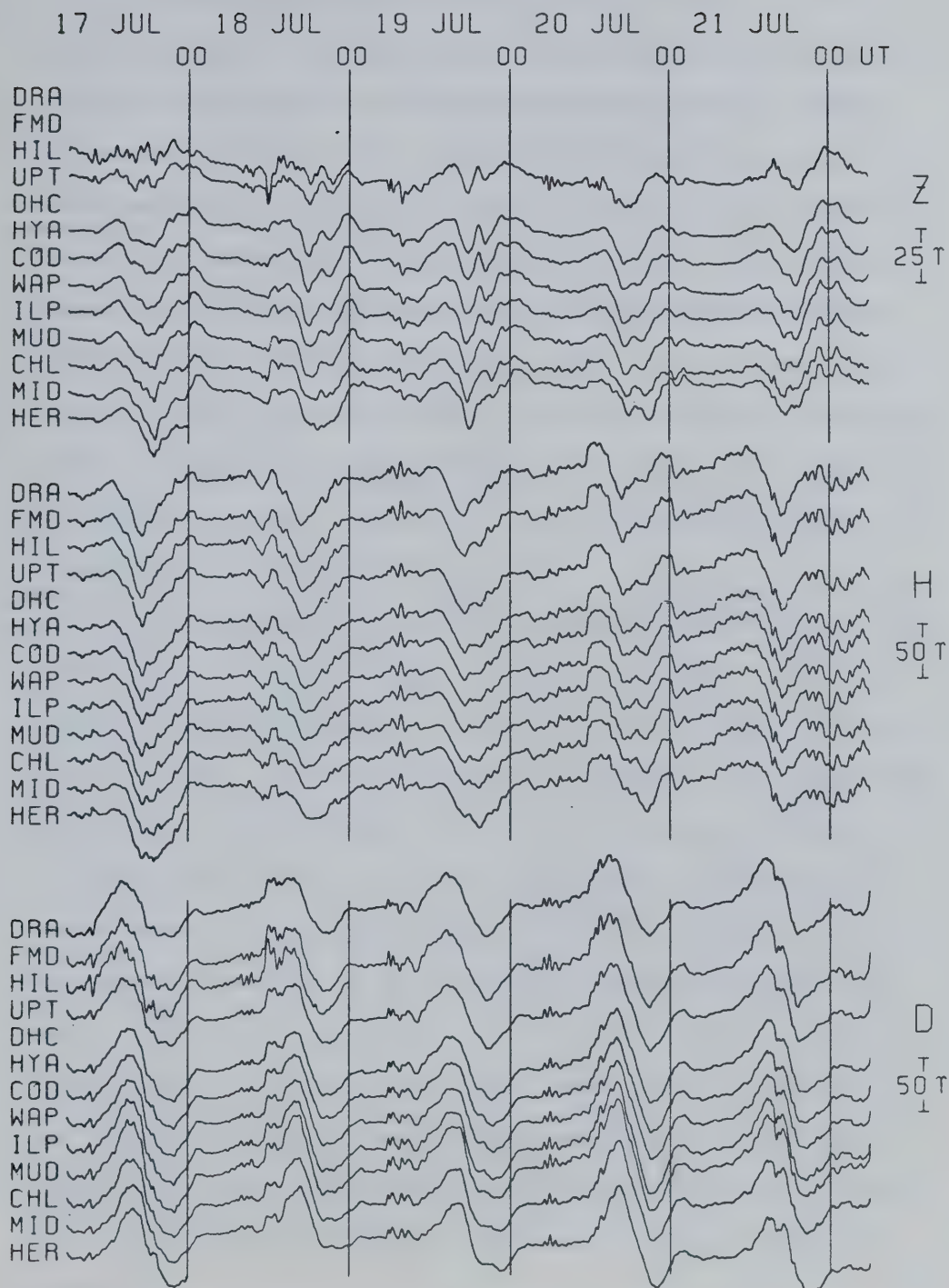


Fig. 4.6  Magnetograms for 17–22 July 1969, line 4.

smaller than the normal H or normal D fields.

Turning from the daily-variation wave for a moment, short-period events in Z, in these data at for example 08 UT on 19 July and 12 UT on 18 July, are strongly attenuated at stations towards the west end of line 1 (Fig. 4.3) and line 2 (Fig. 4.4). This characteristic has already been discussed in the previous chapter on substorm fields, and is the main effect on these fields of the transition from the Great Plains to the Northern Rockies at these latitudes (Caner, 1971; Porath et al., 1971). It is obvious from an inspection of the magnetograms that *the daily variation in Z does not suffer the attenuation that characterizes the short-period events in the Northern Rockies.* Caner (1971) reports the same observation in this region, as mentioned in Section 4.1.

The North American Central Plains anomaly (Camfield et al., 1971; Porath et al., 1971) is present in Z over a wide range of periods, including the daily variation, at BEL (Fig. 4.4), RDR (Fig. 4.5) and HIL (Fig. 4.6). The daily variation in Z appears to have double the amplitude at BEL and RDR that it has at the respective adjacent stations CUL and BKR, which in turn have slightly suppressed amplitudes compared to their respective neighbours HIS and CAV. In D, the anomaly shows only at short periods for RDR and BKR (Fig. 4.5) and for FMD and HIL (Fig. 4.6). It is present but less prominent at short periods in D for CUL (Fig. 4.4). Thus *at the long periods of the daily variation, the Central Plains anomaly affects the vertical component far more strongly than the transverse horizontal component,* an unusual result for which an explanation is suggested in the next chapter.

Notice, for the long-period variations in the magnetograms, that anomalous Z at BEL (Fig. 4.4) and RDR (Fig. 4.5) does not look like normal D, as it did for short-period substorms (e.g. Figs. 3.1-2), but that anomalous Z looks like an amplified version of normal Z. This suggests that for the daily variation the vertical field is the inducing field. This is verified by the phase relationships between the Fourier transforms of the components, to be presented in Section 4.5. This mechanism contrasts with the process of induction by the horizontal field at short periods.

## 4.4 Fourier Spectra

Discrete Fourier transforms of the time series were computed to study the frequency content of the variation fields and the frequency response of anomalies. As in Section 3.3, the Fourier amplitude is the square root of the sum of the squares of the Fourier coefficients, and the Fourier phase is defined so that a more positive value for phase implies a waveform shift to a later time. A rotation of the horizontal components to geographic coordinates was first carried out to correct for the change of declination across the array. A straight line fitted by least squares to the data points of each series was subtracted from the series to remove the mean and any linear trend before transformation. A cosine-bell window was not applied to the data before transformation, as is often done to reduce leakage from spectral peaks (Black, 1970), because tests with synthetic data showed that leakage would be negligible in this particular case. A fast Fourier subroutine, DES002 from the Applications Program Library,

Computer Science Centre, Dept. Energy, Mines and Resources, Ottawa, was used to compute the coefficients for the 1440-point series; this subroutine is based on the multi-radix development by Singleton (1968) of the algorithm of Cooley and Tukey (1965).

With a subroutine which will handle a series representing an integral number of complete days, coefficients could be calculated at frequencies corresponding exactly to those known for harmonics of the daily variation. The daily variation consists essentially of the harmonics at 1, 2, 3 and 4 cpd (cycles per day) i.e. periods of 24, 12, 8 and 6 hours, although higher harmonics may be important at low geomagnetic latitudes (Gupta and Chapman, 1969). Because these frequencies are fixed and not distributed randomly, a smoothing of the Fourier coefficients was not attempted in the way usually carried out in a spectral analysis where no prejudgment is made of frequencies present in the data (Gupta and Chapman, 1969). The frequency resolution of the transform is the reciprocal of the length of the time series (Black, 1970, p. 239); here it is 0.2 cpd. This relatively poor resolution, a reflection of the rather short length of data available, also contributed to the decision not to smooth the estimates since this would have reduced the resolution further. The data length (5 days) is long enough, however, to prevent distortion of the Fourier amplitude at the lowest frequency of interest (1 cpd) due to the finite length of data (Toman, 1965).

The Fourier amplitude spectra for frequencies 0.2 to 9 cpd are plotted in Figs. 4.7 (line 1), 4.8 (line 2), 4.9 (line 3) and 4.10 (line 4). The peaks at 1, 2 and 3 cpd are well-developed in all three
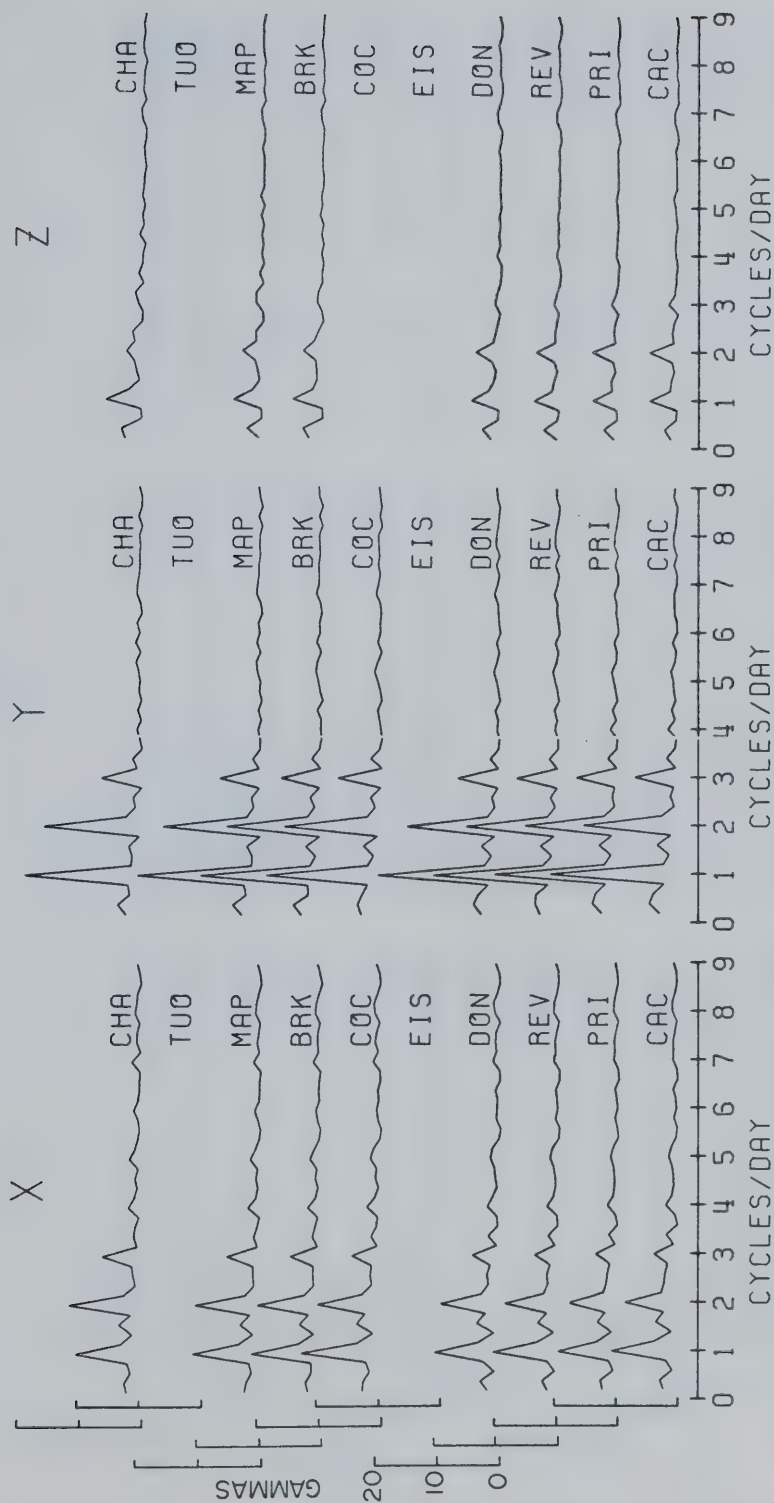
Fig. 4.7  Fourier amplitude spectra for daily variation on line 1.
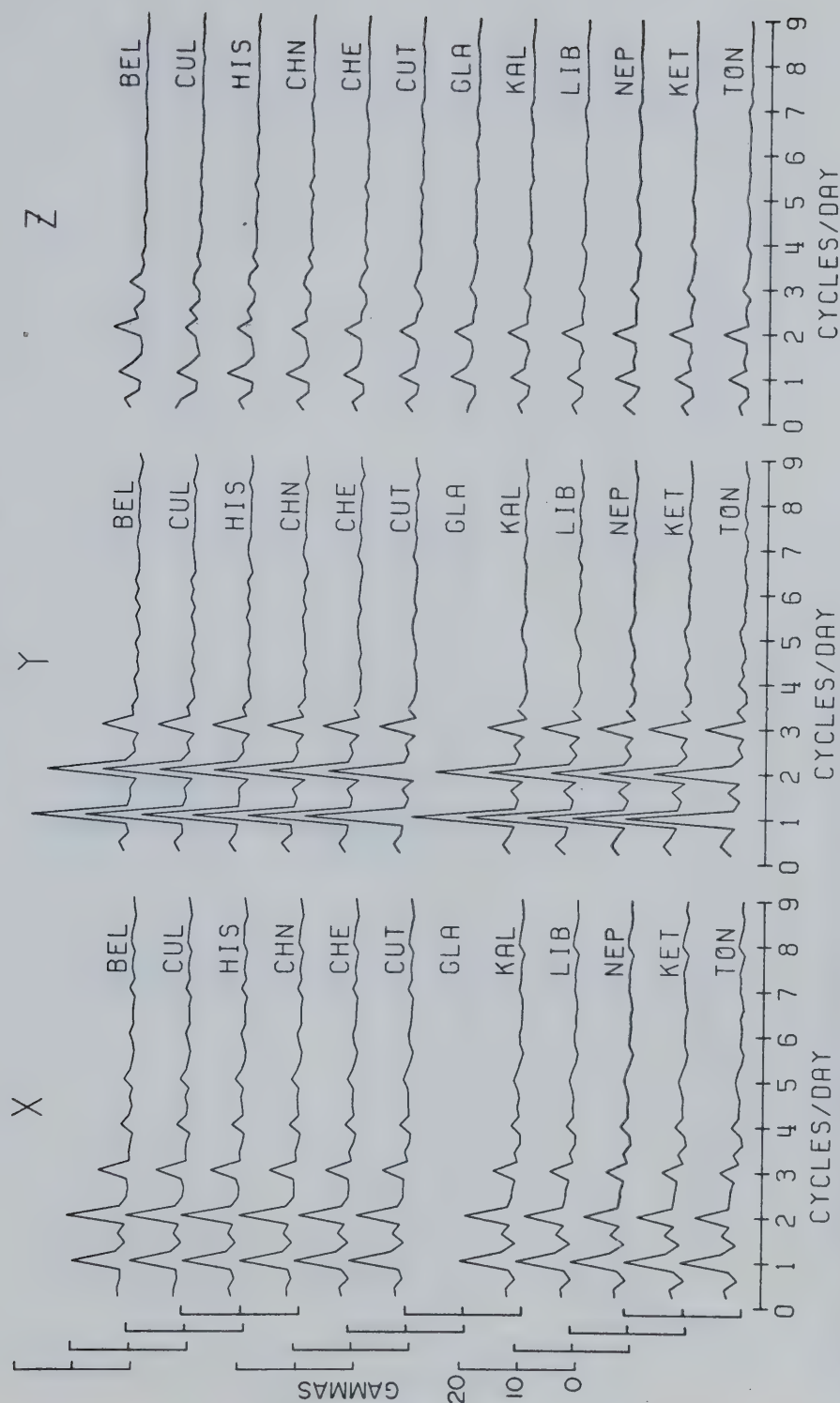
Fig. 4.8  Fourier amplitude spectra for daily variation on line 2.
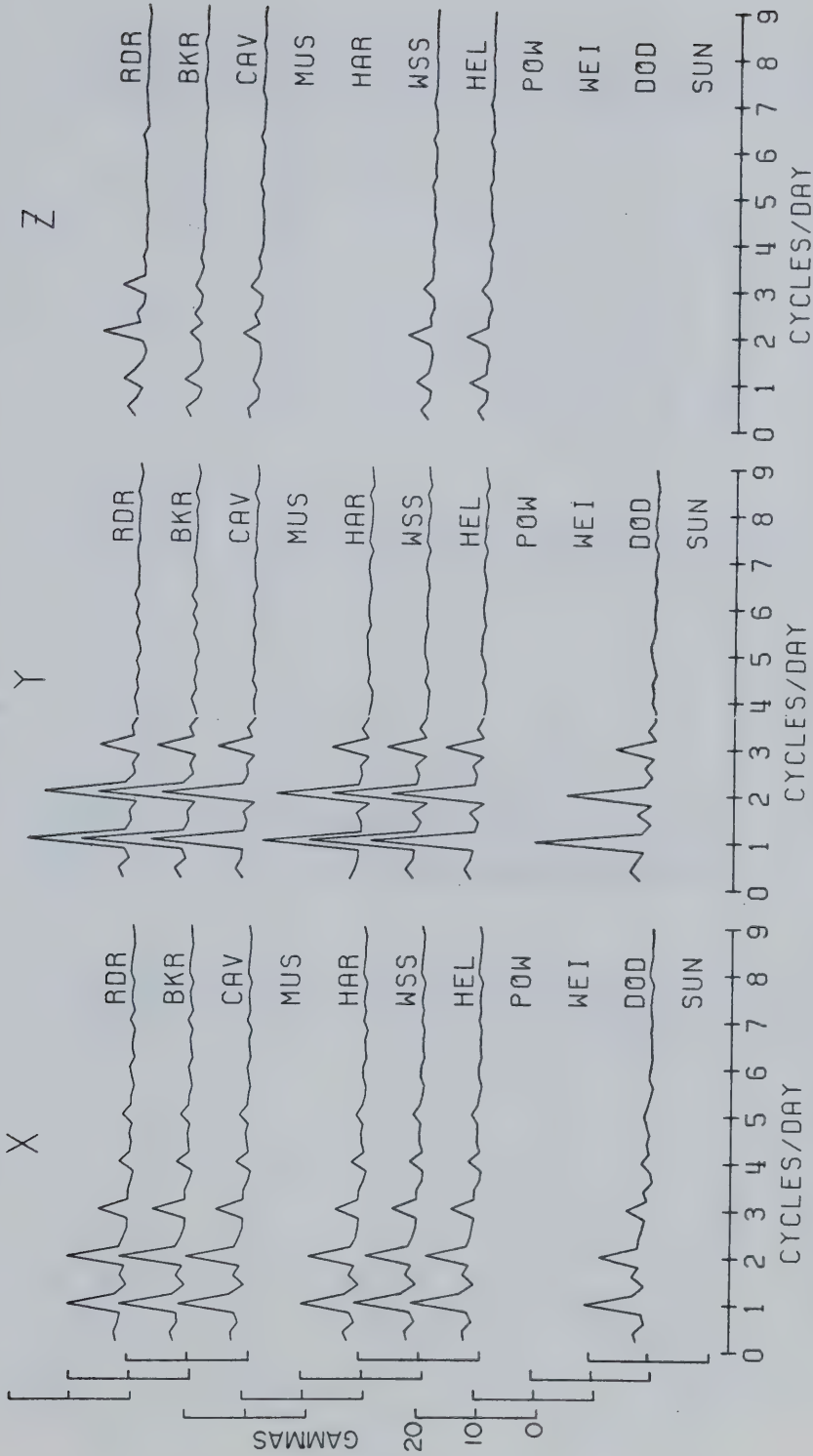
Fig. 4.9  Fourier amplitude spectra for daily variation on line 3.
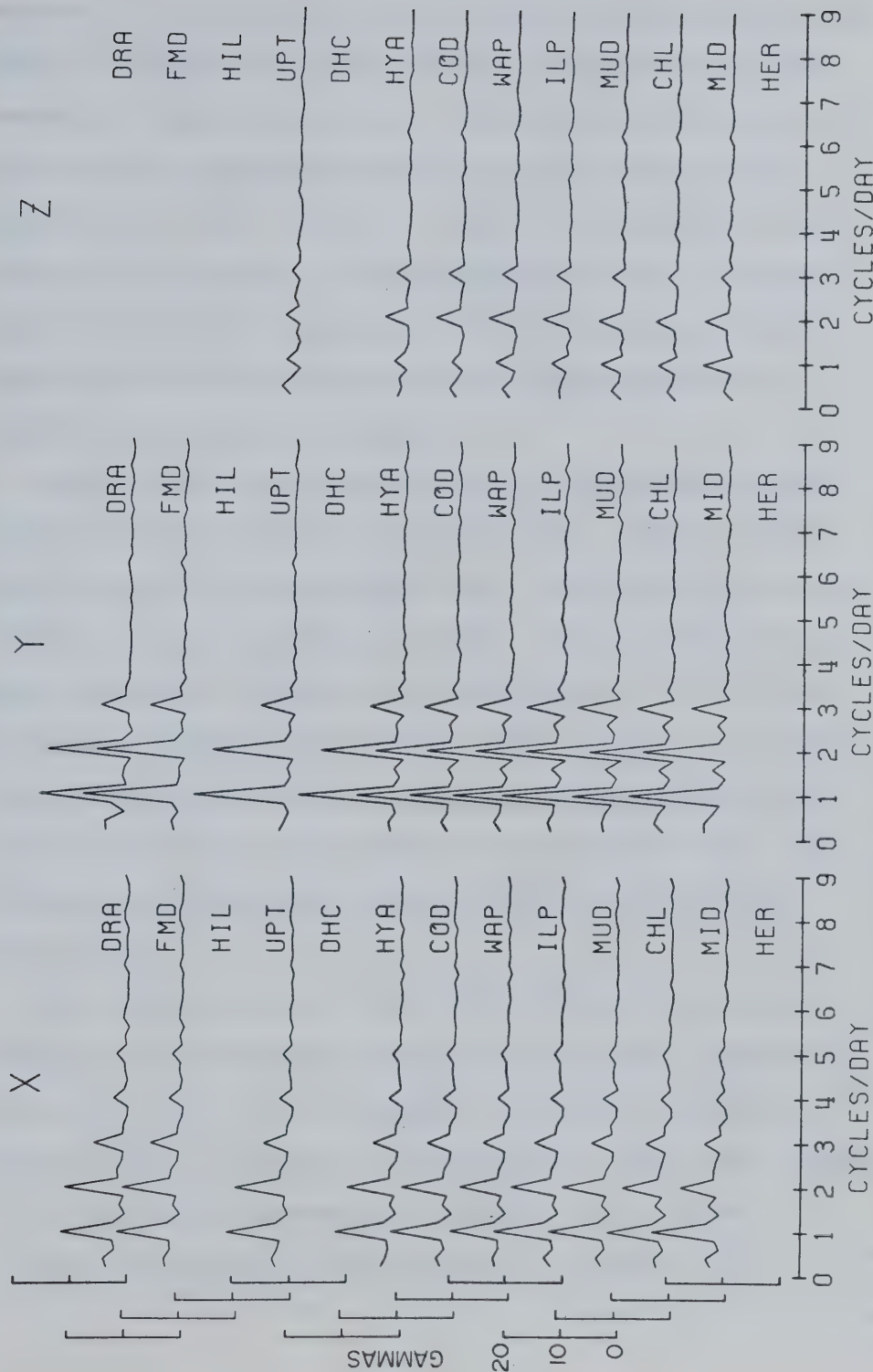
Fig. 4.10  Fourier amplitude spectra for daily variation on line 4.

components. The 1 and 2 cpd peaks have about the same amplitudes; the peaks at 3 cpd have about half the height of those at the two lower frequencies. Small peaks at 4 and 5 cpd (6- and 4.8-hour periods), and sometimes at higher frequencies, can be seen in most of the X spectra but are absent in Y and Z. A look back to the magnetograms of Figs. 4.3-6 shows that the daily variation in D and Z is fairly smooth and sinusoidal in shape, while H is more angular, and hence suggests that H will require more energy at higher harmonics to represent it in a Fourier synthesis.

Fisher's (1929) test of significance in harmonic analysis, as extended by Nowroozi (1967) and Shimshoni (1971), provides a formal way of determining the plausibility that a certain peak in a spectrum represents a real periodicity in the data and is not simply due to a random fluctuation. A check of the coefficients for BEL utilizing the tables of Shimshoni shows that the peaks in X up to and including 5 cpd are significant at the 99% confidence level; peaks in Y and Z can be accepted at this level only up to and including 3 cpd. This confirms what one might have suspected simply by looking at the spectral plots.

Since the calculation of the Fourier coefficients $a_i$ and $b_i$ is equivalent to a least-squares process (see, for example, Hildebrand, 1962, p. 252), one can use the results of analysis of the least-squares procedure to estimate the errors in the coefficients. Formulae given by G.V. Haines (personal communication) are as follows:

The standard error in the coefficients is given by $S\sqrt{2/n}$ ,

where $S^2 = \dfrac{\sum\limits_{i=1}^{n} y_i^2 - n\bar{y}^2 - \dfrac{n}{2} \sum\limits_{i=1}^{p} (a_i^2 + b_i^2)}{n - 2p - 1}$ (4.1)

for $n - 2p - 1$ degrees of freedom. $\bar{y}$ is the mean of the n data points $y_i$; $\bar{y} = 0$ in this case. Similar formulae are given by Braddick (1954, pp 40-43).

The second summation in the expression for $S^2$ was evaluated using only the $a_i$ and $b_i$ corresponding to the 1, 2 and 3 cpd peaks for Y and Z, and to those of 1 to 5 cpd for X. The significance test outlined above and the prominence of these peaks in the spectra of Figs. 4.7-10 provide the rationalization for this selection. Hence p is 3 for Y and Z and 5 for X, implying, with n = 1440, degrees of freedom numbering 1433 for Y and Z and 1429 for X. Repeated calculations which included more terms yielded smaller standard errors, so estimates given below with p = 3 or 5 are upper limits.

Results for RDR, BKR and CAV show standard errors for the amplitudes at both 24 h and 12 h of 2% for X, 1% for Y, and up to 8% for Z. At 8 h the standard errors for X and Y are larger (4%) because the amplitudes at 8 h are smaller than at 12 h and 24 h, while for Z the errors are about the same (up to 9%). These estimates may be somewhat conservative.

Morrison et al. (1968) have determined that the rms amplitude of a sinusoid, digitized sufficiently often, can be estimated numerically to better than 1% if at least 4 cycles of data are available. This gives one further confidence that the 24 h Fourier coefficients, computed here from 5 cycles of data, are sound.

The spectral peaks for Y at 1 and 2 cpd in Figs. 4.7-10 have the same relationship to each other at all stations, with the 1 cpd peak being consistently greater than the 2 cpd. For X, on the other hand, this is not the case. The 1 cpd peak is less than the 2 cpd in the northeastern part of the array; the former then increases while the latter decreases as one traverses southwesterly, until the relative peak heights are reversed, with the 1 cpd peak being larger than the 2 cpd in the southwest. Along any one line of stations this appears as an east-to-west trend; if all four lines are considered together, it is really northeast-to-southwest. In section 4.3, the magnetograms indicated a general decrease in H amplitude from northeast to south-west, and it is suggested that the change in the ratio of the 1 and 2 cpd peak heights is the manifestation in the spectra of this obser-vation. If the daily variation in H is crudely visualized as a single cycle of a sine wave at 12-hour period which repeats once every 24 hours, then the decrease in the height of the 2 cpd peak would represent the decrease in the H amplitude.

The spectra also show the effects which were noted in the magneto-grams in Section 4.3 in the Northern Rockies and in the Central Plains. Passing from stations in the Great Plains into the Northern Rockies, the peaks in Z do not change significantly; this is best seen on line 2 (Fig. 4.8) where the data are complete, but it is also evident on line 1 (Fig. 4.7). For the Central Plains anomaly, the peaks in Z at 2 and 3 cpd are strikingly enhanced at BEL (Fig. 4.8) and RDR (Fig. 4.9), while at the stations adjacent to each of these, CUL and BKR respectively, these peaks are somewhat attenuated relative to their

respective neighbours HIS and CAV. At these stations the peaks in
Y, which is transverse to the structure, show no apparent modifica-
tion, an unusual effect which has already been noted in the previous
section on magnetograms.

4.5 Maps of Spectral Components

Contour maps of Fourier amplitude and phase for the three main
harmonics of the daily variation at stations in the array are shown
in Figs. 4.11 (period 24 h), 4.12 (12 h) and 4.13 (8 h). In addition,
amplitudes and phases for X at 4 and 5 cpd (periods 6 h and 4.8 h)
are presented in Fig. 4.14; Fisher's test of significance in harmonic
analysis accepted these peaks for X but not for Y or Z. (See
Section 4.4). X maps at 8 h from Fig. 4.13 are included in Fig. 4.14
for comparison. Contouring has been done by hand using linear
interpolation between stations. Small circles on the maps indicate
the location of magnetometers; stations for which there are no data
are not shown. These are the primary results of the investigation
of the daily variation, but discussion of them will be delayed until
some relevant points have been made concerning related phase maps
(Figs. 4.15-17).

Phases are in minutes of time, i.e. in fractions of a cycle
multiplied by the appropriate period in minutes. Uncorrected phases
are relative to 06 UT. They have then been adjusted for the motion
of the source field due to the rotation of the earth by subtracting
from them the local time difference (geographic longitude difference
multiplied by 4 min per degree) between each station and the

1969 July 17-22   T = 24 h

X amplitude

X phase

Y amplitude

Y phase

Z amplitude

Z phase

Fig. 4.11   Fourier amplitudes (in gammas, with contour interval 0.2γ)
and corrected phases (in minutes of time, with interval 10
min for X and Y and 25 min for Z) for the 24-hour component
of the daily variation.
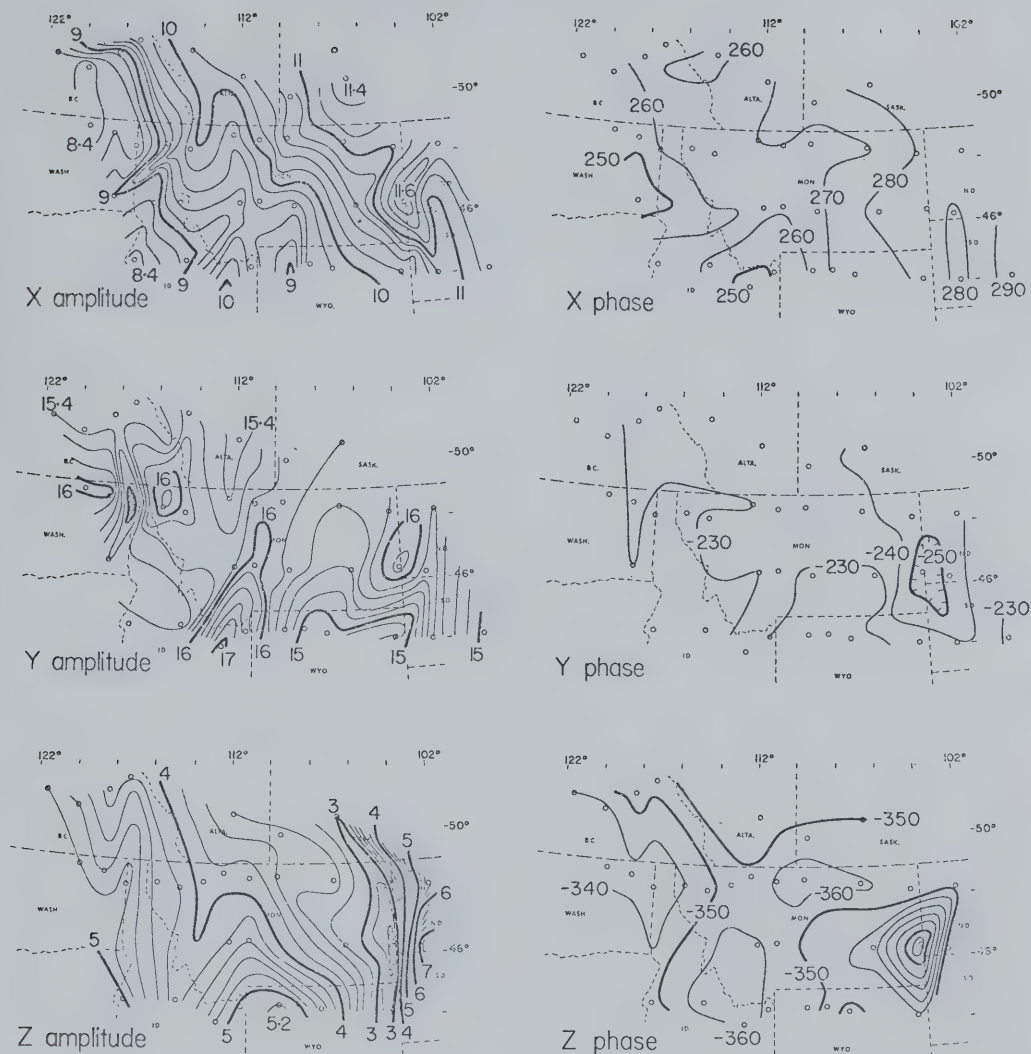
1969 July 17-22   T = 12h



Fig. 4.12   Fourier amplitudes (in gammas, with contour interval 0.2γ) and corrected phases (in minutes of time, with interval 10 min) for the 12-hour component of the daily variation.

1969 July 17-22   T = 8h
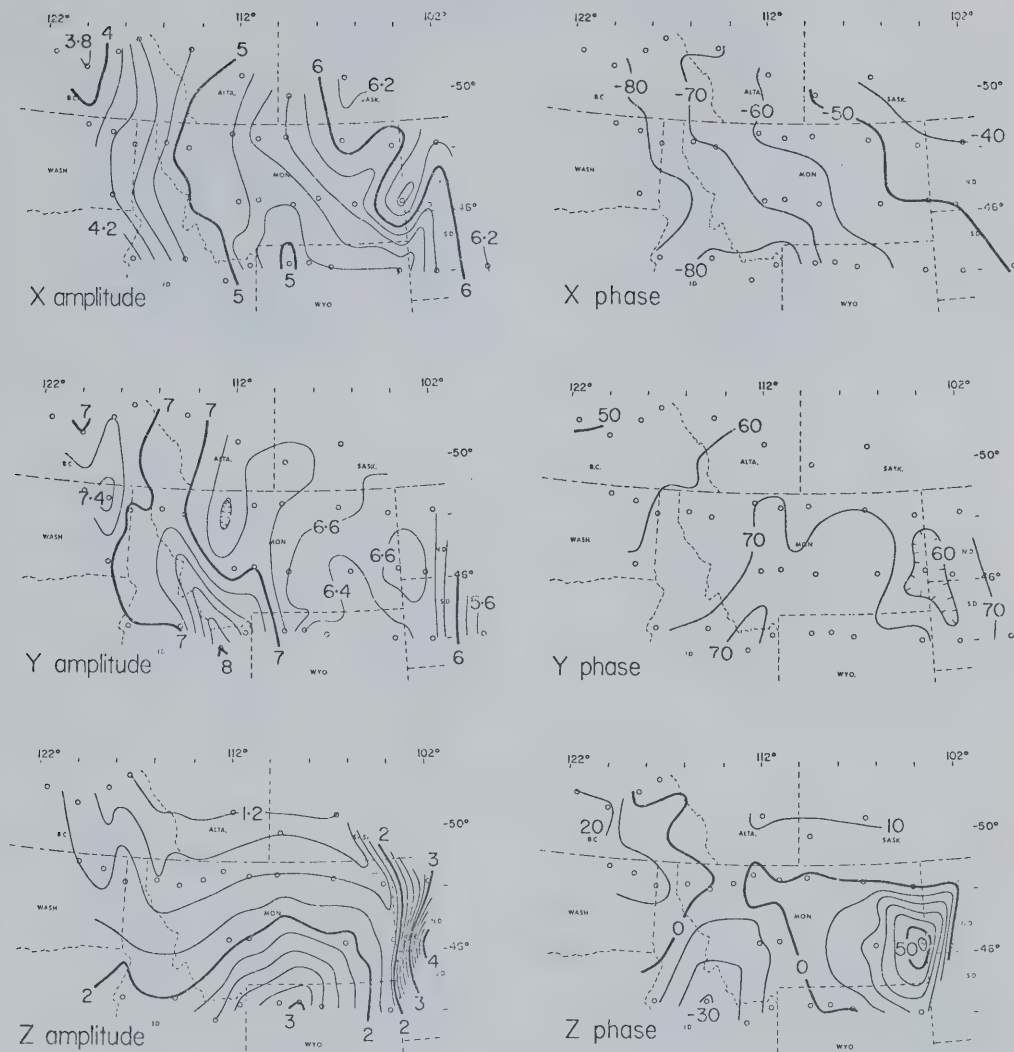


Fig. 4.13  Fourier amplitudes (in gammas, with contour interval 0.2γ)
            and corrected phases (in minutes of time, with interval 10
            min) for the 8-hour component of the daily variation.
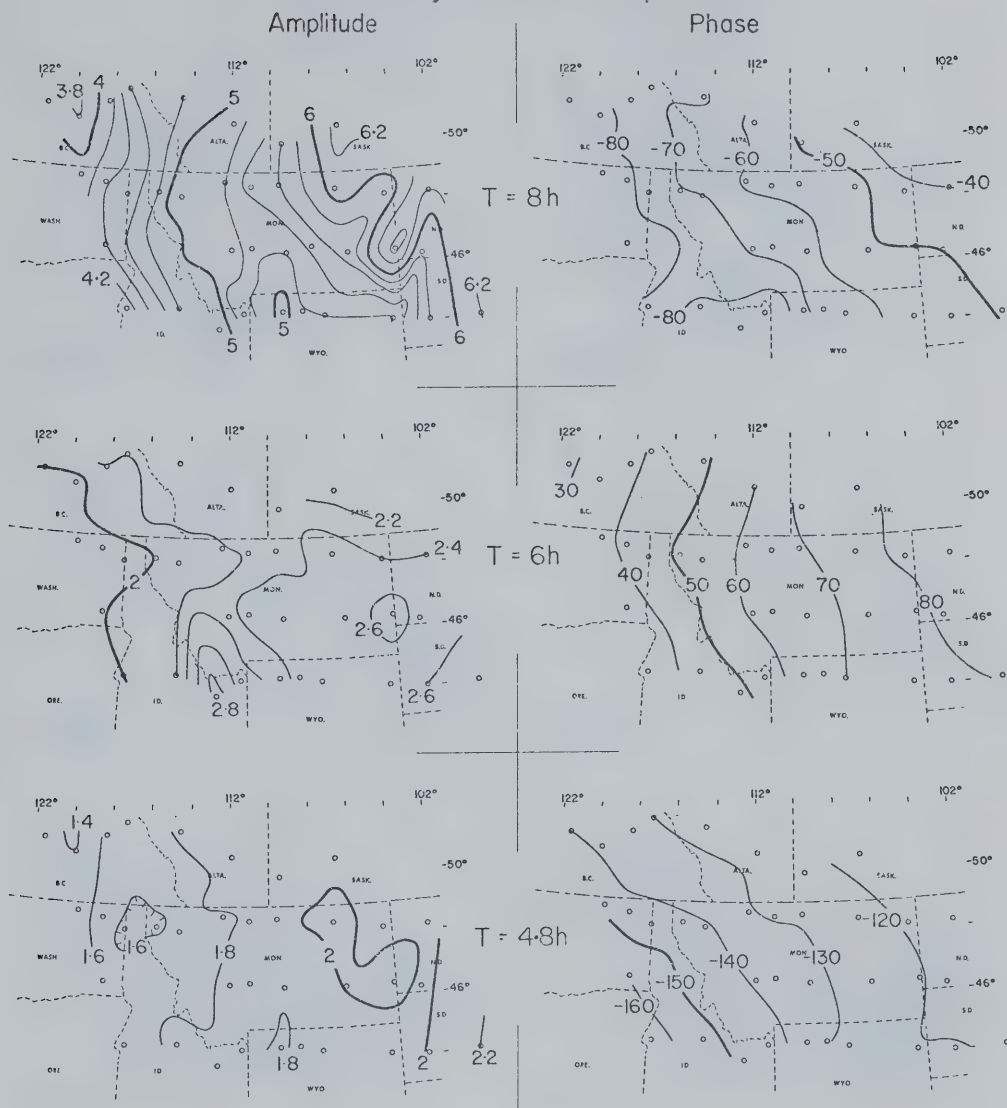
Fig. 4.14   Fourier amplitudes and corrected phases for the X component
of the daily variation at periods 8, 6 and 4.8h.
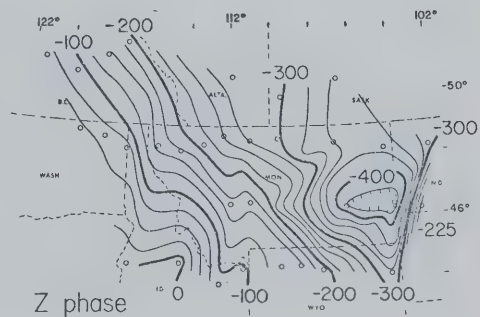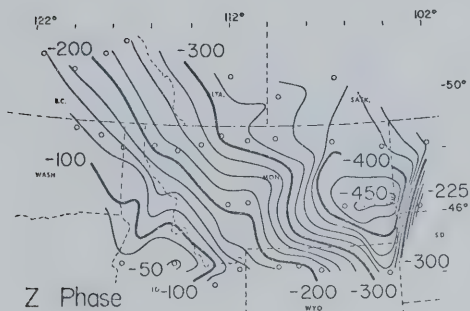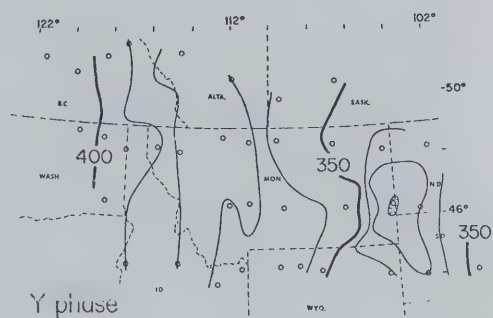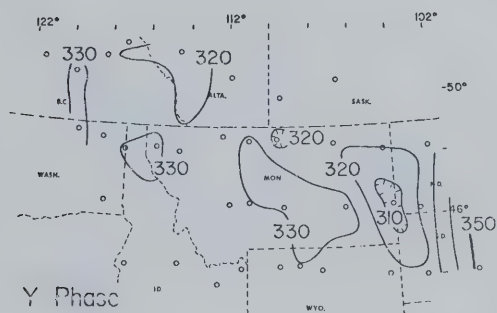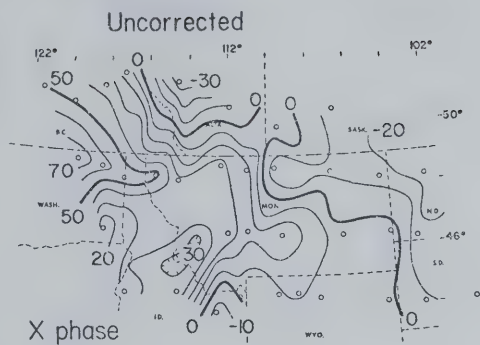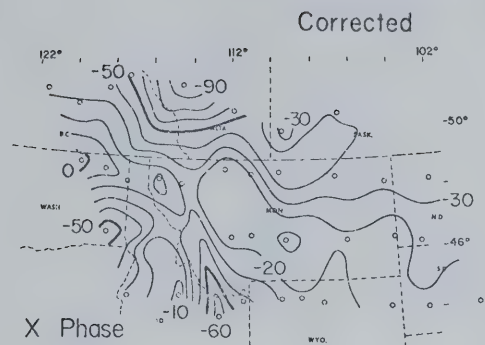
Fig. 4.15   Fourier phases, uncorrected (right) and corrected (left) for the local time difference between each station and the easternmost (DRA), for the 24-hour component of the daily variation.   Contour interval 10 min for X and Y, 25 min for Z.
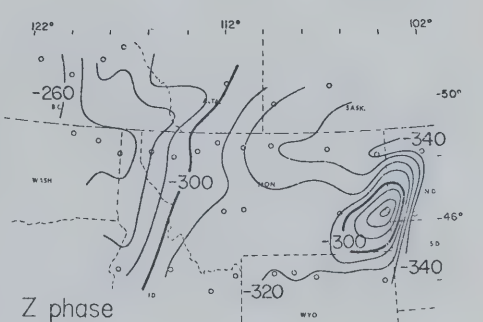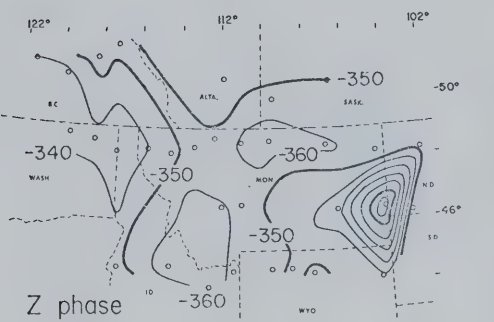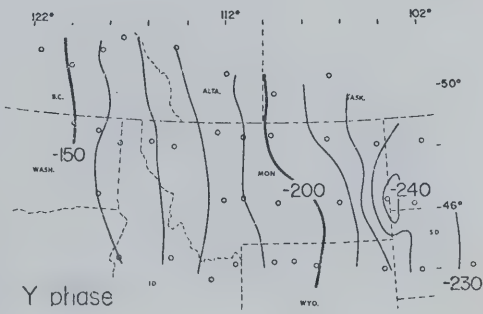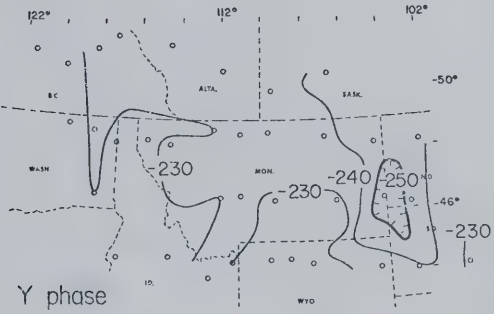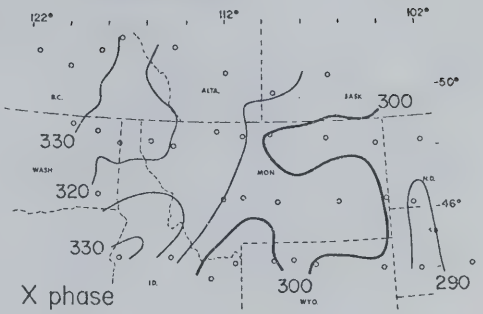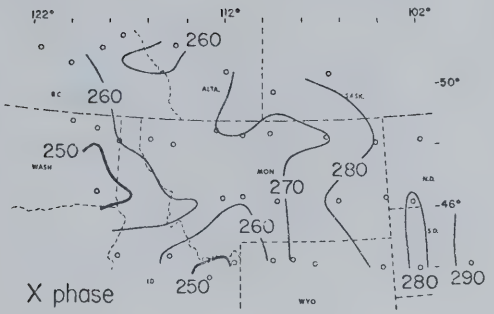
Fig. 4.16  Fourier phases, uncorrected (right) and corrected (left) for the local time difference between each station and the easternmost (DRA), for the 12-hour component of the daily variation.  Contour interval 10 min.

Fig. 4.17 Fourier phases, uncorrected (right) and corrected (left)
for the local time difference between each station and
the easternmost (DRA), for the 8-hour component of the
daily variation. Contour interval 10 min.
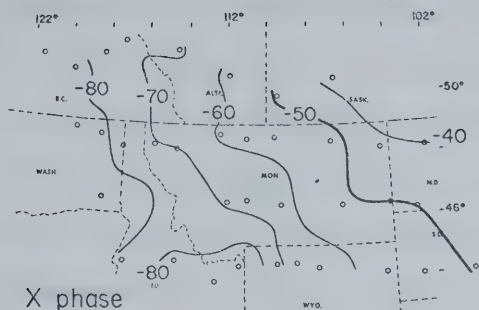
easternmost station DRA (longitude 100.5°W). This yields the corrected values. Both the uncorrected and the corrected phases are mapped in Figs. 4.15 (period 24 h), 4.16 (12 h) and 4.17 (8 h).

In the uncorrected phase maps for the Y component at all three periods, a westerly motion of the source field is clearly evident in the east-to-west phase increase; recall that a phase increase implies a waveform shift to a later time, from east to west. This can also be seen in the magnetograms in Figs. 4.3-6; the daily variation in D arrives at an increasingly-later universal time across the array. The corrected Y maps show no smooth trend, confirming that the proper allowance has been made for the rotation of the earth. The Z maps at 12 h (Fig. 4.16) and 8 h (Fig. 4.17) support the same observation, although it is somewhat masked by local phase anomalies due to induction. In the Z map at 24 h (Fig. 4.15), there is a local phase anomaly at the eastern edge of the array, but over the rest of the map the effect of the earth's rotation is completely hidden in a dominant regional change which will be discussed later.

In the phase maps for X (Figs. 4.14-17), the correction seems merely to reverse the direction of the regional gradient and does not produce any significant clarification. This may be related to the way the phase of a Fourier component is affected both by change in shape of a waveform and by its arrival time. In the magnetograms of line 2 (Fig. 4.4), for example, the shape of the D waveform for the daily variation does not change very much along the line for four of the five days, the exception being 19 July where the minimum appears considerably broadened towards the west

end of the line.  Thus the phase for D, and for Y, should reflect

mainly the steadily-increasing delay in the arrival of the waveform

at stations from east to west.  For H, on the other hand, the

opposite comment can be made about the waveform :  only on one day

(17 July) does it have relatively-constant shape.  The change in

shape would affect the phases for X, and hence these phases cannot

be interpreted as unambiguously as could those for Y.

To return to the primary results of this section, amplitudes

and corrected phases for the three main harmonics of the daily

variation are mapped in Figs. 4.11-13.  In an attempt to verify the

results, especially at 24 h, the Fourier coefficients were

recomputed for the first four days 17-21 July only, to check their

stability.  These values are plotted in Fig. 4.18 for period 24 h.

The small differences which exist between this set of maps and

that at the same period in Fig. 4.11 are due as much to the incon-

sistencies of hand-contouring as to changes in the coefficients

themselves, and probably indicate the degree of uncertainty which

should be associated with this method of data presentation.  The

anomalies in Fig. 4.11 are at least several times as large as the

standard errors in the Fourier transform amplitudes discussed in the

previous section.

The general impression of the data is one of rather surprising

complexity in all components except for phases at 12 h (Fig. 4.12)

and 8 h (Fig. 4.13) and Y phase at 24 h (Fig. 4.11).  The anomalies

in Z amplitude and phase at 12 h and 8 h near the eastern edge of

the array are associated with the Central Plains feature, and will
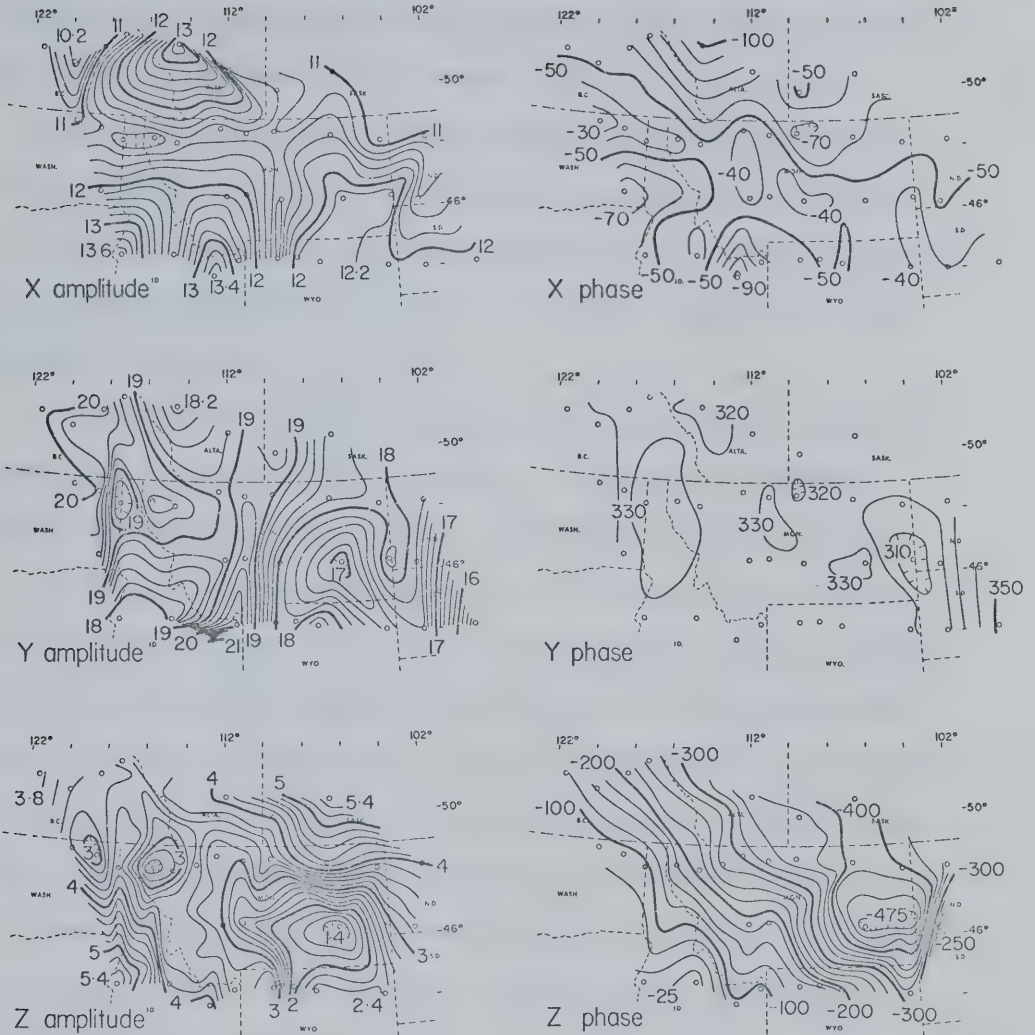
Fig. 4.18  Fourier amplitudes and corrected phases at period 24 h, as computed from four days' data.

be discussed later. If they are disregarded for the moment, *the amplitude maps become increasingly complex with increasing period.* Most of the complexity can be explained in terms of anomalous fields associated with the local conductors detected by the short-period fields, as discussed in the previous chapter, or in terms of variable lateral transmission, through these or other conductors, of anomalous fields originating by induction in conductive bodies outside the array.

Consider first the anomalies associated with local conductors detected by the short-period fields. It is useful to consult again the location map (Fig. 2.1). The Wasatch Front is marked in northern Utah, near the centre of the southern edge of the map, at the contact between the Basin and Range Province and the Middle Rockies. In Section 3.4, it was noted that the Y and Z amplitude maps at short periods may just show the variation anomaly associated with the Wasatch Front, as reported further south by Reitzel et al. (1970). At the longer periods of the daily variation, there is clearer evidence of this anomaly. In the Y fields at 8 h (Fig. 4.13) and 12 h (Fig. 4.12) a ridge of high values decreases northwards from south eastern Idaho into southwestern or western Montana, respectively. For both these periods, a corresponding broader semi-circular anomaly in the Z fields is appropriately positioned in northwestern Wyoming and central Montana, to the east of the feature in Y. At 24 h (Fig. 4.11), the northward extension of the high Y amplitudes can be seen in western Montana, as at 12 h, but the Z anomaly in northwestern Wyoming is cut off by the intense minimum in Z over

eastern Montana.  Observations supporting an anomaly at the Wasatch

Front can also be found in X amplitude and phase, especially at

24 h (Fig. 4.11).

The anomalies in Y and Z, with the exception of Z at 24 h,

terminate north of line 3 in the centre of the array, even though

the short-period results suggested that the actual structure ends

south of the array near latitude 44°N.  This is quite conceivable;

the large skin depths at the periods of the daily variation (see

Table 4.2) would certainly permit the detection of fields due to

anomalous currents flowing some distance from the array.  From

both the short- and long-period results, then, we would conclude

that there is no reason to believe that the Wasatch Front anomaly

continues northward to connect with the Northern Rockies anomalies.

Before the other features on the maps are discussed in

detail, a digression will be taken to consider the expected depth

of penetration of the daily-variation fields, and seismic evidence

for a laterally-heterogeneous upper mantle.

A uniform electromagnetic wave incident on a uniform infinite

half-space (flat earth) will have a penetration depth, or skin

depth, at which the amplitude is attenuated to 1/e of its surface

value, given by

$$\delta = \frac{1}{(2\pi\omega\sigma\mu)^{\frac{1}{2}}} \tag{4.2}$$

where $\omega = 2\pi/T$ is the angular frequency of the wave, $\mu$ the magnetic

permeability of the half-space (usually assumed to be that for free

space) and σ the electrical conductivity of the half-space [all in
e.m.u. (c.g.s.) units]. In deriving this expression, an assumption
equivalent to $\delta \ll \lambda/2\pi$ must be made, where $\lambda$ is the wave length
characteristic of the spatial non-uniformity of the incident field.

In convenient units, for T in hours and σ in mhos per metre,

$$\delta = 30.2 \sqrt{\frac{T}{\sigma}} \text{ km} \tag{4.3}$$

See, for example, Schmucker (1969) and Bullard (1967). Table 4.2
shows some representative numbers.

Table 4.2

Skin depth vs. conductivity for a uniform half-space

| Conductivity $\sigma, \Omega^{-1} m^{-1}$ | Skin Depth $\delta$, km | | |
|---|---|---|---|
| | T = 24 h | T = 12 h | T = 8 h |
| 1 | 148 | 105 | 86 |
| $10^{-1}$ | 468 | 331 | 270 |
| $10^{-2}$ | 1480 | 1050 | 860 |
| $10^{-3}$ | 4680 | 3310 | 2700 |

These numbers refer to a uniform flat earth. For a uniform
spherical earth, Bullard (1967) remarks that, for the correct use
of the concept,

... the skin depth should be much less than both the
radius and the wave length of the applied field ...

A non-uniform spherical earth, such as that of Lahiri and Price

(1939), is more realistic for investigating the penetration of the

daily variation. The conductivity distribution proposed by these

authors, which fits the observed ratio of external to internal

spherical harmonics for both the daily variation and the storm-

time variation $D_{st}$, has three main features: a thin conductive

outer shell (as, for example, a uniform ocean of depth 0.5 km); a

resistive zone ($10^{-3}$ to $10^{-4}$ $\Omega^{-1}$ $m^{-1}$) to a depth from the surface

of at least 200 to 300 km, and possibly to 600 km; and a very

rapid increase in conductivity to at least 1 $\Omega^{-1}$ $m^{-1}$ over the

depth range 600 to 700 km. If the conductivity is assumed to

continue to rise with increasing depth, this radial distribution can

be represented in functional form (model "d" of Lahiri and Price)

by

$$\sigma(r) = (2 \times 10^3) \, \delta(r-a) + (4 \times 10^{-3}) \, (r/a)^{37} \tag{4.4}$$

in metric units, where a is the radius of the earth and $\delta(r-a)$

is the Kronecker-delta function, in order to calculate the depth

of penetration of the induced currents. For the daily variation

at T = 12 h, more specifically for the surface spherical harmonic

$P_3^2$, Lahiri and Price predict that the induced currents flow mainly

between the depths 300 and 1000 km, being maximum at 800 km and

negligible below 1300 km. At T = 24 h, the current maximum will

be at a depth greater than at T = 12 h, but not by factor $\sqrt{2}$ as in

a uniform flat earth, because of the very rapid increase in

conductivity below 600 km.

Schmucker (1970b) gives curves of attenuation vs. depth for the tangential component of the magnetic field in a non-uniform spherical earth "d*" modified from "d" of Lahiri and Price by the inclusion of a conductive zone in the upper-most mantle (80-100 km depth). Skin depths for the $P_3^2$ harmonic are listed for various conductivities of a 4 km-thick surface layer:

<div align="center">

Table 4.3

Skin depths at T = 12 h for
radially-symmetric earth models

</div>

| | Surface layer conductivity $\Omega^{-1} \, m^{-1}$ | Skin depth km |
|---|---|---|
| (ocean) | 4 | 410 |
| (sedimentary basin) | 0.5 | 710 |
| (standard continent) | 0.1 | 730 |

Thus theory predicts that the incident daily variation field will sample to increasingly greater depths in the earth as period increases, and so observations which show increasing complexity of the field with increasing period such as those in Figs. 4.11-13 can be interpreted as evidence against increasing homogeneity with depth in the electrical conductivity of the upper mantle.

Previous geomagnetic deep sounding by our groups (Reitzel et al., 1970; Porath and Gough, 1971; Porath, 1971a) has suggested lateral heterogeneity in the electrical properties of the upper mantle in the western U.S. In the same region, seismic studies have also reported lateral heterogeneity in the upper mantle, in

this case in the structure of body-wave and surface-wave velocities,
and in the absorption factor Q; see, for example, Hales et al. (1968)
and Archambeau et al. (1969). More generally, in his review,
Kanamori (1970) writes:

... Based upon the surface-wave and body-wave results
it is now agreed that the mantle beneath shields has
much higher seismic velocities than those beneath
ocean and tectonically-active regions. At such tec-
tonically-active regions as Japan, Basin and Range
Province of the western U.S., and the Pacific Ocean
side of South America, the upper mantle velocities
have been found to be significantly lower than the
average ... Horizontal heterogeneities as large as a
few percent in velocity and one order of magnitude in
Q have been found beneath mid-oceanic ridges and island
arcs ... These ... can be interpreted in terms of many
factors such as composition, temperature and [/or]
partial melting ...

See also Herrin (1969).

Thus seismic evidence supports the premise of heterogeneity
of the upper mantle on the scale of tectonic provinces. Evidence
from geomagnetic depth sounding, in the maps of Figs. 4.11-13,
could suggest that such heterogeneity may exist in the upper
mantle on smaller distance scales, but one cannot be dogmatic
about this on the basis of this limited amount of data. It must
be recognized, however, that the anomalies in the daily-variation
fields in Figs. 4.11-13 are spatially much too sharp to arise

from sources several hundreds of kilometers below them, ruling out small-scale heterogeneities in the upper mantle.

So, we have the apparent contradiction that the increasing complexity of the fields with increasing period points to inhomogeneity in electrical conductivity structure with increasing depth, at depths appropriate to induction at the periods of the daily variation, while the spatial characteristics of the anomalies in the fields will not support sources at such depths. An explanation of these observations begins with interpreting the massive regional change in the phase of Z at 24 h (Fig. 4.11). If the local phase anomaly in eastern Montana is disregarded, the corrected data show a uniform phase increase totalling *5 to 6 hours* from north-east to south-west across the array. This contrasts with the Z phases at 12 h and 8 h (Figs. 4.12-13), which show essentially no regional phase variation.

This detachment of the 24 h spectral phases of Z from those at 12 h and 8 h is quite different from the phase anomaly for the daily variation of Z in Japan, as reported by Rikitake et al. (1956) and summarized by Rikitake (1959) and Rikitake (1966, pp 261-2). Observatories in central Japan show corrected phases at all the periods 24 h, 12 h and 8 h which are 60 to 80 min less than phases at locations in both northern and southern Japan, expressing the earlier occurrence of the mid-day minimum in Z which is easily seen on magnetograms from central Japan. Rikitake et al. (1956) suggested that this phase anomaly could be explained if the resistive zone in the upper mantle under central Japan

extended to a depth of 700 km, 300 km deeper than a world-wide average depth of 400 km. Rikitake (1956) speculated that the thickening of the resistive zone might be caused by the penetration of a slab of resistive material with geometry similar to that of the inclined seismic zone beneath Japan, into the more-conductive mantle below; in the terms of plate tectonics, Rikitake (1971) interprets the resistive slab as the cold (hence resistive) down-going lithospheric plate beneath Japan.

Again, though, the Japanese anomaly in the phase of the Z daily variation is not the same as the result for the array in southwestern Canada and the northwestern U.S., primarily because the feature in Japan shows at all three periods 24 h, 12 h and 8 h, while the North American one is only at 24 h. Any model which explains the Japanese situation is not likely to help resolve this puzzle unearthed by the 1969 array.

The clue to escaping from this dilemma hinges on noticing in Fig. 4.11 what happens to the phase of Z at 24 h after it has changed so dramatically by 5 hours from northeast to southwest (D.I. Gough, personal communication). In the southwest, *Z is now in phase with X.* This means that anomalous Z associated with X must contribute to the Z field at the daily variation periods, and at 24 h must dominate the phase pattern. The lateral inhomogeneity at which the anomalous east-west currents flow is not the Cordillera but can only be the northern edge of the huge conductive region beneath the Basin and Range and the Southern Rockies, which is within a slant distance laterally from the array equal to the skin depth at 24 h.

Confirmation for this idea of anomalous Z induced by H in the southwest can be seen by looking back to the magnetograms, especially those for MID (Fig. 4.6) on 18 July when the Z and H traces have very similar form. By comparison, there is no resemblance between Z and H at CHA, MAP or BRK in Fig. 4.3; these stations are too far from the induced currents to detect the anomalous fields.

Why, though, does the Z phase map at 24 h (Fig. 4.11) differ so greatly from those at 12 h and 8 h (Figs. 4.12 and 4.13)? First, the amplitudes of the anomalous Z fields over the array at 12 h and 8 h are attenuated by exp ($\sqrt{2}$) and exp ($\sqrt{3}$) with respect to those at 24 h because of the lateral distance, measured in skin depths, between the anomalous currents and the array. Second, normal Z and normal X at 12 h and 8 h in the northeast of the array are almost in phase anyway; in terms of shifting Z into phase with X, anomalous Z could affect the normal Z phase by at most 90 min at 12 h and 50 min at 8 h. Such possible phase changes are small compared with the potential of the corresponding figure of almost 7 h at period 24 h. These two factors combine to yield negligible phase effects at 8 h and 12 h but the massive one at 24 h.

Having established from the phase map at 24 h that the Z field is strongly influenced at 24 h, and presumably to a lesser extent at 12 h and 8 h, by anomalous fields associated with currents under the Basin and Range province, we return to the amplitude maps of Figs. 4.11-13 to see how they can be interpreted in the light of this evidence for fields reaching the array obliquely from beneath.

Large minima in Y and Z amplitude exist in eastern Montana

at 24 h (Figs. 4.11 and 4.18) but are not seen at 12 h (Fig. 4.12)

or at 8 h (Fig. 4.13). The explanation for this feature must lie

in the phenomenon of variable lateral transmission of anomalous

fields originating outside the array, especially here because the

anomaly is present only in the Y and Z minima at 24 h, the longest

period, at which the fields have the greatest lateral diffusion

distance. The "illuminating" source is the induced currents in the

Basin and Range conductor, and the "target" which casts the Y and

Z "shadows" (minima) would be the conductive ridge beneath the

Wasatch Front (Porath and Gough, 1971). Notice that the same conduc-

tor is responsible for both a direct induction anomaly (discussed

earlier in this section) and also a variable transmission anomaly.

This example illustrates the conditions under which a variable

transmission anomaly will occur (Camfield and Gough, 1972):

   a) a large conductor laterally displaced from the array,

      as source of the anomalous field

   b) large variations in conductivity in the region inter-

      vening source and array

   c) suitable slant distance from source to array: less

      than the absorption length in the resistive sectors of

      the intervening region, but greater than this length

      in the conductive sectors. Here, absorption length

      is numerically equal to skin depth. This condition

      will probably be met only at long periods.

Both absorption and refraction will be involved in the process

of variable lateral transmission. If absorption predominates, then

one can argue that the absence of the Y and Z minima in eastern
Montana at 8 h and 12 h (Figs. 4.12-13) implies that insufficient
anomalous field diffuses through the resistive sectors between
source and array at 8 h and 12 h to provide the background against
which a variable transmission anomaly could be seen.  The presence
at 24 h and the absence at 8 h and 12 h suggest, from slant skin-
depth considerations alone, that the average conductivity along
resistive transmission paths must be of the order of  0.02 to
0.04 $\Omega^{-1}m^{-1}$.  Recognition that the X inducing fields, and hence
the anomalous sources, decrease in magnitude with decreasing
period (see the X amplitude maps of Figs. 4.11-13) points to
values at the smaller end of this range.

On the other hand, refraction will be important in cases of
even moderate lateral conductivity contrast, because the index
of refraction for an electromagnetic wave in a conductive medium
involves the square root of the conductivity.  An upwelling or
ridge on the surface of a good conductor, such as the Wasatch Front
conductive ridge, could behave as a crude and irregular cylindri-
cal lens and would produce a distorted, defocussed image (D.I.
Gough, personal communication).  If the eastern Montana anomaly
at 24 h is produced in this way, by refraction of the anomalous
fields through the Wasatch Front conductor, then the geometry will
be critical, and the appearance of the anomaly at 24 h only may be
related to the appropriately-greater average depth of induced
(source) currents under the Basin and Range at this period.

It could be mentioned in passing that seismic results from

LASA, the large-aperture seismic array in this part of eastern
Montana, suggest significant variations in the thickness and/or
velocities of the crust (Glover and Alexander, 1969) and perhaps
in the thickness of the low-velocity layer in the upper mantle
(Iyer and Healy, 1972). If the variation anomaly at 24 h is related
in any way to either of these results, it would most likely be to
the second.

More difficult to interpret are the local anomalies in the
region of the Northern Rockies found in the long-period data at
positions similar to those indicated by the short-period results.
At 24 h, a profile extracted from the amplitude maps in Fig. 4.11
along line 2 would show, for Y, high values at the west end (stations
TON and KET) decreasing sharply to a minimum at NEP, followed by
a rise to a maximum at LIB and KAL. The Z maximum corresponding
to the western Y maximum is shifted eastward to NEP; a Z minimum
centred at LIB separates the western Z peak from a second peak over
GLA. The location of these Y and Z features would be consistent
with two internal current systems flowing approximately at the
Rocky Mountain Trench and at the front range of the Northern
Rockies; the Y and Z maps show that the currents would be confined
to an approximate north-south orientation. Lack of data here in
Y at GLA, in Z at DOD, and in Y and Z at POW and WEI may have
reduced the definition of these anomalies.

A detailed consideration of the Y and Z amplitude maps at
12 h (Fig. 4.12) and 8 h (Fig. 4.13) could lead to the same
suggestion of two internal currents. The evidence at 12 h is as

good in Y but not quite as clear in Z as at 24 h; at 8 h it is
somewhat less so again, in both components. Possibly this could
arise because the normal Y field which would induce the anomalous
currents is larger at 24 h than at the other two periods; the
Fourier component amplitudes for normal Y are about 20, 16 and 7γ
at 24, 12 and 8 h respectively.

Thus one interpretation of the local anomalies at long periods
in the Northern Rockies region would be in terms of internal
currents along conductive structures. However, there are a number
of objections. The ratio of anomalous Z to normal Y, a measure of
the induction effect which assumes that normal Y is the driving,
or inducing, field, can be extracted from the amplitude maps of
Figs. 4.11-13. An approximate separation assigns short-wavelength
features to the anomalous part and the residual smooth long-
wavelength field to the normal part (Porath et al., 1971); such
a procedure would have produced very much the same results for the
1967 array as the formal surface-integral separation by Porath
et al. (1970). At the daily variation periods the maximum value of
the ratio in the Northern Rockies is about 0.05; at short periods
it is somewhat greater than 0.1 (Porath et al., 1971). A model of
medium-depth two-dimensional conductivity structure given by Gough
and Camfield (1972b) to fit the short-period data (see also Chapter
5) has a response at long periods which is much too small (maximum
value of ratio, 0.005; D.I. Gough, personal communication). To
obtain the appropriate response at long periods would require much
deeper structures; these in turn would be ruled out by the spatial

sharpness of the anomalies, which demand shallow or medium-depth sources.

Further, one should ask why, if the long-period anomalies are induction effects and deep structures are not admissible, the anomalies appear most prominently in fields at the longest period (24 h, in Fig. 4.11), and least of all at the shortest ( 8 h, in Fig. 4.13) which should presumably be most affected by shallow or intermediate inhomogeneities.

There is also evidence from the phase maps that the Northern Rockies anomalies are induction effects at short periods but not at long periods. In those contour maps at short periods (Figs. 3.12-18), in which the anomalies are clearly formed in Y and Z amplitude, the Y and Z phases in the region are almost equal, and an induction process can be implied. For events which do not resolve the anomalies (Figs. 3.14 and 3.17), there is no clear relationship among the phases of the three components. At long periods where small anomalies do appear above the Northern Rockies (Y and Z amplitudes in Fig. 4.11, at 24 h; Y in Fig. 4.12, at 12 h), the phase maps are not consistent with induction by Y in north-south structures. Z is not in phase with Y; if anything, it is closer to the phase of X.

The phase information is summarized more quantitatively in Fig. 4.19, which shows the phase differences $\phi_X - \phi_Z$ and $\phi_Y - \phi_Z$. Strictly speaking, the phases of anomalous Z and normal X and Y should be considered, but the unseparated observed values have been used since anomalous Z is large compared with normal Z, and
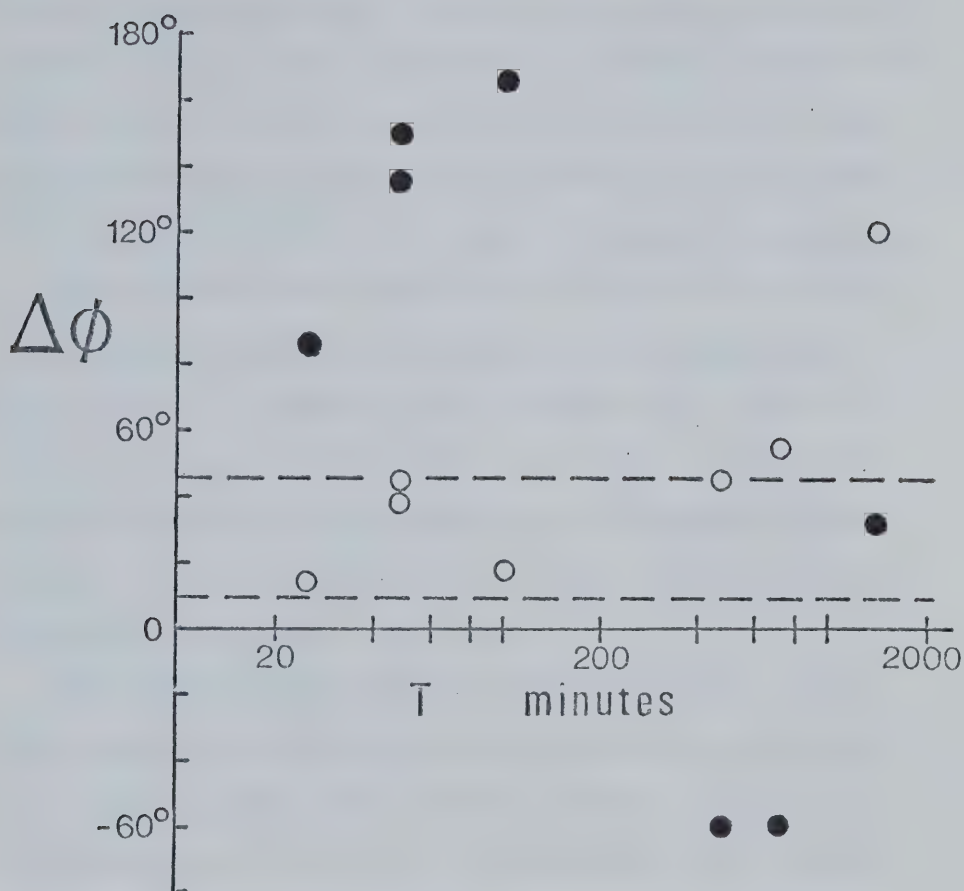
Fig. 4.19 Phase differences in degrees between horizontal and vertical variation fields at six periods, near the Northern Rockies. Dots, $\phi_X - \phi_Z$. Circles, $\phi_Y - \phi_Z$. Broken lines show the range of phase values expected for induction of Z by a horizontal field. (From Camfield and Gough, 1972)

anomalous X and Y are small relative to normal X and Y. In the case of induction by normal Y in a large deep conductor for which self-inductance is larger than resistance, anomalous Z should lead normal Y by 10° to 45°, so $\phi_Y - \phi_Z$ should be small and positive. The difference $\phi_X - \phi_Z$ should have significance only with regard to the source field and not with regard to the induction processes.

These conditions are certainly met in Fig. 4.19 at periods up to 102 min, at which the anomalies are well defined in the maps of Chapter 3. Apparently they also hold at 8 h, where the anomalies are very poorly developed (Fig. 4.13), and where they are unlikely to be induction features from the arguments already advanced. The assumption that normal Z makes negligible contribution to $\phi_Z$ is probably at fault here.

Recognition in Fig. 4.19 of the small value of $\phi_X - \phi_Z$ at 24 h, together with the foregoing discussion, leads Camfield and Gough (1972) to suggest that the Northern Rockies anomalies at daily-variation periods are also due to variable lateral transmission, this time through southward extensions of the medium-depth conductors in the model of Gough and Camfield (1972b) which fits the short period data, of anomalous fields associated with currents induced by X in the Basin and Range upper-mantle conductor to the south. This could explain the observed period-dependence; the fields at the longest period would have the greatest propagation distance (skin depth) and hence the amplitude maps at 24 h (Fig. 4.11) would be more complex than those at the other two periods, the fields having travelled further through more-varied

conductive structure.

Refraction would likely predominate in the case of thin conductive structures such as these, upon which the anomalous fields might fall with angles of incidence of 80° or more. Thus the geometry alone, i.e. the relative location of source and thin conductor, could be decisive in explaining the observed period-dependence.

Camfield and Gough (1972) have coined the term vartran (variable transmission) to describe this type of anomaly. Quantitative interpretation of vartran anomalies, to estimate depths to the anomalous currents, for example, seems virtually impossible. They involve diffusion paths many times longer than the vertical dimensions of the poorly-known or unknown absorbing structures, and very large angles of incidence, with associated refraction effects. Nevertheless, they must be recognized, if only to avoid fruitless attempts to interpret them as induction anomalies.

Thus it seems possible to explain the general results of the long-period data. Some details are discussed in the remainder of this chapter.

North American Central Plains Region

The anomaly in short-period geomagnetic variations in the North American Central Plains (Camfield et al., 1971) persists in the Z component of the daily variation to periods 8 h (Fig. 4.13) and 12 h (Fig. 4.12) in both amplitude and phase. At 24 h (Fig. 4.11)

the Z amplitude map has become highly complex, but the phase map

can perhaps be interpreted at its eastern edge as still showing

the Central Plains feature.  In the Central Plains, the similarity

of the 8 h and 12 h Z fields to those at short periods is illus-

trated in Fig. 4.20, a composite of Z amplitude maps from this

chapter and the previous one.

In contrast to the Z maps at 8 h and 12 h, and to the Y and

Z maps at short periods, the Y component amplitude and phase at

12 h (Fig. 4.12) and at 8 h (Fig. 4.13), and phase only at 24 h

(Fig. 4.11) show only a weak anomaly in this region, as already

noted from the magnetograms and Fourier spectra.  At 24 h the Y

amplitude map is complicated, like those for X and Z at this

period, and bears no obvious relation to the maps at shorter periods.

A first-order explanation of this anomaly is given in the next

chapter.

Northern Rockies Region

In this study of the daily variation, the author hoped to

be able to clarify the difference between the observations by

Reitzel et al. (1970) and Schmucker (1970a) in the western and

southwestern U.S. and those of Caner (1971) in southwestern Canada.

It can be stated from the results presented here that there is

definitely no attenuation in normal Z at long periods towards the

west side of the 1969 array in southwestern Canada and the north-

western U.S.  Fig. 4.20 makes this very clear.  The maps in the

figure also point out that the westward attenuation effect is strong

Fig. 4.20   Z amplitudes for substorm August 20 (in the same arbitrary
            units for T = 25.3 min and T = 102.4 min, and different
            arbitrary units for T = 47.6 min) and for daily variation
            July 17-22 (in gammas).

at 25 and 48 min (also at 85 min, in Fig. 3.17 of the previous chapter) but is tapering off by the time the period has increased to 102 min. So the long-period results of Caner (1971) are confirmed, and it may be concluded that the conductor which attenuates Z variations at short periods must be too shallow or have a conductivity-thickness product too small to influence the much longer periods of the daily variation. This is contrary to the rejection of a shallow, high-conductivity layer by Porath et al. (1971) and Porath (1971b), to whom, however, this daily variation study was not yet available.

The daily variation in Y and Z at all three long periods in Figs. 4.11-13 shows evidence of two small anomalies associated with the Northern Rockies, as discussed earlier in this section. The anomalies at long period cannot be due to induction in the local conductors which fit the short-period data (at the depth of the seismic low-velocity zone: Gough and Camfield, 1972b), for these reasons: the observed anomalous amplitudes are too large to arise from induction in such a conductive configuration; the observed anomalies are too sharp to be caused by deeper structure; and the observed period dependence, with maximum anomalous fields at the longest period, is not consistent with the induction process. In addition, the phase relationships in Fig. 4.19 support induction at short periods but not at long periods. It is suggested that the small anomalies in the daily variation fields are due to variable lateral transmission of anomalous fields, originating from the Basin and Range conductor

to the south, through southward extensions of the conductive structure beneath the Northern Rockies. In such a case, fields at the longest period would diffuse furthest with appreciable amplitude because they have the largest skin depth. This would explain why the field maps at 24 h have the greatest relief, and how the distribution of the anomalies in amplitude and spatial wavelength could be obtained.

The results given in this chapter are discussed in a paper by Camfield and Gough (1972).

CHAPTER V

INTERPRETATION:  CENTRAL PLAINS AND NORTHERN ROCKY MOUNTAINS

5.1  Introduction:  Modelling Techniques

Interpretation of the data described in the previous two
chapters has been concentrated on the straightforward induction
anomalies defined by the array in the North American Central
Plains and in the Northern Rocky Mountains.  In both regions,
the Fourier component maps show that conductive inhomogeneities
carrying anomalous currents are long and narrow (two-dimensional),
with the currents being much more tightly confined in the Central
Plains than in the Northern Rockies.  This makes a first-order
quantitative inversion of the data at least possible; techniques
for calculating the response of arbitrarily-shaped three-
dimensional conductive bodies are embryonic at this time (Jones
and Pascoe, 1972).  In addition, we must determine layered
conductive structures for the areas east and west of the Northern
Rockies, adequate to explain the suppressed normal Z amplitudes
at short periods west of the Cordillera.  The layered structure
from normal fields and the inhomogeneous structure from anomalous
fields must obviously be consistent with one another.

For a layered flat earth, the amplitude relationship between
the perpendicular and tangential magnetic components of an incident
uniform oscillating electromagnetic field is well known.  Price
(1962, pp 1907-1913) provides an excellent introduction to the
detailed derivation of Schmucker (1970a, pp 61-65).  The general

solution of Maxwell's equations in a stratified conductor, neglecting

displacement currents, involves exponentials increasing both upwards

and downwards. Since the incident field disappears at great depth,

the solution in the ultimate layer (which extends to infinity) cannot

contain the downwardly-increasing term; this solution is iterated

to the surface using the continuity condition on the magnetic field

at the interfaces between conductive layers, to yield the theoretical

amplitude ratio $Z/\sqrt{X^2 + Y^2}$.

Besides the distribution of conductivity with depth for the

model, the period of the incident field and its scale length or

wave number k must be specified in the calculation. From versions

of the contour maps which have been smoothed to remove local

anomalous fields, the scale length can be estimated by using

Schmucker's (1970a, p. 64) equation:

$$k = \left| \left( \frac{\partial X}{\partial x} + \frac{\partial Y}{\partial y} \right) \Big/ \sqrt{X^2 + Y^2} \right| \tag{5.1}$$

The theoretical amplitude ratios can then be compared with the

observations, values which have been averaged over areas of

interest in the contour maps of Fourier amplitudes.

In order to model the anomalous fields by conductive inhomo-

geneities with two-dimensional geometry buried in a layered flat

earth, data were extracted from the Fourier amplitude maps along

profiles transverse to the conductive structures. Such measured

data Y and Z are the resultant of the regional normal field

(external part, and internal part induced in the absence of inhomo-

geneities) and the anomalous fields (associated with currents

induced in the inhomogeneities by the normal field). An approximate

separation assumes that short-wavelength features are anomalous,

and assigns the residual, smooth, long-wavelength field to the

normal part (Porath et al., 1971); as mentioned in Section 4.5,

this technique would have yielded almost the same results for the

1967 array as the formal surface-integral separation by Porath

et al. (1970).

In this way one can estimate the anomalous fields $Y_a$ and $Z_a$,

and normalize them with respect to the regional inducing field

(at short periods, $Y_n$; see Section 3.2).

$$\frac{Y_a}{Y_n} = \frac{Y - Y_n}{Y_n} \qquad ; \qquad \frac{Z_a}{Y_n} = \frac{Z - Z_n}{Y_n} \tag{5.2}$$

Initial estimates of the maximum depth to the top of conductive

structures carrying anomalous currents can be obtained using simple

models such as infinitely-long line and sheet currents. For a

horizontal line current of I amperes at depth d metres below the

surface of the earth, the anomalous fields in gammas along a

transverse profile are

transverse: $Y = 200 \; Id/(y^2 + d^2)$ \hfill (5.3)

vertical: $Z = 200 \; Iy/(y^2 + d^2)$ \hfill (5.4)

where y is the horizontal distance from the line current. Y has

its maximum value 200 I/d at $y = 0$, directly above the current;

Z has extrema ($\pm$ 100 I/d) at $y = \pm$ d, and is zero at $y = 0$. Both

components fall to zero far from the current. Note that the range

of Y (from 0 to 200 I/d) is equal to the range of Z (from - 100 I/d
to 100 I/d). The formulae reveal that the half-width of Y along
the profile (full width at half-peak amplitude), and the separation
of the Z extrema, are both equal to twice the depth to the line
current.

Measurements of Y half-widths and Z peak separations on the
data profiles (equations 5.2) can thus give estimates of the maximum
depths to the top of conductive structures carrying current concen-
trations. In reality, a conductive body of finite cross-section
and conductivity, in which flow currents whose fields resemble
those of a line current, would be located at considerably less than
the depth of the line current. Parasnis (1966, p. 120) remarks
that in mining geophysics, depth estimates from the line-current
model are often too large by a factor 2-4.

For a buried sheet current of I amperes and width 2a metres,
at depth d metres, the analogous fields in gammas are

$$\text{transverse:} \quad Y = 200 \, \frac{I}{2a} \, \tan^{-1} \frac{2ad}{d^2 + y^2 - a^2} \tag{5.5}$$

$$\text{vertical:} \quad Z = 100 \, \frac{I}{2a} \, \ln \frac{(a + y)^2 + d^2}{(a - y)^2 + d^2} \tag{5.6}$$

The distance y is measured horizontally from the centre point of the
sheet. Again, Y is maximum at $y = 0$, and has a peak value of
400 (I/2a) $\tan^{-1}$(a/d) at that point. Z has extrema at
$y = \pm \sqrt{a^2 + d^2}$ with peak values given by equation (5.6) with these
values for y, and is zero at $y = 0$. As expected, both components
go to zero far from the sheet. The ratio of the ranges of Y and Z

is given by

$$\frac{\text{Range of } Y}{\text{Range of } Z} = \frac{2 \tan^{-1}(a/d)}{\ln \frac{1 + [(a/d) + \sqrt{(a/d)^2 + 1}]^2}{1 + [(a/d) - \sqrt{(a/d)^2 + 1}]^2}} \qquad (5.7)$$

This quantity is plotted in Fig. 5.1 for various values of width-to-depth ratio $(2a/d)$; note that for very wide sheet currents $(2a/d > 25)$, the parameter is not very sensitive. The maximum value of the range ratio is one, for $(2a/d) = 0$, as for a line current. Numerical experiments using the technique of Jones and Price (1971), discussed later in this section, suggest that if the conductive body carrying the current has appreciable extent in depth, so that a sheet approximation no longer holds, the range ratio can become greater than one. With these limitations in mind, calculation of the range ratio from observed profiles yields a width-to-depth ratio for sheet current models of the anomalous currents in the conductive inhomogeneities, giving at least some indication of the geometry involved.

From these simple line and sheet current models for the anomalous currents, one could proceed to fit more elaborate two-dimensional models of inhomogeneous conductive structure whose response to a uniform alternating electromagnetic field is made analytically tractable through the choice of certain restricted geometries. These might include the conducting cylinder embedded in a resistive medium (Kertz, 1960), generalized by Schmucker (1970a, pp 78-82) to include a perfectly-conducting mantle below
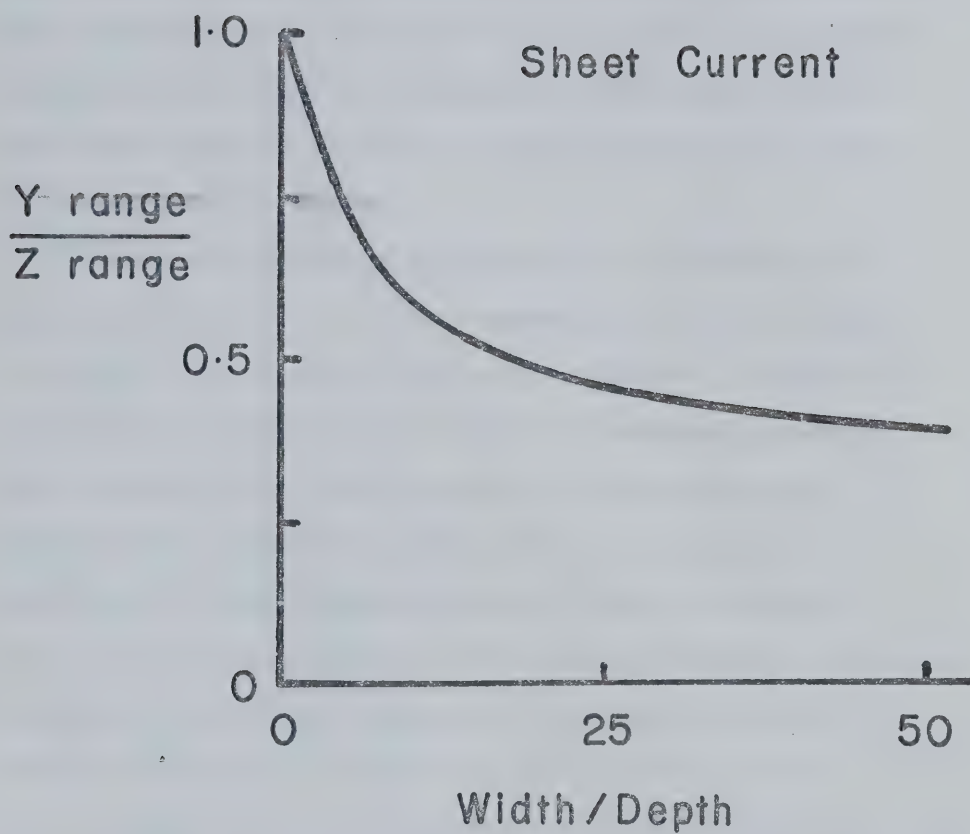
Fig. 5.1 Characteristics of an internal sheet current: ratio of
the range of the transverse (Y) component to the range
of the vertical (Z) component, along a transverse profile;
vs. the width-to-depth ratio. The analytical expression
is given in equation (5.7).

the resistive surface layer which contains the cylinder. Or the modelling might be approached through the conformal mapping used by Schmucker (1970a, pp 86-91) to find the effect of topography on the interface between the resistive surface layer and a perfectly-conducting mantle beneath. Porath et al. (1970) applied most of the foregoing methods to the data of the 1967 array, as reviewed in Chapter I of this thesis.

To deal with conductive inhomogeneities of arbitrary cross-section, recourse must be taken to numerical methods of solving the general electromagnetic boundary-value problem. Computation costs usually restrict one at present to two-dimensional models. In all methods, the conductivity model is approximated by a variably-sized mesh of unit cells, each with homogeneous properties; the edges of the mesh must be placed sufficiently far from lateral discontinuities that local perturbations (anomalous fields) arising from the presence of the discontinuities do not propagate to the edges. Then the boundary conditions become those appropriate to an electromagnetic field in a uniform (or stratified) conductor.

One method of solution, the finite element method (Coggon, 1971; Reddy and Rankin, 1972) involves a variational technique where the quantity to be minimized is the total electromagnetic energy in the mesh. This minimization is equivalent to requiring that the electromagnetic fields satisfy the Helmholtz equation, and so the method is equivalent to the two discussed next which are based more directly on Maxwell's equations.

One of these solves Maxwell's equations via the transmission line, or transmission surface, analogy (Madden and Swift, 1969; Swift, 1967, 1971); the other uses finite difference considerations to achieve the same result (Jones and Price, 1970, 1971). The starting point for both is Maxwell's equations, written here in c.g.s. units with an assumed exp (iωt) time dependence, with negligible displacement current and with magnetic permeability that of free space:

$$\nabla \times \vec{H} = 4\pi\sigma\vec{E} \qquad (5.8) \quad ; \qquad \nabla \times \vec{E} = -i\omega\vec{H} \qquad (5.9)$$

σ is the local conductivity. In the two-dimensional case, all quantities are independent of one coordinate (here, x) and so all partial derivatives in that direction can be ignored. Equations (5.8) and (5.9) can be expanded:

$$\frac{\partial H_z}{\partial y} - \frac{\partial H_y}{\partial z} = 4\pi\sigma E_x \qquad (5.10a)$$

$$\frac{\partial E_z}{\partial y} - \frac{\partial E_y}{\partial z} = -i\omega H_x \qquad (5.11a)$$

$$\frac{\partial H_x}{\partial z} = 4\pi\sigma E_y \qquad (5.10b)$$

$$\frac{\partial E_x}{\partial z} = -i\omega H_y \qquad (5.11b)$$

$$-\frac{\partial H_x}{\partial y} = 4\pi\sigma E_z \qquad (5.10c)$$

$$-\frac{\partial E_x}{\partial y} = -i\omega H_z \qquad (5.11c)$$

With two-dimensional geometry, then, Maxwell's equations separate into two polarizations. Equations (5.10a), (5.11b) and (5.11c) make up the E polarization (Jones and Price, 1970) or the case of E parallel to strike (Madden and Swift, 1969), with the electric field in the x-direction only ($E_x$, with $H_y$ and $H_z$).

Equations (5.11a), (5.10b) and (5.10c) describe the H polarization

or the E perpendicular case, in which the magnetic field is

restricted to the x-direction    ($H_x$, with $E_y$ and $E_z$).  The E

polarization, with vertical and transverse-horizontal magnetic

fields, is the one usually of interest in geomagnetic induction

studies.

Motivation for solving these equations via the transmission

surface analogy comes from their similarity to the equations

governing current and voltage on a transmission line.  Although

a transmission line is strictly one-dimensional, the idea can be

generalized to a two-dimensional transmission surface with two

directions of current flow, to correspond to the two-dimensional

electromagnetic problem.  Swift (1971) describes the concept:

... First, the continuous conductivity cross-section

is represented by an equivalent transmission surface;

then, a lumped-circuit approximation is constructed

from the transmission surface; and, finally, the

system of node equations resulting from the lumped-

circuit network [when Kirchoff's law of current

continuity is written for each node] is solved

directly.  T.R. Madden of MIT developed this approach ...

Boundary conditions are applied to the network by considering that

the layers which make up the half-space in which the inhomogeneity

is buried are, at their "ends", one-dimensional transmission lines

whose characteristic impedance can be used to terminate the

network.

Porath et al. (1971) have used the transmission surface

analogy, as programmed by Wright (1969, 1970), in the model

studies of the Central Plains and Northern Rockies anomalies

described in the remainder of this chapter.

The finite difference method as introduced by Jones and

Price (1970) proceeds from the E or H polarization equations

(5.10-11) to obtain a single equation for the polarized component

by eliminating the other two components:

$$\frac{\partial^2 F}{\partial y^2} + \frac{\partial^2 F}{\partial z^2} = i\eta^2 F \tag{5.12}$$

or     $\nabla^2 F = i\eta^2 F$ (5.13)

where F is either $E_x$ or $H_x$, and $\eta^2 = 4\pi\sigma\omega$. If F is complex

(F = f + ig), then we have

$$\nabla^2 f + i\nabla^2 g = i\eta^2 f - \eta^2 g \tag{5.14}$$

which can be decomposed by equating real and imaginary parts into

$$\nabla^2 f = -\eta^2 g; \quad \nabla^2 g = \eta^2 f \tag{5.15}$$

These equations must be satisfied at any particular point within

the mesh of cells. Jones and Pascoe (1971) expand f and g in

second-order Taylor series in the four directions about the point,

and by approximating first derivatives by finite differences they

obtain from equations (5.15) finite difference expressions for f

and g. These are modified to satisfy continuity conditions at

the internal boundaries between cells. Boundary values are

assigned to the edge grid points, and initial values at interior

points are interpolated from the edges. Then the finite difference

equations are solved simultaneously by the Gauss-Seidel iterative

scheme to yield the polarized component. The other components

follow from derivatives of this component, as suggested by equations

(5.10-11, b and c).

The boundary values referred to above are essentially solutions

of equation (5.12) simplified by assuming that the boundaries are

far enough from the conductive inhomogeneities (at a distance of

several skin depths in the most resistive medium) that anomalous

fields due to the inhomogeneities are negligible there. Then

equation (5.12) becomes independent of y, and has solutions:

$$F = D_1 \exp(-\sqrt{i}\eta z) + D_2 \exp(\sqrt{i}\eta z), \quad \eta \neq 0 \tag{5.16}$$

$$F = D_1 + D_2 z, \qquad \qquad \eta = 0 \tag{5.17}$$

The field components must vanish at great depths, so $D_2$ in equation

(5.16) must be zero at the bottom boundary of the mesh. If $D_1$ is

set to 1 at that point, then F and its vertical derivative are

defined for that level. From the continuity conditions (for the

E polarization, for $E_x$ and $H_y$, where $H_y$ is proportional to

$\partial E_x / \partial z$, as in equation 5.11b), and from the functional forms for

the fields given by equations (5.16-17), the bottom boundary values

can be carried up the sides of the mesh to the top boundary. Jones

and Price (1970), Jones and Pascoe (1971) and Pascoe and Jones (1972)

discuss the boundary conditions in some detail.

An anonymous reviewer of the paper by Porath, Gough and

Camfield (1971) stressed that the work of Jones and Price

... was concerned essentially with the perturbation

of current distributions (and the resulting surface

field anomalies) produced by two-dimensional conduc-

tivity structures.  It is important to note that

the currents may originate from inducing fields over

large areas at a considerable distance from the

anomaly ...  The inducing fields will certainly not

be horizontal and the large conductor need not

itself be two-dimensional.  Useful approximations

might be attained ... provided only that the

conductivity model in the immediate neighbourhood

of the anomaly can be taken as two-dimensional ...

Swift (1971) makes a comparable point in discussing solutions by

the transmission surface analogy.

Gough and Camfield (1972b) have used the finite difference

technique as programmed by Jones and Pascoe (1971) and Pascoe

and Jones (1972) in modelling the variational anomalies associated

with the Northern Rocky Mountains.  This work is described in

Section 5.3.

A brief reminder should be made about the non-uniqueness of

a model whose response, computed by the above methods, may match

a set of observations over a limited frequency range.  In an

example discussed in Chapter I, Porath (1971a) shows two different

models which apparently both fit the same substorm data equally

well; while·the models have similar form, they have inhomogeneities
of quite different conductivity at quite different depths.    In
general, broadening the frequency range to include micropulsations
and the daily variation as well as  substorms will reduce the
uncertainty, as will the requirement of consistency between models
fitting anomalous fields and those appropriate for normal fields.
In the end, however, other geophysical and geological constraints
and an awareness of the limitations of the model computations will
likely be needed in making the subjective choice of the best model
from a group of acceptable ones.

5.2  Conductive Structures in the North American Central Plains

        The observations discussed in Chapters III and IV indicate a
long narrow conductor in the Central Plains, striking from south
of the Black Hills of South Dakota north to the region of the U.S.-
Canada border.  This section is concerned with models for the
conductive inhomogeneity and the induction process which produces
the enhanced variations, as interpreted by Porath, Gough and
Camfield (1971) and Camfield and Gough (1972).

        To start the modelling, profiles of Fourier data have been
drawn for the southernmost line of variometers, where coverage at
substorm periods is most complete.  Anomalous field amplitudes $D_a$
and $Z_a$ have been separated from the normal fields and normalized
with respect to a normal field $D_n$ taken as the mean of amplitudes
at stations DRA and HYA; see equations (5.2).  These stations
are assumed far enough from the anomaly that they recorded only

the normal field. Phase differences between normal and anomalous

fields are very small, as can be seen in the magnetograms of

Section 3.2; the Fourier phases of Figs. 3.12-18 show that Z is

closely in phase with Y on one side of the anomaly and in anti-

phase on the other.

Normalized anomalous field amplitudes along this profile are

shown in Fig. 5.2 at various periods (25 to 120 min) for two

substorms. The response of the anomaly is strongly period-

dependent, with maximum amplitudes at period 50 min. Note that

these maximum values for $D_a$ are more than twice the normal field

$D_n$. This immediately indicates the complicated nature of the

conductive system and induction process, because induction in a

half-space of infinite conductivity (the limiting case) can do no

more than double the tangential component of an incident field

(see, for example, Skilling, 1948, p. 147). Thus the anomaly

cannot result from induction solely in a local conductor but must

require concentration, by the conductor, of current induced over

a much wider region of the crust. This concept has been considered

by Price (1964) in general terms and by Dyck and Garland (1969)

for the Alert (Ellesmere Island, Canada) anomaly in geomagnetic

variations. Current from the upper mantle is assumed in this case

not to reach the conductor; the crust is taken as insulated

from the upper mantle zone of thermally-excited semi-conduction

by a resistive section (Brace, 1971).

From the location of the Y maxima and the Z cross-overs on the

profiles of Fig. 5.2, the centre of the internal current lies

Fig. 5.2 Normalized anomalous eastward ($D_a/D_n$) and vertical ($Z_a/D_n$) variation field amplitudes along the profile HYA-DRA across the North American Central Plains anomaly. From Porath et al. (1971).
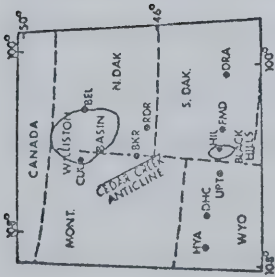
NORMALIZED ANOMALOUS FIELDS

o — $D_Q/D_N$
x — $Z/D_N$

100 km

AUGUST 10, 1969

T = 120.5 MIN.

T = 50 MIN.

T = 24.4 MIN.
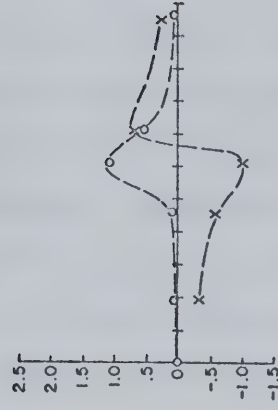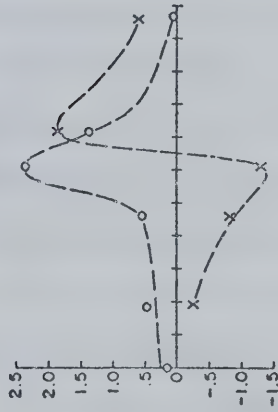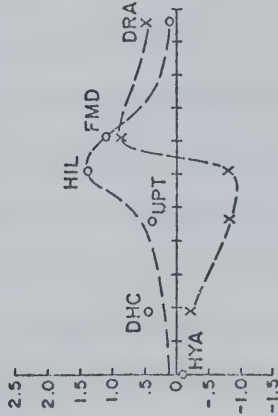
AUGUST 20, 1969

T = 85.3 MIN.

T = 47.6 MIN.

T = 25.3 MIN.
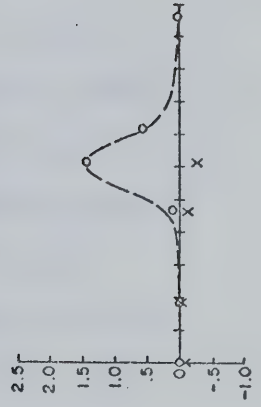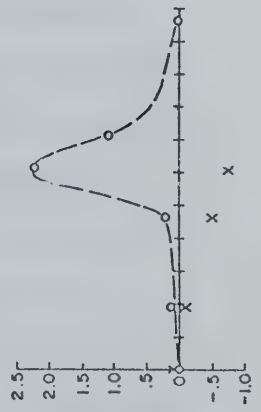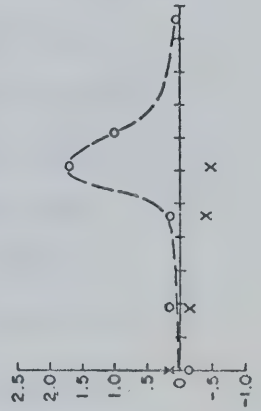
between stations HIL and FMD near the eastern edge of the Black
Hills. The positive and negative Z peaks are not symmetrical in
amplitude; this may be due to any or all of the following: a
too-large station spacing, an incomplete separation of the Z
field, or a non-uniform distribution of internal current. Depth
estimates place a line current at 35-50 km; the actual conductor
will be considerably shallower. Measurement of amplitude ranges
yields width-to-depth ratios for a sheet current (Fig. 5.1)
between 5:1 and 9:1 for the various periods, with some indication
that the sheet becomes wider as period increases.

Dr. H. Porath (Porath et al., 1971) used the transmission
surface solution of the induction problem, as programmed by Wright
(1969), to model the anomaly with a long, narrow, highly-conducting
body in the crust. The inhomogeneity was given a rectangular
cross-section (30 km wide, 3 km thick) with its upper surface at
depth 2 km. With such a conductor of $10 \ \Omega^{-1}m^{-1}$ embedded in a
normal conductivity section (Cantwell-McDonald model; see Madden
and Swift, 1969, Table 3), the model has approximately the observed
vertical field amplitude at period 50 min. Horizontal fields
were calculated using an integral transformation of the vertical
fields. Computed phase differences between normal and anomalous
fields were small (less than 10°) as observed. However, the
calculated field amplitudes changed very little with period,
unlike the observations. By decreasing the conductivity of the
body, the amplitudes could be made more dependent on period, but
the observed maximum response at 50 min could not be duplicated

with any model conductivity. A further complication arose with conductivities less than $5 \ \Omega^{-1}m^{-1}$: phase differences became too large (greater than 30°) to fit the observations.

A two-dimensional model will thus not describe the observations, as predicted from the evidence of maximum anomalous fields more than twice the normal fields. This implies the current concentration effect mentioned earlier, with a linear conductor joining much larger regions where an important part of the induction takes place; the structure is three-dimensional. It also implies that a normal horizontal field from stations relatively close to the anomaly, as used above, is not the correct source field amplitude with which to normalize the anomalous fields. Note that the correct choice would be exceedingly difficult to make because of the unknown geometry. Finally, this reasoning implies that the frequency response of the anomaly will be controlled by the characteristics of the three-dimensional region.

A schematic illustration of the three-dimensional conductor envisaged above is given in Fig. 5.3. C is the long, narrow conductor in the crust under the anomaly; it joins the much larger but less conductive regions A and B also in the crust. These two regions are further joined by other paths D, presumably multiple, also in the crust. As mentioned, the entire crustal system is assumed insulated from the upper mantle.

Porath et al. (1971) suggest a qualitative explanation for the period response of the anomaly in the period-band of substorms,

152
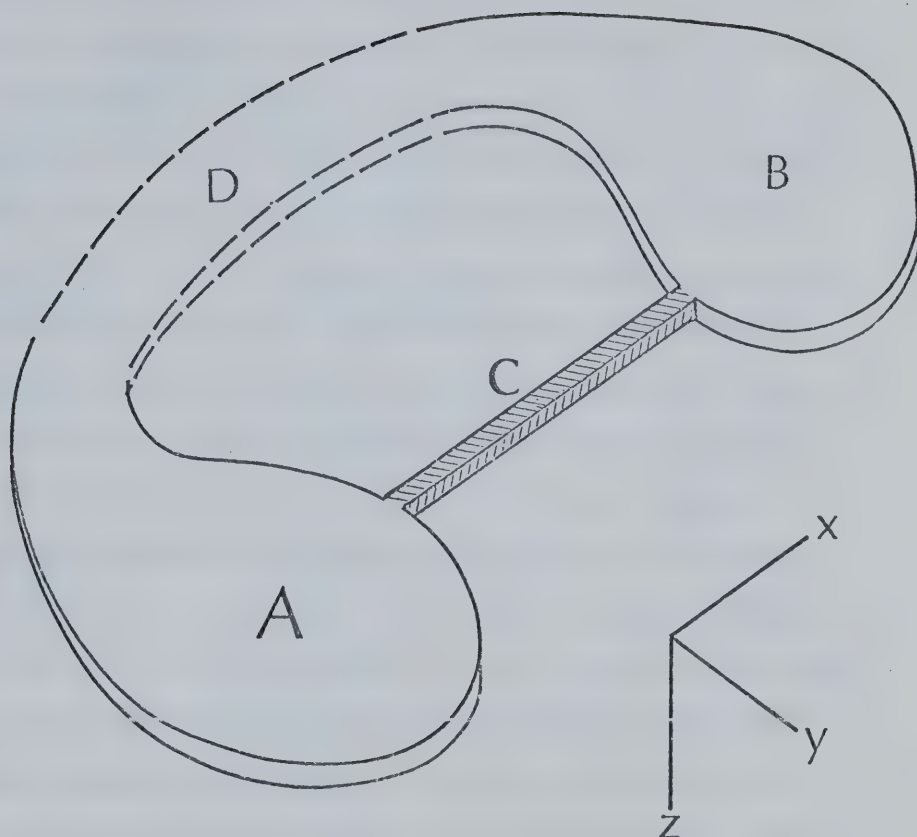


Fig. 5.3  Schematic representation of the conductive system believed
         responsible for the North American Central Plains anomaly.
         A and B are large undefined regions of the continental
         crust and D represents multiple connections between them.
         C is a conductor of much higher conductivity (2 orders of
         magnitude) joining A and B.  The anomaly is observed near
         C.  From Camfield and Gough (1972).

with the assumption that the anomaly arises from concentration
of current induced in a large area of the upper crust such as
the Great Plains Province. At the short period end of the band,
induction in the upper crust will be important, and little of the
incident field will penetrate to the upper mantle. At periods
greater than about 1 h, the efficiency of induction in the crust
has diminished, and most of the incident field will reach the
upper mantle and will induce current there. So, at the longer
end of the band, anomalous fields will be smaller because of
reduced induction in the crust, while the normal horizontal
field will increase by the added contribution from currents in
the upper mantle. As a result the normalized anomalous fields
will fall as the period increases. At the other end of the band,
the increase in normalized anomalous fields with decreasing
period, expected on the basis of this model, would be cut off
by the reduced source-field spectrum at shorter periods. Hence
the maximum response of the anomaly at period 50 min would
result from the combined effects of these two factors.

When the daily variation data became available, Camfield
and Gough (1972) combined them with the substorm data to give
a more detailed description of the conductivity structure and
induction process which give rise to the Central Plains anomaly.
Table 5.1 lists some of the observations which a model must
satisfy; these have been discussed in detail in Chapters III
and IV.

Table 5.1

Characteristics of the Central Plains Anomaly

| Period band | Substorms (25-102 min) | Daily variation (8-12 h) |
|---|---|---|
| Magnetograms show: | $Z_a(t)$ resembles $D_n(t)$ | $Z_a(t)$ resembles $Z_n(t)$ |
| Phase maps show: | small anomaly in $\phi_Y$ large anomaly in $\phi_Z$ | very small anomaly in $\phi_Y$ small anomaly in $\phi_Z$ |
| Amplitude maps show: | large anomaly in Y large anomaly in Z | very small anomaly in Y large anomaly in Z |

On the basis of these observations, Camfield and Gough (1972) have suggested two main ways in which induction can take place in the conductor of Fig. 5.3, with the importance of one or the other being a function of the period of the incident field and of the geometry:

1.  Induction by the normal vertical field $Z_n$ in the whole laminar structure ABCD.

2.  Induction by the normal transverse horizontal field $Y_n$ in the linear conductor C. $Y_n$ is several times $Z_n$, so it should be relatively more important in this local induction. Opposing induction by $Y_n$ in D will probably complicate the current in C without annulling it, since the link D is multiple and of unknown configuration, and much of it may be at distances of the order

of the spatial wavelength of the field.

At substorm periods we believe that induction by $Y_n$ in C is most important, but that there is a significant contribution by $Z_n$ in ABCD. The dominance of $Y_n$ in C is evident from some aspects of the model studies of Porath et al. (1971) described above, and from the variograms and Fourier component maps. If $Y_n$ is the main driving field, then $Z_a(t)$ should have a waveshape like that of $Y_n(t)$. There should be little or no phase anomaly in Y, since the anomalous current is induced by Y itself; on the other hand, a large phase anomaly in Z is expected where induction is by Y. In amplitude, the Y and Z anomalies should be comparable, and both will be related to $Y_n$. In addition, we require some induction by $Z_n$ in the entire conductor ABCD to explain the discrepancies between the substorm observations and the response of the two-dimensional model of Porath et al. (1971).

In terms of the processes discussed so far, we have not found a model which correctly predicts the $Y_a$ and $Z_a$ amplitudes at the long periods. From Figs. 4.12-13, the ranges of $Z_a$ are ~4$\gamma$ at 12 h and ~2$\gamma$ at 8 h; the ranges of $Y_a$ cannot be estimated accurately but are about 1$\gamma$ and 0.5$\gamma$ respectively. So at both periods the Y range-to-Z range ratio is about 0.25. Recall from Section 5.1 that this ratio is 1 for a line current, somewhat greater than 1 for a current of rectangular cross-section with appreciable thickness, and less than 1 for a sheet current. However, a sheet current with range ratio 0.25 would have a width-to-depth ratio of about 500:1; the corresponding value mentioned above at substorm

periods is between 5:1 and 9:1. This large difference forced

Camfield and Gough (1972) to conclude that no crustal current

distribution of credible cross-section could by itself produce

the observed large $Z_a$ but small $Y_a$ amplitudes at long periods.

To suggest an explanation, Camfield and Gough (1972)

postulated another source of anomalous fields above the conductor

C in Fig. 5.3. Currents induced by the daily variation in the

conductive part of the upper mantle (which is assumed insulated

from the crustal conductor) will contribute to the variation

field measured at the surface; if these mantle-current fields

are absorbed in the conductor C, then perhaps the observations

above the conductor can be understood. Qualitatively, $Y_a$ will

be reduced by the absorption, since in the absence of the

conductor the mantle currents would in the usual case increase

$Y_n$. How they will effect $Z_a$ is less clear; they would decrease

$Z_n$ if they were not absorbed, so presumably they would increase

$Z_a$ above the conductor. In addition, the Z anomaly will undoubtably

be shifted laterally and might have its range increased.

Essentially we suggest that the Y range-to-Z range ratio may be

smaller when a conducting upper mantle is included in the model

than it would be for the same current concentration process above

an insulating mantle. Further numerical experimentation is

needed on this point.

In summary, it is proposed that the North American Central

Plains anomaly at substorm periods (1/2 to 2 h) results mainly

from induction by $Y_n$ in the linear conductor C, with a smaller

contribution by $Z_n$ in the entire structure ABCD to explain the
deviations from a two-dimensional model. At the daily varia-
tion periods of 8 h and 12 h, the process has switched mainly
to induction by $Z_n$ in the whole laminar conductor, with upper
mantle currents also being important.

Vozoff et al. (1969) present magnetotelluric data in
eastern Montana. Their telluric lines, up to 80 km long, covered
most of the centre of the triangle formed by the array stations
CUL, BKR and CAV. Rotated tensor apparent resistivities support
the existence of shallow two- and three-dimensional conductivity
structures only to the extent that they show an apparent anisotropy
with average strike N 20°W or N 70°E over most of the period
range 0.2 sec to 8 h, which could result from such structures.

The geological interpretation for the linear conductor C
has developed in a very satisfying way, as outlined by Gough and
Camfield (1972a). In the initial paper, Camfield et al. (1971)
recognized from the narrowness of the anomaly that the conductor
must be in the crust. They mentioned that the anomaly might be
caused by the combined effect of three known crustal structures
(the Black Hills uplift, the Cedar Creek anticline and the
Williston sedimentary Basin), but preferred a single structure;
it is thoroughly improbable that three structures could connect
to channel the anomalous current so intensely.

Hot springs exist in the Black Hills uplift, but the few
heat flow measurements (Blackwell, 1969; Sass et al., 1971)
are too scattered to define a regional heat flow for the Black Hills.

In any case it is improbable that a long narrow conductor in the crust could be produced by high temperature alone. Thus Camfield et al. (1971) sought a compositional explanation. Mathisrud and Sumner (1967) had reported graphite bodies of very high conductivity in the Lead district in western South Dakota. This was the origin of our suggestion that a graphite schist body in the basement could provide the enhanced conductivity and linear form required to concentrate the induced current and cause the anomaly.

Shortly after this idea had been published, Lidiak (1971) presented a geological map of the Precambrian rocks of South Dakota. He had used gravity and vertical intensity magnetic data to outline the rock units characterizing the Precambrian basement which underlies the younger sedimentary rocks. Rock samples from outcrops and wells drilled into the basement served to identify the units. Lidiak's (1971) map shows the outcropping metamorphic rocks which form the Black Hills, and indicates schist in one well west of the outcrop areas. Lidiak interpreted the geophysical data to extend this direct lithological information, and the results show a metamorphic belt striking just west of north, and centred on the Black Hills (Fig. 5.4). The figure includes for comparison the Y component Fourier amplitude map at 47.6 min taken from Fig. 3.16; the conductor of course lies beneath the maximum of the Y field. The correspondence between the metamorphic belt and the induction anomaly is striking; the array study has supported Lidiak's mapping of the metamorphic belt, and suggests further that it contains some highly conductive
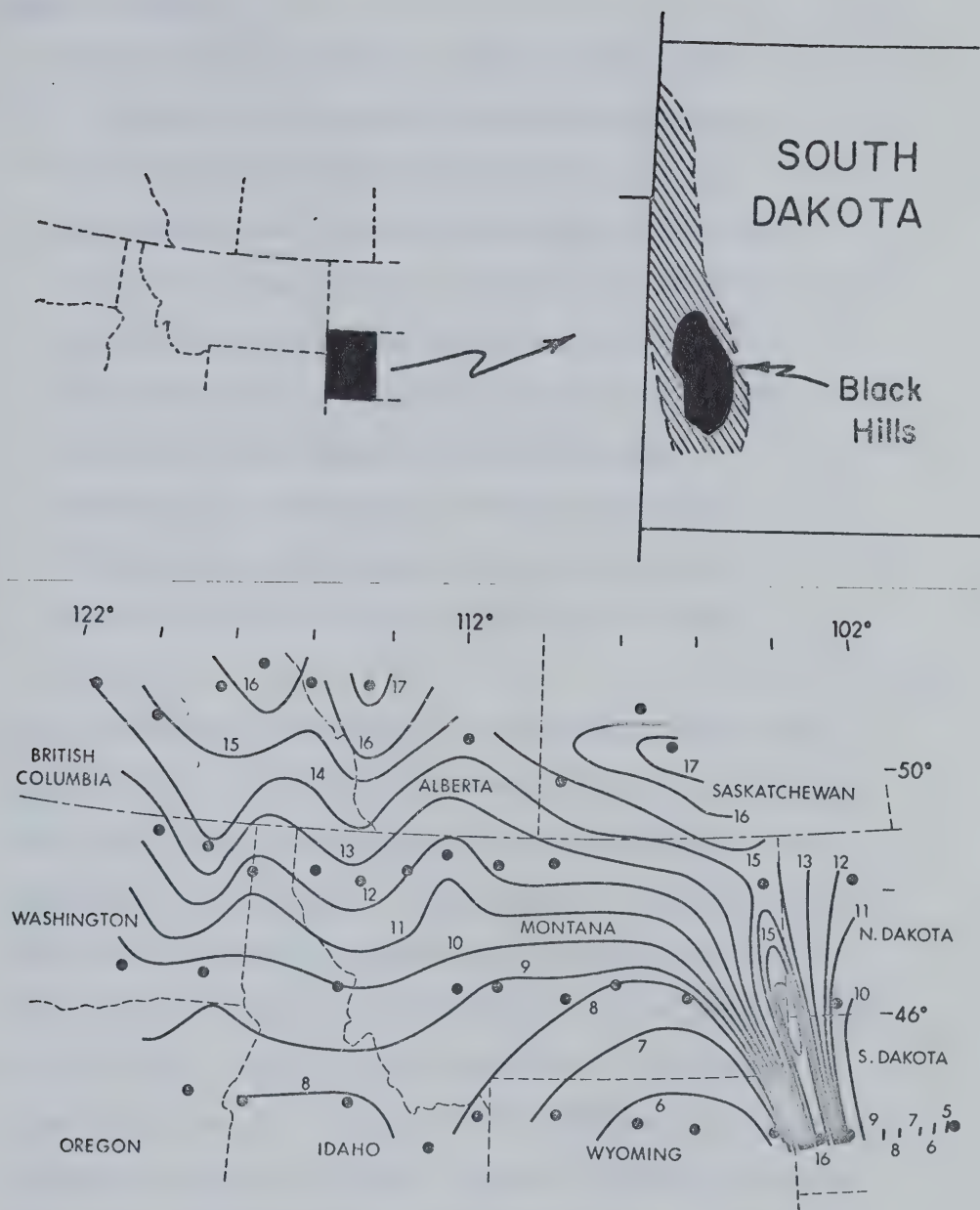
Fig. 5.4 The sketch map of western South Dakota (upper right) gives the location of the metamorphic belt (shaded) mapped by Lidiak (1971). The key map relates the sketch map to the contour map (lower) of Y Fourier-transform amplitudes at period 48 min repeated from Fig. 3.16.

graphite schist.

> Lidiak (1971) comments that the metamorphic belt
>
> ... is part of a prominent basement high of mainly
>
> metamorphic rocks which includes the Chadron and
>
> Cambridge arches of Nebraska [see Lidiak, 1972] and
>
> the central Kansas uplift ... Metamorphic rocks are
>
> not continuous throughout the extent of this high.
>
> Accordingly, the southern continuation of the Black
>
> Hills belt is ... doubtful where the magnetic
>
> anomalies lose definition. Granitic rocks occupy
>
> a large area in northwestern Nebraska, and they
>
> probably continue into the adjacent part of South
>
> Dakota ...

Here the reference is, of course, to anomalies in the static

magnetic field. The observation by Reitzel et al. (1970) at

their station CRW in northwestern Nebraska of enhanced Y and

Z variation fields similar to those recorded at the Black Hills

station HIL of this array suggests that the continuity of the

metamorphic belt southward into Nebraska, at least electrically,

must be stronger than Lidiak has indicated. In addition, the

basement granites in southwestern South Dakota and northwestern

Nebraska must contain sufficient graphite to maintain the high

conductivity evident further north in the belt.

Zietz et al. (1971) show aeromagnetic data in eastern Montana,

in the region northward along the strike of the induction anomaly,

which is also the extrapolated strike of the Black Hills metamorphic

belt. Prominent magnetic features trend rather more west of north than does the induction anomaly, and have been associated with the Cedar Creek anticline, a sedimentary rather than a basement structure. On the other hand, the anticline is reported to have its steep west limb overlying a recumbent fault in the basement; to some extent it must reflect the control by basement structures of those in the sediments, and hence the magnetic anomalies may indicate the trend of the basement structure. Whether or not this is true, it appears that aeromagnetic data in eastern Montana will not be as helpful as the magnetic and gravity anomalies in South Dakota in mapping independently the basement conductor which is responsible for the Central Plains induction anomaly.

In the most relevant seismic study, Borcherdt and Roller (1968) have derived a crustal model for eastern Montana from a seismic refraction profile; the model is also shown in the more accessible reference Glover and Alexander (1969). The profile traverses the Central Plains conductor at a point which is about 50 km south of CUL or about 160 km north of BKR. A three-layer crust consists of a 2 km upper layer (sediments) with P velocity 3.0 km/sec, a middle layer (6.1 km/sec) and a bottom layer (6.7 km/sec); the upper mantle (8.3 km/sec), whose top surface is flat, begins at depth 50 km. The middle layer is thinnest (depth range 2 to 15 km), or, equivalently, the bottom layer is thickest (from 15 to 50 km) *directly beneath the conductor.*

Electrical conductivity and seismic velocity are usually unrelated at these depths, but the lack of topography on the Moho,

together with the intra-crustal seismic structure, could indicate that the conductive structure is confined to the crust, as we have postulated. This conclusion is tenuous, however, because of the very detailed seismic results for the crust beneath the Large Aperture Seismic Array, 200 km in diameter centred 200 km from the axis of the conductor. Iyer and Healy (1972), by assuming a crust with uniform velocity 6.5 km/sec, calculate local varia- tions in total crustal thickness of up to $\pm$ 20%. Conclusions about topography on the Moho, or lack of it, obviously depend on the initial assumptions in the seismic interpretation.

The North American Central Plains anomaly is similar in form to the Kirovograd anomaly in the Ukranian Shield (Rokityanskiy and Logvinov, 1972) but has anomalous fields of greater magnitude.

## 5.3  Conductive Structures under the Northern Rocky Mountains

This section describes the work of Porath et al. (1971) and Gough and Camfield (1972b) in interpreting the observations in the Northern Rocky Mountains. As has been emphasized many times in this thesis, the major induction effect in the region is the attenuation of the vertical normal field of substorms at stations west of the Cordillera, relative to its value in the Great Plains. The daily variation field is however not attenuated in this way. The substorm results thus cannot be explained by a westward rise of the highly-conducting part of the upper mantle; the conductor must have limited thickness, if it is to be transparent to the

daily variation.

In addition to the normal field observations, small anomalous fields in Y and Z were recorded at substorm periods near the front range of the Rockies and just west of the Rocky Mountain Trench. These anomalies can be attributed to internal currents flowing in conductive structures which strike approximately north-south at 48°N (variometer line 2). North of line 2 the anomalies in X increase (Figs. 3.12-18), suggesting that the conductors follow the northwest trend of the Rockies in southern Canada. At daily variation periods, twin anomalies are also found in this area, but as discussed in Section 4.5, they differ markedly from the short-period features, and are thought to arise not by direct induction but by variable transmission of fields passing obliquely through the same structures.

As remarked previously, models of layered structure from normal fields and of inhomogeneous structure from anomalous fields must be consistent. Gough and Camfield (1972b) note that while the inversion of this two-part data set does not yield a unique conductivity distribution, it does impose appreciable constraints, detailed below, on the range of possible solutions.

To fit layered structures to the normal fields requires numerical estimates at various periods of the amplitude ratio $Z/\sqrt{X^2 + Y^2}$ (here abbreviated Z/H) and the spatial wave number k. Gough and Camfield (1972b) estimated Z/H from the mean value of each component over two windows in the Fourier amplitude maps, one east of the Cordillera in the Great Plains (46° to 50°N, 106°

to 108°W) and one west (47° to 51°N, 118° to 120°W).  The eastern

window is well clear of the Central Plains anomaly.  The observed

Z/H ratios at both substorm and daily variation periods are

listed in Table 5.2.  At the three short periods these are the

same as the ratios previously reported from the same maps by

Porath et al. (1971).  The values at period 1440 min (24 h) must

be considered less reliable estimates of the normal field than

those at the other periods, since the discussion in Section 4.5

concluded that over much of the array, most of the Z field at 24 h,

and certainly part of the X and Y fields, are not normal fields

but anomalous fields associated with currents in the Basin and

Range conductor.

Table 5.2

Observed parameters for fitting layered structures

| Period, min | Wave Number k $km^{-1}$ | Observed ratios Z/H western | eastern |
|---|---|---|---|
| 25 | $10^{-3}$ | 0.08 | 0.22 |
| 48 | $10^{-3}$ | 0.18 | 0.32 |
| 102 | $10^{-3}$ | 0.24 | 0.34 |
| 480 | $6.28 \times 10^{-4}$ | 0.19 | 0.20 |
| 720 | $4.71 \times 10^{-4}$ | 0.26 | 0.18 |
| 1440 | $3.14 \times 10^{-4}$ | 0.18 | 0.19 |

The spatial wave number k can be estimated from the contour

maps using equation 5.1.  Since the wave number for the incident

field is required, the fields of internal currents must be removed. A formal separation via surface integrals must be supplemented by an arbitrary division of the inseparable fields, which have wavelengths larger than the size of the array (Porath et al., 1970), so it is virtually as effective to smooth the maps assuming that the short-wavelength anomalies have internal sources. This is justifiable here since the anomalies occur at approximately the same locations for different geomagnetic events. The smoothing is still rather subjective, of course, and there is a corresponding uncertainty in the estimate for k. On the other hand, an estimate can at least be attempted from the array data, whereas with data on a short linear profile this is hardly possible. Thus Caner (1971) could not fit models to Z/H for eastern and western regions independently but had to work with the M-ratio $(Z/H)_{west}$ to $(Z/H)_{east}$ defined in equation 1.8.

Porath et al. (1971) estimated k at substorm periods from smoothed versions of the amplitude maps in Figs. 3.12-18: $0.9 < k < 1.3 \times 10^{-3} \, km^{-1}$. This corresponds to $5000 < \lambda < 7000$ km. Porath et al. (1971) and Gough and Camfield (1972b) adopted the value $k = 10^{-3} km^{-1}$ for the short periods. For the daily variation, Chapman's analysis of $S_q$ (Chapman, 1919) showed that each of the first four harmonics (m = 1 to m = 4) could be approximately represented by the single spherical harmonic $P_{m+1}^m$, for which $k = (m+1)/a$ where a is the earth's radius. Thus for T = 24, 12 and 8 hours we have $k = 2/a$, $3/a$ and $4/a$ respectively, the values listed in Table 5.2.

The observed values of the Z/H ratio are plotted against period
T for the eastern region in Fig. 5.5, and for the western region in
Fig. 5.6. The vertical bars show only approximate uncertainties and
are not formal error estimates. It should be kept in mind that for
each observation of Z/H at a given T there is corresponding value
for k which is not plotted in these diagrams; the Z/H response of
a conductive structure is a single-valued function of T only for
a particular set of incident fields with fixed wave numbers k.

In Fig. 5.5, the responses of two different models of conduc-
tivity vs. depth are compared with the observations in the eastern
region. One model was proposed by Caner (1970, 1971) and supported
by Cochrane and Hyndman (1970); see also Fig. 1.7. The other was
suggested by Porath et al. (1971). Both models are undoubtably over-
simplified, but are probably as sophisticated as the data justify.
At the daily variation periods both agree reasonably well with the
data. At substorm periods Caner's model with our wave numbers has
a response well below the observed values, while the model of Porath
et al. does fit the substorm ratios satisfactorily. The latter has
a 2 km surface layer with $\sigma = 0.2 \ \Omega^{-1}m^{-1}$, then a resistive zone,
with $\sigma = 0.001 \ \Omega^{-1}m^{-1}$ to depth 350 km, which rests upon the ultimate
conducting half-space of $\sigma = 0.2 \ \Omega^{-1}m^{-1}$. The surface layer repre-
sents the sedimentary resistivities found by Vozoff and Ellis (1966)
from magnetotelluric studies in the Alberta Basin northwest of
the eastern window. Caner's model does not have the surface layer;
note that the inclusion of such a layer would make the fit of
Caner's model slightly worse. In the model of Porath et al., the
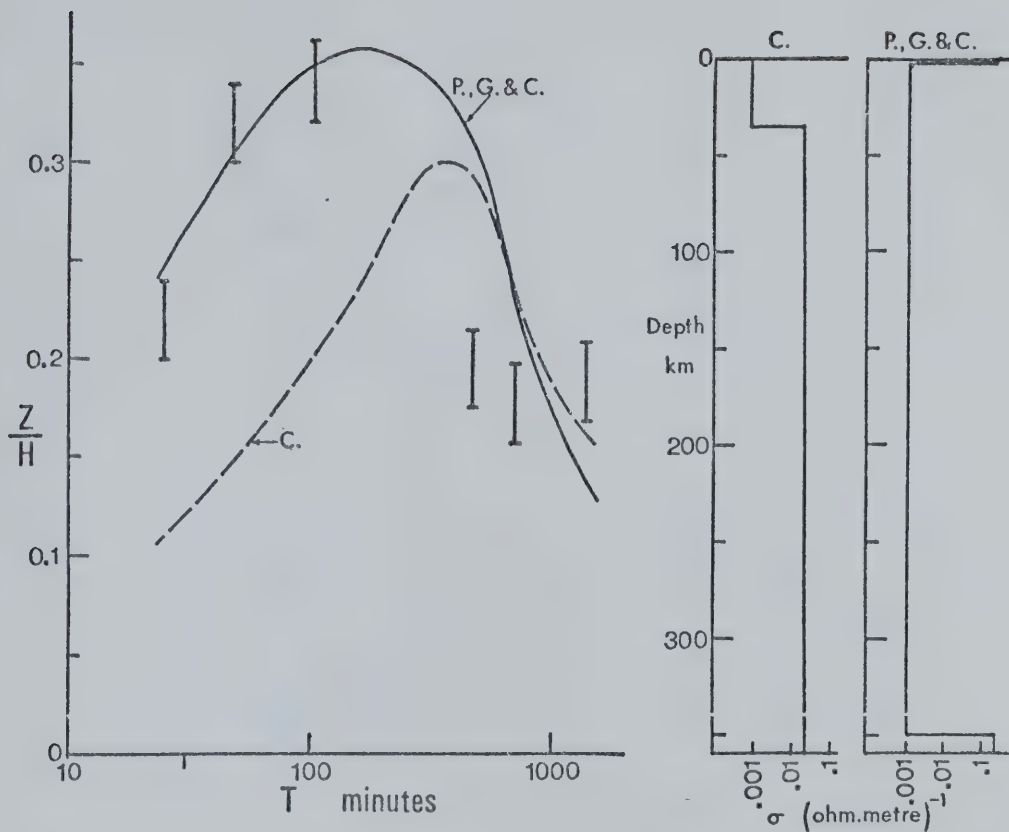
Fig. 5.5 Observed and calculated ratios of vertical to horizontal normal
fields in the eastern region (Great Plains), at six
periods.  The wave numbers associated with the observed
values are given in Table 5.2.  The curves correspond to
the conductivity-depth profiles proposed by Caner (1970,
1971) and by Porath, Gough and Camfield (1971).  From
Gough and Camfield (1972b).

Fig. 5.6   Observed and calculated ratios of vertical to

horizontal normal fields in the western region

(Cordillera), at six periods.   The wave numbers

associated with the observed values are given in

Table 5.2.   The curves correspond to the conduc-

tivity-depth profiles given by

a) Caner (1970, 1971)

b) Porath, Gough and Camfield (1971)

c) Gough and Camfield (1972b)

Figure taken from Gough and Camfield (1972b)

(a)

(b)

(c)
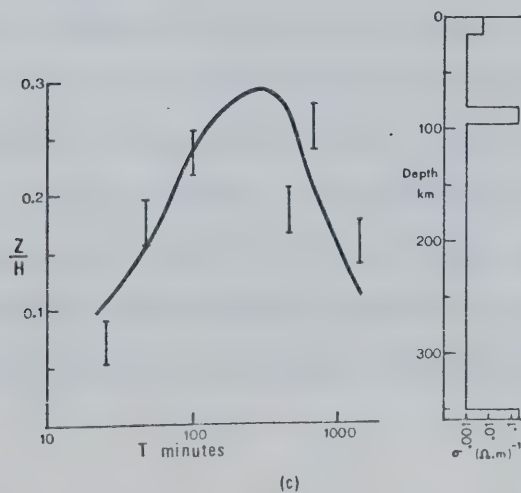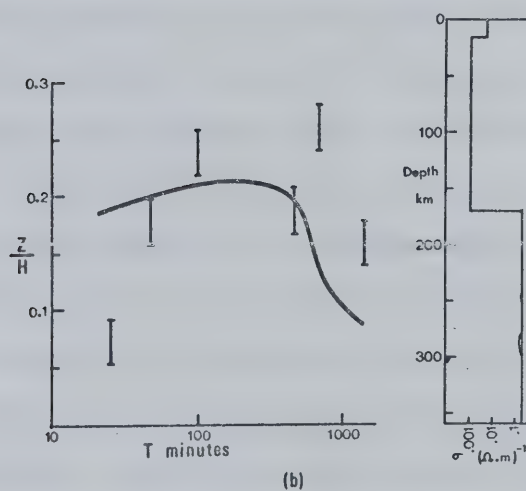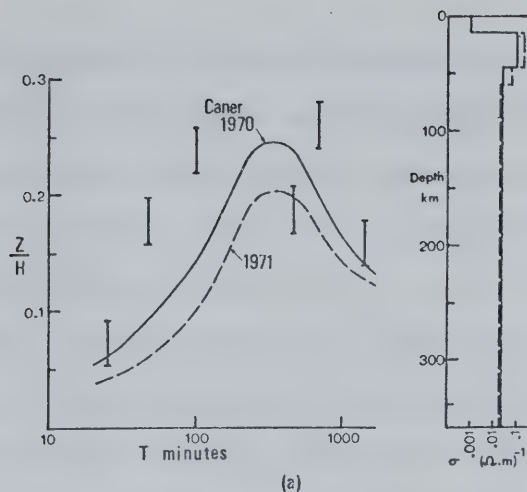
depth to the half-space and its conductivity are consistent
with laboratory measurements by Mao and Bell (1972) on olivine
and spinel in the pressure range 100-300 kb (corresponding to a
depth range 300-800 km in the earth model of Haddon and Bullen as
tabulated by Stacey, 1969, p. 281).

In the western region, three different types of conductivity-
depth profiles have been proposed to account for the westward
attenuation of the vertical field of substorms:  a) the conductive
layer in the lower crust, of Caner (1970, 1971) and Cochrane and
Hyndman (1970); see again Fig. 1.7; b) the rise in the level of the
conductive mantle, relative to its depth in the east, of Porath
et al. (1971); and c) the conductive layer in the resistive upper
mantle chosen by Gough and Camfield (1972b).  These profiles and
their response are shown in Fig. 5.6.  Caner's data covered both
substorm and daily variation period bands, but while  his lower
crustal layer fits some of our observations, it requires, with our
wave numbers, much more Z attenuation at 48 and 102 min than our
Z/H ratios will allow.  The western model of Porath  et al.,
derived from substorm data alone, is the same in form as their
eastern model but has these differences:  the top of the conducting
mantle is raised to half the depth it has in the eastern region,
and the surface layer is thickened to 15 km to take in the entire
upper crust, not just the sediments.  The surface layer is also
made less conductive ($\sigma = 0.005 \ \Omega^{-1}m^{-1}$) following the deep
resistivity soundings of Cantwell et al. (1965).  As mentioned
earlier, this model had to be rejected when the daily variation data

became available, because its response has quite the wrong shape;
it predicts for the daily variation a westward attenuation of Z/H
which is not observed.

The reasoning behind profile c, with a conductive layer in the
resistive upper mantle, proceeds as follows:  first, there is good
evidence from seismological studies for a low-vecocity layer in the
upper mantle in the western United States and western Canada beneath
the array; for example, Wickens and Pec (1968) and Wickens (1971)
place such a zone in the depth range 50 to 90 km present only in the
Cordillera.   Second, Hales and Doyle (1967) find indications of
partial  melting in the low-velocity zone under tectonic regions such
as these, and third, Presnall et al. (1972) report that at fusion,
the conductivity of an artificial basalt rises by two orders of magni-
tude during laboratory experiments at atmospheric pressure.  Finally,
geomagnetic data require a conductive layer of limited thickness, so
it was reasonable from the above considerations to try such a layer at
depths typical of the seismic low-velocity zone.  Caner and Cannon
(1965) and Lambert and Caner (1965) had noted the apparent correlation
of the zone of     suppressed Z amplitudes in the western region with
the zone of low $P_n$ seismic velocities mapped in the review of Herrin
(1969).  In a more general way, Fournier et al. (1963) had also been
thinking along these lines.  At that time, however, neither petrolo-
gical nor continental heat flow data gave good evidence for partial
melting at these depths, nor does the hypothesis of partial melting
as a mechanism to both reduce seismic velocities and increase
electrical conductivity seem to have been favoured.

Following the above considerations, Gough and Camfield (1972b) arrived at their western profile by adding a conducting layer in the upper mantle to their eastern model and by making minor changes in the near-surface conditions. The additional layer is 15 km thick with $\sigma = 0.2\ \Omega^{-1}m^{-1}$ in the resistive upper mantle $(\sigma = 0.001\ \Omega^{-1}m^{-1})$. The conductive mantle $(\sigma = 0.2\ \Omega^{-1}m^{-1})$ begins at 350 km, as in the east, while the upper crust at the top of the section is retained from the western model of Porath et al. (15 km at $\sigma = 0.005\ \Omega^{-1}m^{-1}$). The Z/H response of the model, plotted in Fig. 5.6c, fits reasonably well at all periods. The thickness of the conducting layer, with $\sigma$ fixed at the value above, lies in the range 10 to 20 km; the depth of the top of the layer is poorly defined, and may be anywhere between 50 and 150 km while still satisfying the data. The maximum depth is reduced when this model for the normal fields is made consistent with the model for the anomalous fields, to be discussed next.

The anomalous fields in the Northern Rockies (Fig. 5.7) were derived using the approximate scheme described in Section 5.1 (equations 5.2) to separate them from the normal fields. The two local anomalies in this region are smaller relative to the normal fields and broader than the anomaly in the Central Plains, so the results have a rather larger uncertainty. Small errors here in the assumed normal fields can have drastic effects on the amplitudes of the normalized anomalous fields, and in fact the estimation of the normal fields sets the limit to the precision of the interpretation. Porath et al. (1971) adopted at each of the substorm periods a linear east-west variation for $Y_n$ and a smooth curve

joining the different levels of eastern and western Z fields for

$Z_n$. For two of the magnetic events described in Chapter III, the

observed fields at latitude 48°N on variometer line 2, just south

of the Canada-U.S.A. border, are shown in Fig. 5.7 along with the

assumed normal fields and the separated, normalized anomalous

fields. Normalization is with respect to $Y_n$, which is assumed to

be the inducing field for these north-south trending anomalies.

These is an internal inconsistency for the easternmost anomaly

on these profiles which must be considered. As discussed in

Section 5.1, a north-south line current will have a maximum in Y

and a cross-over in Z directly above it, and a Z maximum on one

side matched by a Z minimum on the other. Fields due to currents

in extended conductors are less easily predicted, but in general

maxima in Y and Z will be displaced from one another. However, the

observations in Fig. 5.7 for all three periods of the substorms

on 20 August show coincident Y and Z maxima at station KAL (Fig.

2.1) at 390 km on the profile scale. For the western anomaly in

this event, and for both anomalies in the event of 10 August, the

maxima in Z lie to the east of those in Y.

Porath et al. (1971) attribute this inconsistency to the

uncertainty in defining the normal and anomalous parts of the

variation field. Gough and Camfield (1972b) are more specific in

suggesting that it is an inhomogeneous part in the external field

which displaces the Z maximum on 20 August westward by one or

more station spacings. Whatever the cause, it is unlikely that

fields with coincident Y and Z maxima will be caused by induction

Fig. 5.7 Variation field components along an east-west profile

from Tonasket, Washington (TON) to Chinook, Montana

(CHN) at latitude 48°N. In each set of three diagrams,

that on the left gives three field components in

arbitrary units, those on the right the normalized

anomalous field ratios as indicated. $Y_a$ and $Z_a$ are

the eastward horizontal and vertical anomalous fields;

$Y_n$ is the regional, normal east-west field. The

curves of long dashes are the assumed normal fields.

From Porath et al. (1971).

AUGUST 20, 1969
T = 47.6 MIN.

NORMALIZED FIELDS

$Y_o/Y_n$

$Z_o/Y_n$

800 km

0.2

0

0.2

0

Y

X

Z

14

11

7

800 km

0

AUGUST 10, 1969
T = 47.6 MIN.

NORMALIZED FIELDS

$Y_o/Y_n$

$Z_o/Y_n$

800 km

0.2

0

0.2

0

Y

X

Z

8

800 km

0

AUGUST 20, 1969
T = 25.3 MIN.

NORMALIZED FIELDS

$Y_o/Y_n$

$Z_o/Y_n$

800 km

0.3

0

0.2

0

Y

X

Z

3

800 km

0

AUGUST 20, 1969
T = 102.4 MIN.

NORMALIZED FIELDS

$Y_o/Y_n$

$Z_o/Y_n$

800 km

0.2

0

0.2

0

Y

X

Z

9

800 km

0

E

W
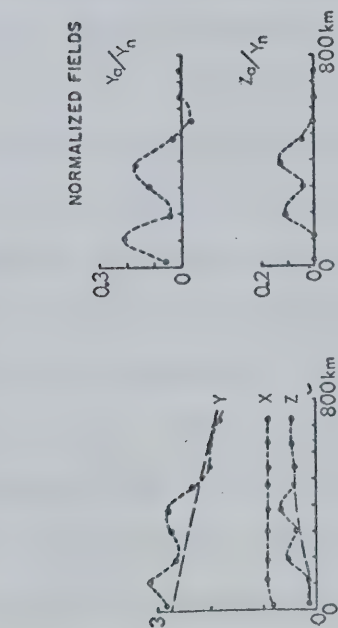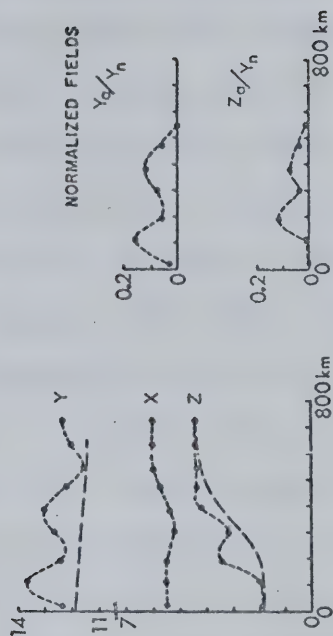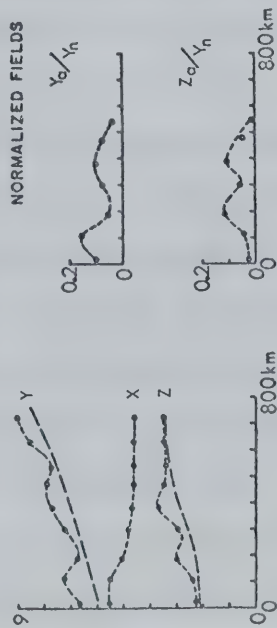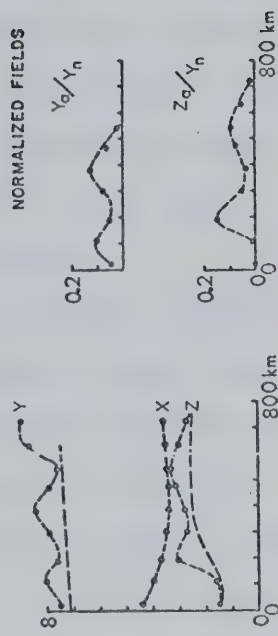
in internal conductivity structures alone. In the models which follow, we have tried to fit calculated fields to both Y maxima and the western Z maximum, and have accepted a displacement of the eastern Z maximum providing it had the right magnitude and shape. The models do have their eastern Z peak at the location required by the observations at period 47.6 min on 10 August.

Porath et al. (1971) used the transmission surface modelling technique discussed in Section 5.1. The program of Wright (1969) was employed to calculate anomalous fields due to ridges and steps on the surface of a conducting mantle which had been initially placed at the depths suggested by the normal field models of Porath et al. (1971), 350 km in the east and 170 km in the west. It must be remembered that the daily variation data were not available at this point. Half-widths of the computed anomalies were considerably larger than the observed anomalies, so the structure was raised to the depth of the low-velocity zone; see the sketch in Fig. 5.8.

The response of the model of Fig. 5.8 fits the anomalous fields reasonably well, but the model itself had to be rejected because it is not consistent with the optimum layered structures derived by Gough and Camfield (1972b) for east and west. The daily variation data demand that the conductor in the west be a thin layer underlain by resistive material. Porath et al. (1971) remark that induction in a structure like that in Fig. 5.8 differs only slightly from induction in a layer of finite thickness but with the same surface features, provided the thickness is everywhere greater than the skin depth in the layer (see Porath and Gough, 1971, Fig. 10). But the

Fig. 5.8  Observed normalized fields (circles and ×'s) across

the Northern Rockies (from Fig. 5.7) and calculated

fields (solid curves) for induction in a two-

dimensional conductive structure.  From Porath et al.

(1971).
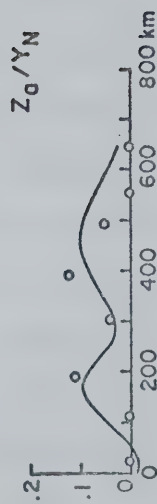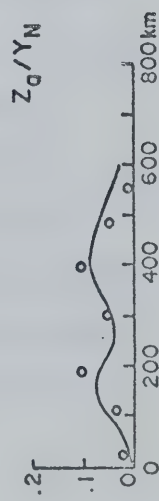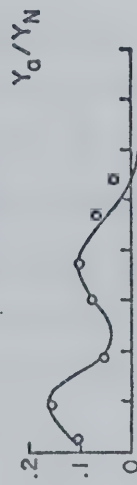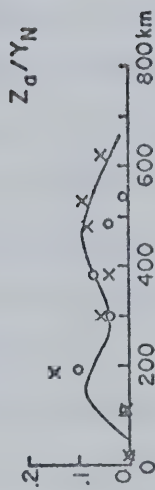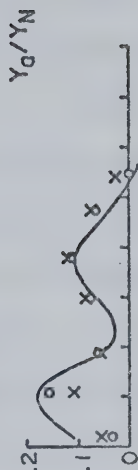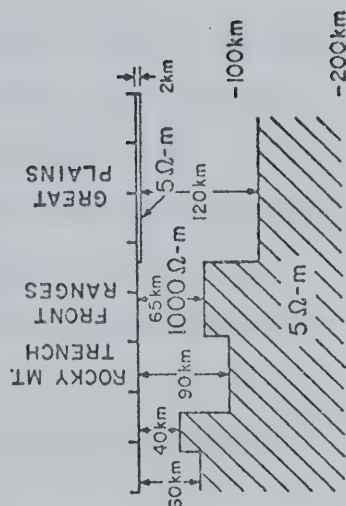
thickness of the conductor in the western normal-field model of
Gough and Camfield (1972b) is less than the skin depth at even the
shortest period, so a different model had to be sought.

In making a fresh attempt at the modelling, Gough and Camfield
(1972b) have used the finite difference technique, also discussed
in Section 5.1, rather than the transmission surface solution.
Using the computer program of Jones and Pascoe (1971) and Pascoe and
Jones (1972), they have investigated about thirty models which
progressively elaborate on the western conductive layer determined
from the normal field observations of Fig. 5.6.  The final model,
drawn in Fig. 5.9, fits the anomalous fields of Fig. 5.7 just as
well as the model of Porath et al. (1971) shown in Fig. 5.8.  This
anomalous-field model, unlike that of Porath et al., is consistent
with the model for the normal fields.

The conductive sediments of the Great Plains in the model of
Gough and Camfield (1972b) are taken from the magnetotelluric results
of Reddy and Rankin (1971).  These were measured at sites in central
Alberta, some hundreds of kilometers north of the profile, but
nevertheless are the best information available.  The conductor
thickens but becomes less conductive towards the foothills, or,
conversely, thins but becomes more conductive away from the foothills.
The latter trend to higher conductivities is supported by the long-
line magnetotellurics of Vozoff et al. (1969) in eastern Montana,
beyond the eastern edge of the model in Fig. 5.9.

With the sedimentary conductor fixed, the edge of the conductive
layer in the upper mantle has been progressively modified to fit the

Fig. 5.9 Observed and calculated anomalies near the Northern
Rockies at latitude 48°N for three substorm periods.
Solid bars show data from an event on 20 August 1969;
dotted bars (at T = 48 min) are from an event on 10
August 1969 (from Fig. 5.7). Error bars are a rough
indication of uncertainties arising from the approxi-
mate separations. All six curves correspond to
induction by a uniform east-west field in the assemblage
of conductors shown. Note the vertical exaggeration of
the cross-sections. The upper section represents upper-
mantle conductive layer as an equivalent thickness at
$\sigma = 0.2 \ \Omega^{-1} \ m^{-1}$; all black parts of this figure indicate
this conductivity, which extends to infinite depth.
For convenience of computation, the upper-mantle
layer was elaborated by changing conductivities rather
than thicknesses, as shown at the bottom right. From
Gough and Camfield (1972b)

$\frac{Y_a}{Y_n}$

$\frac{Z_a}{Y_n}$

T - 48 min

$\frac{Y_a}{Y_n}$

$\frac{Z_a}{Y_n}$

T - 25 min

$\frac{Y_a}{Y_n}$

$\frac{Z_a}{Y_n}$

T - 102 min

Midway-Kettle R. Ranges
Idaho Panhandle
R. M. Trench
Front Range
Great Plains

800 km

82 km

380 km

200 km

80 km

0                    800 km

0.001 (ohm.m)$^{-1}$    0.1    0.2

0.001

200 km

8 km

0.1    0.2    0.2    0.06
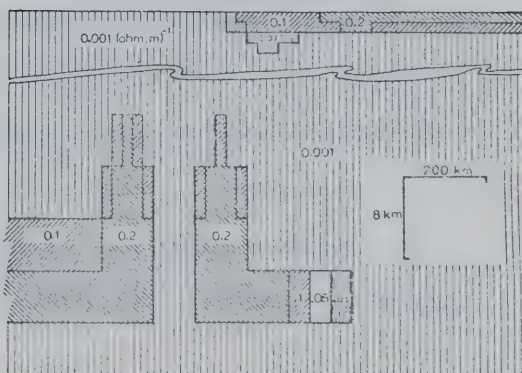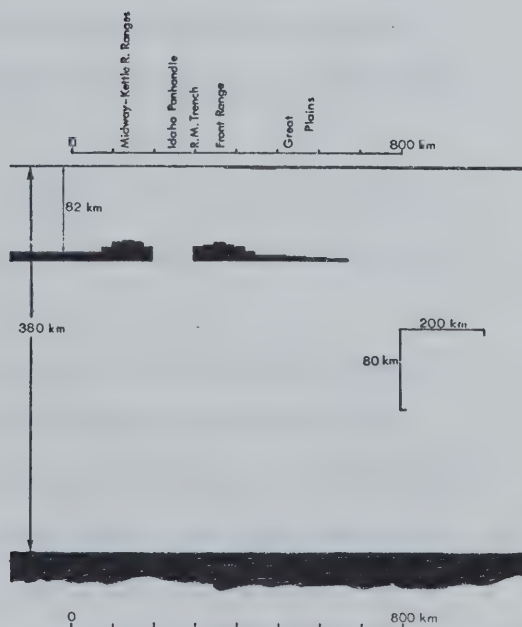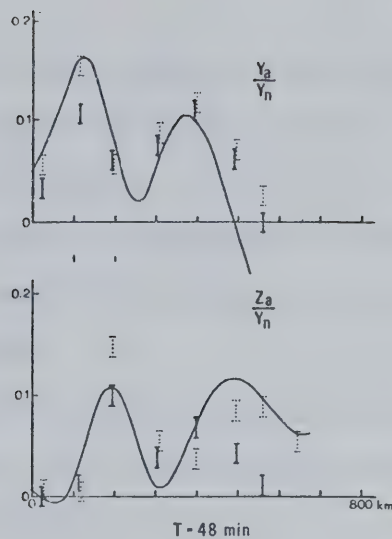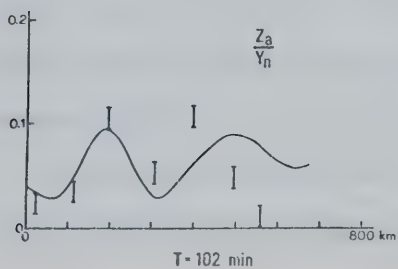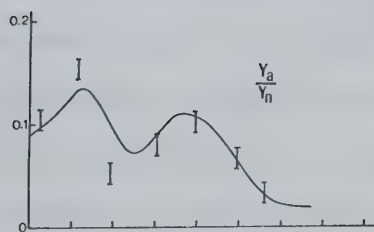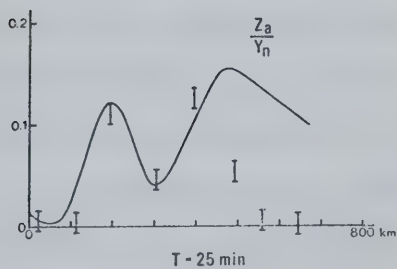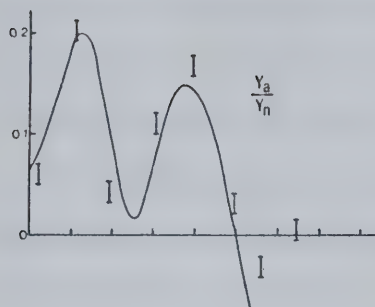
anomalous fields as well as possible. Listed next are some of the constraints which became evident during the model computations.

1. Resistive rock underlies the conductive structures. It must be less conductive, by about two orders of magnitude, than the conductive layer, so that the model predicts the western attenuation of Z with the observed period dependence.

2. The layer must thicken at two places, under the Midway-Kettle River ranges and under the front range. The double anomalies cannot be generated by the sediments and one such thickening alone.

3. The western ridge must be continuous with the western conductive layer, to yield the observed departure from antisymmetry in the western Z anomaly.

4. The resistive gap under the Idaho Panhandle, between the two thickenings, is needed to fit the low values of Y at NEP and of Z at LIB.

5. The conductive layer must extend under the Great Plains, to prevent an otherwise steep eastward fall in Y much below the observed values. The tapered layer has pinched out well before the window used to estimate eastern normal fields. The alternative to the extension seems to be a highly improbable thickening of the sediments by a factor of two, for which the magnetotellurics of Vozoff et al. (1969) and refraction seismology of Borcherdt and Roller (1968) (see Glover and Alexander, 1969) give no evidence in eastern Montana.

6. The half-widths (full widths at half-peak amplitude) of the anomalies in Y are about 150 km. From the discussion in Section

5.1 on line currents, the maximum depth to the top of extended structures of reasonably high conductivity can be no more than half this figure:  75 km.  This narrows the limits on the depth to the conductive layer from the 50-150 km range given by the normal-field Z/H ratios to 50-75 km.

While there is still much freedom within these constraints, Gough and Camfield (1972b) believe that the main features of the model are probably correct.  The structures have been placed at the maximum depth allowed by the  half-widths.

Other workers have carried out induction studies in the region above the resistive gap and the western conductive thickening.  The small-scale variation anomaly investigated by Lajoie and Caner (1970) 100 km north of line 2 above the resistive gap probably reflects secondary structure at depths smaller than those considered here.  Vozoff et al. (1969) report long-line magnetotellurics in Washington State above the western conductive thickening.  Their interpretation has a resistive crust $(0.0007 - 0.001 \ \Omega^{-1}m^{-1})$ to depth 30 km, on top of an upper mantle of $0.003 - 0.005 \ \Omega^{-1}m^{-1}$. Their data suggest that any further increase in conductivity in the mantle must occur deeper than 250 km, agreeing with the model of Fig. 5.9.  From the experience of Caner et al. (1969) with magne-totellurics at PEN and GRA (Fig. 1.5), north of array stations TON and KET respectively, it seems likely that the uniform somewhat-resistive upper mantle of Vozoff et al. (1969) could be reinterpreted in terms of a thin conductive layer sandwiched between two more-resistive layers.  Rapid change in the direction of the principal axis of the

tensor apparent resistivities at periods up to 1/2 h is evidence for nearby two-dimensional structure. It is unfortunate that tensor data were not available at longer periods.

Gough and Camfield (1972b) have given some physical grounds to explain high conductivity in a finite layer, as detailed above. Partial melting is a possible process yielding both the enhanced conductivity modelled here and the low seismic velocities reported by Wickens and Pec (1968) and Wickens (1971). Partial melting requires higher temperatures and/or hydration. Berry et al. (1971) have reviewed geophysical studies in the Canadian Cordillera and point out that Blackwell (1969) brings his Cordilleran Thermal Anomaly Zone of high heat flow into Canada, and hence across variometer line 2, between the Fraser Fault system and the Rocky Mountain Trench. These high heat flow values are supported directly by the measurements of Sass et al. (1971) and indirectly by the aeromagnetic mapping of a coincident region of low-amplitude static vertical-field magnetic anomalies by Haines et al. (1971). The array unfortunately did not extend to the western boundary of the Zone, marked by low heat flow in the western half of Washington State, although Caner et al. (1971) map suppressed Z amplitudes, and hence the conductive layer, as far west as Vancouver Island (see Fig. 1.5). Roy et al. (1972) have postulated from the heat flow data an undivided partially-melted zone in the depth range 50–170 km beneath the Northern Rocky Mountains, not extending as far west as the Pacific coast, at about latitude 47°N just south of line 2. It is not surprising that they have not detected the resistive gap

required in the model of Gough and Camfield (1972b), since it is only about as wide as it is deep.

In tectonic terms, Gough and Camfield (1972b) have speculated, from the depth (50 to 100 km) to the conductive layer, that it may mark the boundary between two overthrust lithospheric plates. If oceanic lithosphere has underthrust the continent as far as the eastern front of the Rockies, following the paleoseismic Benioff zones of Hyndman (1972), one or both of two factors could have produced the conductive layer. The first is dissipative heating, frictional, viscous, or otherwise. The second is the effect of water from the sea, either directly in hydrated minerals (Hyndman and Hyndman, 1968) or through its facilitation of partial-melting (Lebedev and Khitarov, 1964). Both heating and hydration might be important near the interface between the plates, although the heating would be significant only if the overthrust were active now or in the very recent past. This follows from the thermal relaxation time for a hot layer 15 km thick: of order 1 million years for heat transfer by conduction (Carslaw and Jaeger, 1940), or less if other mechanisms are active. The resistive gap under the Idaho Panhandle would be easier to explain with the hydration/partial melt model than with a purely thermal model, since some lateral redistribution of the hydrated ocean-floor rocks would be expected in the large-scale shearing involved in lithospheric underthrust. This model might account for both the thickenings in the conductive layer and the resistive gap.

Gough and Camfield (1972b) also speculate that, alternatively,

the conductive ridge under the front range may be of thermal origin and associated with injection of magma from greater depths. Eardley (1963) and others have postulated that the uplifts of the Rocky Mountains are caused by intrusion of lower-density basaltic megasills or megalaccoliths into the deep crust from a mantle source, with buoyancy being provided when the basaltic material is transferred from the higher confining pressure of the upper mantle to the lower pressures of the crust. These authors have not necessarily located the intrusions above a subduction zone, although this may be the case. The western edge of the eastern ridge in the geoelectric model lies under the Rocky Mountain Trench. The Trench may thus mark the western limit of the front range uplift, if the latter is associated with intrusion. This model for the formation of the front range differs from the widely-accepted hypothesis that uplift of the Omineca Geanticline (a metamorphic fold belt west of the Trench) caused the overlying sediments to slide eastward to build the front range (Price and Mountjoy, 1970).

One can contrast the structure of the Northern Rockies region with that of the western United States covered by the 1967 array (Fig. 1.8), where

1. a seismic low-velocity layer, causing delays in teleseismic arrivals and amplitude attenuation, is well documented (Hales and Doyle, 1967; Hales et al., 1968; Archambeau et al., 1969; Herrin, 1969);

2. heat flow patterns are strongly related to crustal provinces (Blackwell, 1969; Sass et al., 1971; Roy et al., 1972); and

3.   electrical conductivity has a distribution in harmony

with seismological and geothermal results (Schmucker, 1970a; Reitzel

et al., 1970; Porath and Gough, 1971).

The conductive regions under the Southern Rockies, the Wasatch

Fault Zone and the Basin and Range Province are either continuous

with the conductive mantle or are at least of order 100 km thick.

This is true whether the topography on the surface of the conductor

is at the depth of the seismic low-velocity zone (Porath, 1971a)

or deeper (Porath and Gough, 1971; see Fig. 1.11 of this thesis).

It is required by the phase differences between inducing and

induced fields (Porath et al., 1970) and by the anomalies in the

daily-variation fields recorded by the 1967 array (Reitzel et al.,

1970; see Fig. 1.10) and on the Rio Grande profile (Schmucker,

1970a; see Fig. 1.4).

In this study we have confirmed, as Dr. B. Caner long main-

tained in principle, that the conductor under the Northern Rockies

is by contrast thin (a small fraction of the skin-depths of the

incident fields) and has under it a poor conductor of much greater

thickness.   This result, along with many others in geology and

geophysics, suggests that the scale of heating and tectonic distur-

bance, whatever processes of overthrust and lithospheric subduction

have been involved, has been much greater in the Basin and Range,

Colorado Plateau and Southern Rockies than in the Northern Rockies.

5.4  Suggestions for Further Work

The magnitude of anomalous fields and the complexity of induction

effects in the North American Central Plains indicates that further study is worthwhile. An array program with more-closely spaced variometers and better coverage northward in Saskatchewan and Manitoba and southward in Wyoming and Nebraska was undertaken jointly by the University of Alberta and the Earth Physics Branch in the summer of 1972. Preliminary results indicate that the region of enhanced variations extends at least as far north as the Trans-Canada highway near Regina, Saskatchewan. The proximity of auroral-zone substorm currents will require careful selection of events with low external Z fields, so that the fields of internal currents can be recognized.

Further useful examination could be made of the 1969 data in the Central Plains, in an attempt to estimate quantitatively the relation between inducing and induced fields. Cross-power spectral analyses among the three variation components and the computation of transfer functions would be valuable, although the statistical requirements of the latter would require more events than currently available, hence extended digitizing. However, this should be feasible once the automatic digitizing system (flying-spot scanner and mini-computer) becomes fully operational at the University of Alberta.

Similar comments can be made about the region of the Northern Rockies, especially regarding fullest use of available data.

Data in the records at much shorter periods, micropulsations and sudden commencements, should be analysed to widen the period band of the investigation.

BIBLIOGRAPHY

Alpaslan, T., 1968. *Spectral behavior of short period body waves and the synthesis of crustal structure in western Canada.* M.Sc. Thesis, Department of Physics, University of Alberta, Edmonton.

Anderson, C.W., III, 1970. *Geomagnetic depth sounding and the upper mantle in the western United States.* Ph.D. Thesis, Department of Physics, University of Alberta, Edmonton.

Archambeau, C.B., E.A. Flinn, and D.G. Lambert, 1969. Fine structure of the upper mantle. *J. Geophys. Res.*, 74, 5825-5865.

Bennett, D.J., and F.E.M. Lilley, 1972. Horizontal polarization in array studies of anomalous geomagnetic variations. *Nature Phys. Sci.*, 237, 8-9.

Berry, M.J., W.R. Jacoby, E.R. Niblett and R.A. Stacey, 1971. A review of geophysical studies in the Canadian Cordillera. *Can. J. Earth Sci.*, 8, 788-801.

Black, D.I., 1970. Lunar and solar magnetic variations at Abinger: their detection and estimation by spectral analysis via Fourier transforms. *Phil. Trans. Roy. Soc. Lond.*, A268, 233-263.

Blackwell, D.D., 1969. Heat-flow determinations in the northwestern United States. *J. Geophys. Res.*, 74, 992-1007.

Borcherdt, C.A., and J.C. Roller, 1968. Preliminary interpretation of a seismic-refraction profile across the Large Aperture Seismic Array, Montana. Open file report, 31 pp, U.S. Geological Survey, Menlo Park, California.

Brace, W.F., 1971. Resistivity of saturated crustal rocks to 40 km based on laboratory measurements. In The Structure and Physical Properties of the Earth's Crust, ed. J.G. Heacock, Geophysical Monograph 14, A.G.U., Washington, D.C., 243-255.

Braddick, H.J.J., 1954. The Physics of Experimental Method. Chapman and Hall, London.

Bullard, E.C., 1967. Electromagnetic induction in the earth. *Quart. J.R. astr. Soc.*, 8, 143-160.

Camfield, P.A., and D.I. Gough, 1972. Anomalies in daily variation magnetic fields in the northwestern United States and southwestern Canada. In preparation.

Camfield, P.A., D.I. Gough and H. Porath, 1971. Magnetometer array studies in the northwestern United States and southwestern Canada. *Geophys. J.R. astr. Soc.*, 22, 201-221.

Caner, B., 1970. Electrical conductivity structure in western Canada and petrological interpretation. *J. Geomag. Geoelec.*, 22, 113-129.

Caner, B., 1971. Quantitative interpretation of geomagnetic depth-sounding data in western Canada. *J. Geophys. Res.*, 76, 7202-7216.

Caner, B., D.R. Auld, H. Dragert and P.A. Camfield, 1971. Geomagnetic depth-sounding and crustal structure in western Canada. *J. Geophys. Res.*, 76, 7181-7201.

Caner, B., P.A. Camfield, F. Andersen, and E.R. Niblett, 1969. A large-scale magnetotelluric survey in western Canada. *Can. J. Earth Sci.*, 6, 1245-1261.

Caner, B., and W.H. Cannon, 1965. Geomagnetic depth-sounding and correlation with other geophysical data in western North America. *Nature*, 207, 927-928.

Caner, B., W.H. Cannon and C.E. Livingstone, 1967. Geomagnetic depth sounding and upper mantle structure in the Cordillera region of western North America. *J. Geophys. Res.*, 72, 6335-6351.

Cantwell, T., P. Nelson, J. Webb and A.S. Orange, 1965. Deep resistivity measurements in the Pacific Northwest. *J. Geophys. Res.*, 70, 1931-1937.

Carslaw, H.S., and J.C. Jaeger, 1940. Conduction of Heat in Solids. Oxford U.P., 510 pp.

Carson, J.E., 1963. Analysis of soil and air temperatures by Fourier techniques. *J. Geophys. Res.*, 68, 2217-2232.

Chapman, S., 1919. The solar and lunar diurnal variation of the earth's magnetism. *Phil. Trans. Roy. Soc. London*, A218, 1-118.

Cochrane, N.A., and R.D. Hyndman, 1970. A new analysis of geomagnetic depth-sounding data from western Canada. *Can. J. Earth Sci.*, 7, 1208-1218.

Coggon, J.H., 1971. Electromagnetic and electrical modelling by the finite element method. *Geophys.*, 36, 132-155.

Cook, K.L., and J.R. Montgomery, 1971. East-west transverse
    structural trends in eastern Basin and Range province as
    indicated by gravity data. (Abstract only) *EOS Trans.*
    *A.G.U.*, 52, 350.

Cooley, J.W., and J.W. Tukey, 1965. An algorithm for the machine
    calculation of complex Fourier series. *Math. Comput.*, 19,
    297-301.

Dawson, G.B., and R.G. Fisher, 1964. Diurnal and seasonal ground
    temperature variations at Wairakei. *N.Z. J. Geol. Geophys.*,
    7, 144-154.

Dyck, A.V., and G.D. Garland, 1969. A conductivity model for certain
    features of the Alert anomaly in geomagnetic variation. *Can.*
    *J. Earth Sci.*, 6, 513-516.

Eardley, A.J., 1963. Relation of uplifts to thrusts in the Rocky
    Mountains. In The Backbone of the Americas - Tectonic History
    from Pole to Pole, A Symposium. *Amer. Assoc. Petrol. Geol.*
    *Mem.*, 2, 209-219.

Everett, J.E., and Hyndman, R.D., 1967. Geomagnetic variations and
    electrical conductivity structure in south-western Australia.
    *Phys. Earth Planet. Interiors*, 1, 24-34.

Fisher, R.A., 1929. Test of significance in harmonic analysis.
    *Proc. R. Soc.*, A, 125, 54-59.

Fournier, H.G., S.H. Ward and H.F. Morrison, 1963. Magnetotelluric
    evidence for the low velocity layer. *Space Sci. Lab. Univ. of*
    *California (Berkeley), Publ. Ser.* 4, no. 76, 23 pp.

Glover, P., and S.S. Alexander, 1969. Lateral variations in crustal
    structure beneath the Montana LASA. *J. Geophys. Res.*, 74,
    505-531.

Gough, D.I., and P.A. Camfield (1972a). Convergent geophysical
    evidence of a metamorphic belt through the Black Hills of
    South Dakota. *J. Geophys. Res.*, 77, 3168-3170.

Gough, D.I., and P.A. Camfield, 1972b. Conductive structures under
    the Northern Rocky Mountains. In preparation.

Gough, D.I., and H. Porath, 1970. Long-lived thermal structure under
    the Southern Rocky Mountains. *Nature*, 226, 837-839.

Gough, D.I., and J.S. Reitzel, 1967. A portable three-component
    magnetic variometer. *J. Geomag. Geoelec.*, 19, 203-215.

Gough, D.I., and J.S. Reitzel, 1969. Magnetic deep sounding and local conductivity anomalies. In The Application of Modern Physics to the Earth & Planetary Interiors, ed. S.K. Runcorn, Wiley-Interscience, London, 139-153.

Gupta, J.C., and S. Chapman, 1969. Lunar daily harmonic geomagnetic variation as indicated by spectral analysis. J. Atmosph. Terr. Phys., 31, 233-252.

Haines, G.V., W. Hannaford, and R.P. Riddihough, 1971. Magnetic anomalies over British Columbia and the adjacent Pacific Ocean. Can. J. Earth Sci. 8, 387-391.

Hakura, Y,, 1965. Tables and maps of geomagnetic coordinates corrected by higher order spherical harmonic terms. Rept. Ionosph. Space Res. Japan, 19, 121-157.

Hales, A.L., J.R. Cleary, H.A. Doyle, R. Green and J. Roberts, 1968. P-wave station anomalies and the structure of the upper mantle. J. Geophys. Res., 73, 3885-3896.

Hales, A.L., and H.A. Doyle, 1967. P and S travel-time anomalies and their interpretation. Geophys. J.R. astr. Soc., 13, 403-415.

Hartman, O., 1963. Behandlung lokaler erdmagnetischer Felder als Randwertaufgabe der Potentialtheorie. Abhandl. Akad. Wiss. Göttingen, Math. Phys. Kl., Beitr. I.G.J., 9, 1-50.

Herrin, E., 1969. Regional variations of P-wave velocity in the upper mantle beneath North America. In The Earth's Crust and Upper Mantle, ed. P.J. Hart, Geophysical Monograph 13, A.G.U., Washington, D.C., 242-246.

Herron, T.J., 1967. An average geomagnetic power spectrum for the period range 4.5 to 12,900 seconds. J. Geophys. Res., 72, 759-761.

Hildebrand, F.B., 1962. Advanced Calculus for Applications. Prentice-Hall, Englewood Cliffs, N.J.

Hyndman, R.D., 1963. Electrical conductivity inhomogeneities in the earth's upper mantle. M.Sc. Thesis, University of British Columbia, Vancouver.

Hyndman, R.D., 1972. Plate motions relative to the deep mantle and the development of subduction zones. Nature, 238, 263-265.

Hyndman, R.D., and D.W. Hyndman, 1968. Water saturation and high electrical conductivity in the lower continental crust. Earth Planet. Sci. Lett., 4, 427-432.

Iyer, H.M., and J.H. Healy, 1972. Teleseismic residuals at the LASA-USGS extended array and their interpretation in terms of crust and upper-mantle structure. *J. Geophys. Res.*, 77, 1503-1527.

Jones, F.W., and L.J. Pascoe, 1971. A general computer program to determine the perturbation of alternating electric currents in a two-dimensional model of a region of uniform conductivity with an embedded inhomogeneity. *Geophys. J.R. astr. Soc.*, 24, 3-30.

Jones, F.W., and L.J. Pascoe, 1972. The perturbation of alternating geomagnetic fields by three-dimensional conductivity inhomogeneities. *Geophys. J.R. astr. Soc.*, 27, 479-485.

Jones, F.W., and A.T. Price, 1970. The perturbations of alternating geomagnetic fields by conductivity anomalies. *Geophys. J.R. astr. Soc.*, 20, 317-334.

Jones, F.W., and A.T. Price, 1971. The geomagnetic effects of two-dimensional conductivity inhomogeneities at different depths. *Geophys. J.R. astr. Soc.*, 22, 333-345.

Kanamori, H., 1970. Seismological evidence for heterogeneity of the mantle. *J. Geomag. Geoelec.*, 22, 53-70.

Kertz, W., 1960. Leitungsfaehiger Zylinder im transversalen magnetischen Wechselfeld. *Gerlands Beitr. Geophys.*, 69, 4-28.

Lahiri, B.N., and A.T. Price, 1939. Electromagnetic induction in non-uniform conductors and the determination of the conductivity of the earth from terrestrial magnetic variations. *Phil. Trans. Roy. Soc. London*, A237, 509-540.

Lajoie, J.J., and B. Caner, 1970. Geomagnetic induction anomaly near Kootenay Lake - a strike-slip feature in the lower crust? *Can. J. Earth Sci.*, 7, 1568-1579.

Lambert, A., and B. Caner, 1965. Geomagnetic "depth-sounding" and the coast effect in western Canada. *Can. J. Earth Sci.*, 2, 485-509.

Lebedev, E.B., and N.I. Khitarov, 1964. Dependence of the beginning of melting of granite and the electrical conductivity of its melt on high vapor pressure. *Geochem. Intern.*, 1, 193-197.

Lidiak, E.G., 1971. Buried Precambrian rocks of South Dakota. *Bull. Geol. Soc. Amer.*, 82, 1411-1420.

Lidiak, E.G., 1972. Precambrian rocks in the subsurface of Nebraska. *Neb. Geol. Survey Bull.*, no. 26, 41 pp.

Madden, T.R., and P.H. Nelson, 1964. A defense of Cagniard's magnetotelluric method. ONR Report, project NR-371-401, Geophysics Lab., Massachusetts Institute of Technology.

Madden, T.R., and C.M. Swift, Jr., 1969. Magnetotelluric studies of the electrical conductivity structure of the crust and upper mantle. In The Earth's Crust and Upper Mantle, ed. P.J. Hart, Geophysical Monograph 13, A.G.U., Washington, D.C., 469-479.

Mao, H.K., and P.M. Bell, 1972. Electrical conductivity and the red shift of absorption in olivine and spinel at high pressure . *Science*, 176, 403-406.

Mathisrud, G.C., and J.S. Sumner, 1967. Underground induced polarization surveying at the Homestake mine. *Mining Congress J.*, 53(3), 66-69.

Morrison, H.F., E. Wombwell, and S.H. Ward, 1968. Analysis of earth impedances using magnetotelluric fields. *J. Geophys. Res.*, 73, 2769-2778.

Nowroozi, A.A., 1967. Table for Fisher's test of significance in harmonic analysis. *Geophys. J.R. astr. Soc.*, 12, 517-520.

Oldenburg, D.W., 1969. *Separation of magnetic substorm fields for mantle conductivity studies in the western United States.* M.Sc. Thesis, Department of Physics, University of Alberta, Edmonton.

Parasnis, D.S., 1966. Mining Geophysics. Elsevier, Amsterdam.

Parkinson, W.D., 1959. Directions of rapid geomagnetic fluctuations. *Geophys. J.R. astr. Soc.*, 2, 1-14.

Parkinson, W.D., 1962. The influence of continents and oceans on geomagnetic variations. *Geophys. J.R. astr. Soc.*, 4, 441-449.

Pascoe, L.J., and F.W. Jones, 1972. Boundary conditions and calculation of surface values for the general two-dimensional electromagnetic induction problem. *Geophys. J.R. astr. Soc.*, 27, 179-193.

Porath, H., 1971a. Magnetic variation anomalies and seismic low-velocity zone in the Western United States. *J. Geophys. Res.*, 76, 2643-2648.

Porath, H., 1971b.  A review of the evidence on low-resistivity
    layers in the earth's crust.  In The Structure and Physical
    Properties of the Earth's Crust, ed., J.G. Heacock,
    Geophysical Monograph 14, A.G.U., Washington, D.C., 127-144.

Porath, H., and A. Dziewonski, 1971.  Crustal electrical conduc-
    tivity anomalies in the Great Plains province of the United
    States.  Geophys., 36, 382-395.

Porath, H., and D.I. Gough, 1971.  Mantle conductive structures
    in the western United States from magnetometer array studies.
    Geophys. J.R. astr. Soc., 22, 261-275.

Porath, H., D.I. Gough, and P.A. Camfield, 1971.  Conductive
    structures in the north-western United States and south-west
    Canada.  Geophys. J.R. astr. Soc., 23, 387-398.

Porath, H., D.W. Oldenburg and D.I. Gough, 1970.  Separation of
    magnetic variation fields and conductive structures in the
    western United States.  Geophys. J.R. astr. Soc., 19,
    237-260.

Presnall, D.C., C.L. Simmons, and H. Porath, 1972.  Changes in
    electrical conductivity of a synthetic basalt during melting.
    J. Geophys. Res., 77, 5665-5672.

Price, A.T., 1962.  The theory of magnetotelluric methods when the
    source field is considered.  J. Geophys. Res., 67, 1907-1918.

Price, A.T., 1964.  A note on the interpretation of magnetic
    variations and magnetotelluric data.  J. Geomag. Geoelec.,
    15, 241-248.

Price, R.A., and E.W. Mountjoy, 1970.  Geological structure of
    the Canadian Rocky Mountains between the Bow and Athabasca
    Rivers.  Geol. Assoc. Can. Special Paper 6, 7-26.

Reddy, I.K., and D. Rankin, 1971.  Magnetotelluric measurements
    in central Alberta.  Geophys., 36, 739-753.

Reddy, I.K., and D. Rankin, 1972.  Magnetotelluric response of a
    two-dimensional sloping contact by the finite element method.
    Pure Appl. Geophys. (in press).

Reitzel, J.S., D.I. Gough, H. Porath, and C.W. Anderson, 1970.
    Geomagnetic deep sounding and upper mantle structure in the
    western United States.  Geophys. J.R. astr. Soc., 19, 213-
    235.

Riddihough, R.P., 1969.  A geographic pattern of daily magnetic
    variation over north-west Europe.  Ann. Geophys., 25, 739-745.

Rikitake, T., 1956. Electrical state and seismicity beneath Japan. *Bull. Earthquake Res. Inst., Tokyo Univ.*, 34, 291-299.

Rikitake, T., 1959. Anomaly of geomagnetic variations in Japan. *Geophys. J.R. astr. Soc.*, 2, 276-287.

Rikitake, T., 1966. Electromagnetism and the Earth's Interior. Elsevier, Amsterdam.

Rikitake, T., 1971. Electric conductivity anomalies in the earth's crust and upper mantle. *Earth Sci. Rev.*, 7, 35-65.

Rikitake, T., I. Yokoyama and S. Sato, 1956. Anomaly of the geomagnetic Sq variation in Japan and its relation to the subterranean structure. *Bull. Earthquake Res. Inst., Tokyo Univ.*, 34, 197-235.

Rokityanskiy, I.I., and I.M. Logvinov, 1972. Anomaly of electrical conductivity of Kirovograd block of Ukrainian Shield. *Izvestia, Phys. Solid Earth*, no. 6, 104-110 in the Russian original.

Rostoker, G., 1968. Macrostructure of geomagnetic bays. *J. Geophys. Res.*, 73, 4217-4229.

Rostoker, G., 1972. Polar magnetic substorms. *Rev. Geophys. Space Phys.*, 10, 157-211.

Rostoker, G., C.W. Anderson, D.W. Oldenburg, P.A. Camfield, D.I. Gough, and H. Porath, 1970. Development of a polar magnetic substorm current system. *J. Geophys. Res.*, 75, 6318-6323.

Roy, R.F., D.D. Blackwell, and E.R. Decker, 1972. Continental heat flow. In The Nature of the Solid Earth, ed. E.C. Robertson. McGraw-Hill, New York, 506-543.

Samson, J.C., 1971. *Spectral characteristics of Pc4 and Pc5 geomagnetic micropulsations*. Ph.D. Thesis, Department of Physics, University of Alberta, Edmonton.

Sass, J.H., A.H. Lachenbruch, R.J. Munroe, G.W. Greene, and T.H. Moses, Jr., 1971. Heat flow in the westem United States. *J. Geophys. Res.*, 76, 6376-6413.

Schmucker, U., 1964. Anomalies of geomagnetic variations in the southwestern United States. *J. Geomag. Geoelectr.*, 15, 193-221.

Schmucker, U., 1969. Conductivity anomalies, with special reference to the Andes. In The Application of Modern Physics to the Earth and Planetary Interiors, ed. S.K. Runcorn, Wiley-Interscience, London, 125-138.

Schmucker, U., 1970a.  Anomalies of geomagnetic variations in the southwestern United States.  *Bull. Scripps Inst. Oceanography*, 13, 1-165, Univ. California, San Diego.

Schmucker, U., 1970b.  An introduction to induction anomalies.  *J. Geomag. Geoelec.*, 22, 9-33.

Serson, P.H., 1957.  An electrical recording magnetometer.  *Can. J. Phys.*, 35, 1387-1394.

Shimshoni, M., 1971.  On Fisher's test of significance in harmonic analysis.  *Geophys. J.R. astr. Soc.*, 23, 373-377.

Singleton, R.C., 1968.  Algol procedures for the fast Fourier transform.  *Commun. A.C.M.*, 11, 773-779.

Skilling, H.H., 1948.  Fundamentals of Electric Waves, second edition.  J. Wiley & Sons, New York, (Tenth printing, 1962).

Stacey, F.D., 1969.  Physics of the Earth.  John Wiley & Sons, New York.

Swift, C.M., Jr., 1967.  *A magnetotelluric investigation of an electrical conductivity anomaly in the southwestern United States*.  Ph.D. Thesis, Massachusetts Institute of Technology, Cambridge, Mass.

Swift, C.M., Jr., 1971.  Theoretical magnetotelluric and Turam response from two-dimensional inhomogeneities.  *Geophys.*, 36, 38-52.

Toman, K., 1965.  The spectral shifts of truncated sinusoids.  *J. Geophys. Res.*, 70, 1749-1750.

Tozer, D.C., 1959.  The electrical properties of the earth's interior.  In Physics and Chemistry of the Earth, ed. Ahrens, Press, Rankama, and Runcorn; Pergamon, London, 3,414-436.

Trigg, D.F., P.H. Serson, and P.A. Camfield, 1971.  A solid-state electrical recording magnetometer.  Pub. Earth Physics Branch 41, no. 5, 66-80, Dept. Energy, Mines and Resources, Ottawa.

Vozoff, K., and R.M. Ellis, 1966.  Magnetotelluric measurements in southern Alberta.  *Geophys.*, 31, 1153-1157.

Vozoff, K., A. Orange, and H.S. Lahman, 1969.  Magnetotelluric deep earth resistivity at eight U.S. "type-locations".  Final Report for Contract Nonr 4900(00) NR 081-25/3-23-65, Geoscience Inc., Cambridge, Mass.

Warren, R.E., J.G. Sclater, V. Vacquier, and R.F. Roy, 1969.
    A comparison of terrestrial heat flow and transient geomagnetic
    fluctuations in the southwestern United States. *Geophys.*,
    34, 463-478.

Weaver, J.T., 1964.  On the separation of local geomagnetic fields
    into external and internal parts. *Z. Geophys.*, 30, 29-36.

Wickens, A.J., 1971.  Variations in lithospheric thickness in
    Canada. *Can. J. Earth Sci.*, 8, 1154-1162.

Wickens, A.J., and K. Pec, 1968.  A crust-mantle profile from
    Mould Bay, Canada, to Tucson, Arizona. *Bull. Seism. Soc.
    Amer.*, 58, 1821-1831.

Wright, J.A., 1969.  The magnetotelluric and geomagnetic response
    of two-dimensional structures. *GAMMA*, 7, Inst. Geophys. Met.,
    Techn. Univ. Braunschweig, 102 pp.

Wright, J.A., 1970.  Anisotropic apparent resistivities arising
    from non-homogeneous, two-dimensional structures. *Can. J.
    Earth Sci.*, 7, 527-531.

Zietz, I., B.C. Hearn, M.W. Higgins, G.D. Robinson, and D.A.
    Swanson, 1971.  Interpretation of an aeromagnetic strip across
    the northwestern United States. *Bull. Geol. Soc. Amer.*, 82,
    3347-3372.

APPENDIX

Coordinates of Variometer Stations

On the following pages are listed the geographic coordinates
of variometer locations' (Fig. 1.8), scaled from 1:250,000 topo-
graphic maps, and the corresponding corrected geomagnetic
coordinates interpolated from the tables of Hakura (1965). For
completeness, the 1968 and 1967 arrays are included after the
1969 array. Declination values for the 1969 array were taken
from the relevant charts (D-Isogonic Chart, Canada 1965.0,
Department of Mines and Technical Surveys, Dominion Observatories
Branch, Ottawa; Isogonic Chart of the United States, 1965.0,
U.S. Department of Commerce, Coast and Geodetic Survey,
Washington, D.C.).

COORDINATES OF STATIONS IN 1969 ARRAY

| LINE | STATION | GEOGRAPHIC | | CORRECTED GEOMAGNETIC | | DECLI-NATION |
| | | LAT, DEG N | LONG, DEG W | LAT, DEG N | LONG, DEG E | DEG E |
|---|---|---|---|---|---|---|
| 1 | CHA | 50.5 | 106.7 | 59.9 | 311.0 | 17.5 |
| 1 | TUO | 51.2 | 107.3 | 60.5 | 310.0 | 18.3 |
| 1 | MAP | 50.0 | 109.5 | 58.7 | 307.7 | 19.1 |
| 1 | BRK | 50.6 | 111.9 | 58.8 | 304.6 | 20.3 |
| 1 | CCC | 51.2 | 114.5 | 58.8 | 301.3 | 21.9 |
| 1 | EIS | 51.3 | 116.0 | 58.6 | 299.6 | 22.4 |
| 1 | DON | 51.5 | 117.2 | 58.5 | 298.1 | 22.9 |
| 1 | REV | 51.0 | 118.2 | 57.7 | 297.2 | 22.9 |
| 1 | PRI | 50.7 | 119.8 | 57.0 | 295.6 | 23.0 |
| 1 | CAC | 50.8 | 121.3 | 56.8 | 294.0 | 23.2 |
| 2 | BEL | 48.1 | 102.4 | 58.3 | 317.2 | 13.4 |
| 2 | CUL | 48.2 | 104.5 | 58.0 | 314.5 | 15.0 |
| 2 | HIS | 48.4 | 106.9 | 57.7 | 311.5 | 16.6 |
| 2 | CHN | 48.7 | 109.2 | 57.5 | 308.5 | 18.1 |
| 2 | CHE | 48.6 | 111.0 | 57.0 | 306.4 | 19.0 |
| 2 | CUT | 48.8 | 112.2 | 56.9 | 305.0 | 19.6 |
| 2 | GLA | 48.4 | 113.3 | 56.2 | 303.8 | 19.7 |
| 2 | KAL | 48.2 | 114.4 | 55.8 | 302.6 | 20.1 |
| 2 | LIB | 48.4 | 115.4 | 55.7 | 301.4 | 20.5 |
| 2 | NEP | 48.3 | 117.1 | 55.2 | 299.6 | 20.9 |
| 2 | KET | 48.6 | 118.2 | 55.3 | 298.2 | 21.4 |
| 2 | TCN | 48.7 | 119.4 | 55.1 | 296.9 | 21.7 |
| 3 | RDR | 46.1 | 102.8 | 56.2 | 317.2 | 13.3 |
| 3 | BKR | 46.4 | 104.2 | 56.2 | 315.4 | 14.2 |
| 3 | CAV | 46.3 | 106.5 | 55.6 | 312.6 | 15.6 |
| 3 | MUS | 46.5 | 108.1 | 55.4 | 310.6 | 16.6 |
| 3 | HAR | 46.3 | 109.4 | 54.9 | 309.0 | 17.1 |
| 3 | WSS | 46.6 | 111.0 | 54.9 | 307.1 | 17.8 |
| 3 | HEL | 46.5 | 111.9 | 54.6 | 306.1 | 18.3 |
| 3 | PCW | 46.5 | 114.8 | 53.9 | 302.8 | 19.5 |
| 3 | WEI | 46.4 | 115.9 | 53.6 | 301.6 | 19.8 |
| 3 | DCD | 46.5 | 117.9 | 53.2 | 299.4 | 20.4 |
| 3 | SUN | 46.5 | 120.0 | 52.7 | 297.1 | 20.9 |
| 4 | DRA | 43.9 | 100.5 | 54.4 | 320.6 | 11.2 |
| 4 | FMD | 44.0 | 102.9 | 54.0 | 317.6 | 12.9 |
| 4 | HIL | 44.0 | 103.5 | 53.9 | 316.9 | 13.1 |
| 4 | UFT | 44.0 | 104.5 | 53.7 | 315.6 | 13.6 |
| 4 | DHC | 44.3 | 106.3 | 53.6 | 313.4 | 14.7 |
| 4 | HYA | 44.3 | 107.6 | 53.3 | 311.8 | 15.5 |
| 4 | CCD | 44.5 | 108.7 | 53.2 | 310.5 | 16.1 |
| 4 | WAP | 44.5 | 109.7 | 53.0 | 309.3 | 16.6 |
| 4 | ILP | 44.4 | 111.3 | 52.5 | 307.5 | 17.2 |
| 4 | MUD | 43.8 | 112.4 | 51.7 | 306.5 | 17.5 |
| 4 | CHL | 44.6 | 114.2 | 52.1 | 304.2 | 18.4 |
| 4 | MID | 44.4 | 116.8 | 51.3 | 301.4 | 19.1 |
| 4 | HER | 44.5 | 118.0 | 51.1 | 300.0 | 19.5 |

## COORDINATES OF STATIONS IN 1968 ARRAY

| LINE | STATION | GEOGRAPHIC | | CORRECTED GEOMAGNETIC | | DECLI-NATION |
| | | LAT, DEG N | LONG, DEG W | LAT, DEG N | LONG, DEG E | DEG E |
|---|---|---|---|---|---|---|
| 1 | LEO | 35.9 | 95.9 | 46.9 | 327.7 | |
| 1 | CAN | 35.9 | 100.3 | 45.9 | 322.5 | |
| 1 | DUM | 35.9 | 102.0 | 45.6 | 320.5 | |
| 1 | SFR | 36.4 | 104.7 | 45.5 | 317.2 | |
| 1 | TPD | 36.7 | 106.0 | 45.5 | 315.7 | |
| 1 | GOC | 36.9 | 107.4 | 45.5 | 314.1 | |
| 1 | KAY | 36.7 | 110.2 | 44.6 | 311.0 | |
| 1 | PAG | 37.0 | 111.5 | 44.7 | 309.5 | |
| 1 | KAN | 37.1 | 112.3 | 44.6 | 308.6 | |
| 1 | MCJ | 37.2 | 112.9 | 44.6 | 308.0 | |
| 1 | VEY | 37.3 | 113.6 | 44.5 | 307.2 | |
| 1 | GLC | 36.8 | 114.6 | 43.8 | 306.2 | |
| 1 | SHO | 36.0 | 116.2 | 42.5 | 304.8 | |
| 2 | CHI | 34.4 | 100.2 | 44.4 | 322.8 | |
| 2 | TUL | 34.6 | 101.8 | 44.2 | 320.9 | |
| 2 | GLN | 35.2 | 103.0 | 44.6 | 319.4 | |
| 2 | CLC | 35.0 | 105.6 | 43.8 | 316.4 | |
| 2 | SNF | 35.1 | 107.6 | 43.5 | 314.2 | |
| 2 | GAL | 35.5 | 109.0 | 43.6 | 312.6 | |
| 2 | WIN | 35.1 | 110.7 | 42.8 | 310.9 | |
| 2 | RED | 35.3 | 112.0 | 42.7 | 309.4 | |
| 2 | PEA | 35.5 | 113.2 | 42.7 | 308.1 | |
| 2 | KIN | 35.1 | 114.2 | 42.0 | 307.1 | |
| 2 | ESS | 34.8 | 115.1 | 41.5 | 306.3 | |
| 2 | NEW | 34.8 | 116.6 | 41.2 | 304.7 | |
| 2 | MOJ | 35.1 | 118.2 | 41.2 | 302.9 | |
| 3 | DAL | 32.9 | 96.8 | 43.5 | 327.0 | |
| 3 | BRO | 33.2 | 102.2 | 42.6 | 320.7 | |
| 3 | ROS | 33.6 | 104.4 | 42.6 | 318.1 | |
| 3 | CAZ | 33.7 | 105.9 | 42.4 | 316.4 | |
| 3 | SNM | 33.7 | 107.0 | 42.1 | 315.2 | |
| 3 | LUN | 33.8 | 109.0 | 41.8 | 313.0 | |
| 3 | GER | 33.1 | 110.0 | 40.8 | 312.1 | |
| 3 | PHO | 33.6 | 112.2 | 40.9 | 309.7 | |
| 3 | AGU | 34.0 | 113.3 | 41.1 | 308.4 | |
| 3 | BLY | 33.6 | 114.9 | 40.3 | 306.8 | |
| 3 | CCA | 33.6 | 115.2 | 40.0 | 305.5 | |
| 4 | CLB | 32.5 | 104.2 | 41.4 | 318.5 | |
| 4 | DEM | 32.1 | 107.7 | 40.2 | 314.8 | |
| 4 | DCU | 31.3 | 109.6 | 38.9 | 312.9 | |
| 4 | TUS | 32.2 | 110.8 | 39.6 | 311.4 | |
| 4 | WHY | 32.2 | 112.7 | 39.2 | 309.4 | |
| 4 | TAC | 32.9 | 113.9 | 39.7 | 308.0 | |
| 4 | YUM | 32.6 | 114.5 | 39.3 | 307.5 | |
| 4 | HOL | 32.9 | 115.4 | 39.4 | 306.5 | |

COORDINATES OF STATIONS IN 1967 ARRAY

| LINE | STATION | GEOGRAPHIC | | CORRECTED GEOMAGNETIC | | DECLI-NATICN |
| | | LAT, DEG N | LONG, DEG W | LAT, DEG N | LONG, OEG E | DEG E |
|---|---|---|---|---|---|---|
| 1 | MUL | 42.0 | 101.0 | 52.3 | 320.4 | |
| 1 | CRW | 42.7 | 103.4 | 52.6 | 317.3 | |
| 1 | CAS | 42.8 | 106.5 | 52.0 | 313.5 | |
| 1 | SWE | 42.6 | 108.1 | 51.4 | 311.7 | |
| 1 | FAR | 42.1 | 109.4 | 50.5 | 310.4 | |
| 1 | MCN | 42.2 | 111.2 | 50.2 | 308.3 | |
| 1 | AMF | 42.8 | 112.8 | 50.5 | 306.3 | |
| 1 | MUR | 42.6 | 114.3 | 50.0 | 304.7 | |
| 1 | BRU | 43.0 | 115.6 | 50.1 | 303.2 | |
| 2 | OAK | 39.3 | 100.9 | 49.5 | 321.1 | |
| 2 | IMP | 40.6 | 101.7 | 50.7 | 319.8 | |
| 2 | STE | 40.7 | 103.1 | 50.5 | 318.1 | |
| 2 | LYO | 40.2 | 105.3 | 49.5 | 315.6 | |
| 2 | WAL | 40.6 | 106.4 | 49.6 | 314.2 | |
| 2 | CRA | 40.5 | 107.3 | 49.2 | 312.7 | |
| 2 | JEN | 40.5 | 109.5 | 48.8 | 310.7 | |
| 2 | DUC | 40.3 | 110.4 | 48.4 | 309.8 | |
| 2 | FRA | 40.7 | 111.4 | 48.6 | 308.5 | |
| 2 | GRA | 40.7 | 112.5 | 48.4 | 307.3 | |
| 2 | PIL | 41.0 | 114.1 | 48.3 | 305.4 | |
| 2 | CAR | 40.9 | 116.0 | 47.8 | 303.4 | |
| 3 | PRH | 37.2 | 102.9 | 46.8 | 319.1 | |
| 3 | WLS | 37.7 | 104.6 | 47.0 | 317.0 | |
| 3 | MOF | 37.9 | 105.9 | 46.9 | 315.5 | |
| 3 | SAG | 38.0 | 106.5 | 46.9 | 314.8 | |
| 3 | CIM | 38.3 | 107.5 | 47.0 | 313.6 | |
| 3 | MCA | 38.5 | 109.4 | 46.8 | 311.4 | |
| 3 | EME | 39.1 | 111.0 | 47.0 | 309.5 | |
| 3 | SLN | 39.0 | 111.9 | 46.7 | 308.5 | |
| 3 | HIN | 39.0 | 113.0 | 46.5 | 307.3 | |
| 3 | BAK | 39.0 | 114.0 | 46.3 | 306.2 | |
| 3 | EUR | 39.6 | 116.0 | 46.4 | 303.9 | |
| 4 | TUC | 35.0 | 103.5 | 44.3 | 318.9 | |
| 4 | LVG | 35.8 | 105.2 | 44.7 | 316.7 | |
| 4 | ESP | 36.0 | 106.0 | 44.8 | 315.8 | |
| 4 | CUB | 36.1 | 107.0 | 44.7 | 314.7 | |
| 4 | SHP | 36.5 | 108.6 | 44.8 | 312.8 | |
| 4 | KAY | 36.9 | 110.0 | 44.9 | 311.2 | |
| 4 | GCC | 37.1 | 111.7 | 44.7 | 309.3 | |
| 4 | MCJ | 37.3 | 112.7 | 44.7 | 308.2 | |
| 4 | VEY | 37.4 | 113.5 | 44.7 | 307.3 | |
| 4 | HIK | 37.5 | 115.8 | 44.3 | 304.8 | |